ABSTRACT OF THESIS

Name of Candidate Elizabeth Anne IRVINE

Address 24 Bonaly Gardens, Colinton, Edinburgh 13.

Degree Doctor of Philosophy *Date* July 1976

Title of Thesis Reactions on Mixed Tin-Antimony Oxides

An investigation of the catalytic properties of stannic oxide, antimony tetroxide and a range of tin-antimony mixed oxides has been carried out using two pretreatment methods. The two pretreatment methods were a L.T. method (outgassing the catalyst for 5 hr at a temperature of 293 K) and a H.T. method (outgassing the catalyst for 16 hr at a temperature of 698 K). The object of the investigation was two-fold.

i) To gain an insight into the acidic properties of the catalysts by studying the dehydration of isopropanol and the isomerization of 3,3-dimethylbut-1-ene, cyclopropane, and n-butenes.

ii) To increase the existing information about the oxidizing properties of the catalysts by studying the oxidative dehydrogenation of n-butenes.

With the exception of stannic oxide, H.T. pretreatment, which dehydrogenates isopropanol, the individual oxides are inactive. Combining the two oxides results in an acidic catalyst. The number and nature of the acidic sites are determined by the percentage composition of the catalyst and their pretreatment. Brønsted-type acidic sites are believed to be responsible for isopropanol dehydration, 3,3-dimethylbut-1-ene, cyclopropane and n-butene isomerization over the L.T. series mixed oxides. Similar sites are thought to be responsible for isopropanol dehydration, 3,3-dimethylbut-1-ene and cis but-2-ene isomerization over the H.T. series mixed oxides. However, Brønsted and Lewis type sites may account for cyclopropane and but-1-ene isomerization over the H.T. series mixed oxides.

A redox mechanism, involving the cations Sb^{5+} and Sn^{4+} found in the saturated solid solution of antimony tetroxide in stannic oxide, is thought to be responsible for the oxidative dehydrogenation of n-butenes to butadiene.

Use other side if necessary.

To my family

Reactions on Mixed Tin-Antimony Oxides

A thesis presented for the degree of Doctor of Philosophy in the Faculty of Science of the University of Edinburgh

by

Elizabeth Anne Irvine, B.Sc.

July 1976

Abstract

An investigation of the catalytic properties of stannic oxide, antimony tetroxide and a range of tin-antimony mixed oxides has been carried out using two pretreatment methods. The two pretreatment methods were a L.T. method (outgassing the catalyst for 5 hr at temperature of 293 K) and a H.T. method (outgassing the catalyst for 16 hr at a temperature of 698 K). The object of the investigation was two-fold.

i) To gain an insight into the acidic properties of the catalysts by studying the dehydration of isopropanol and the isomerization of 3,3-dimethylbut-1-ene, cyclopropane, and n-butenes.

ii) To increase the existing information about the oxidizing properties of the catalysts by studying the oxidative dehydrogenation of n-butenes.

With the exception of stannic oxide, H.T. pretreatment, which dehydrogenates isopropanol, the individual oxides are inactive. Combining the two oxides results in an acidic catalyst. The number and nature of the acidic sites are determined by the percentage composition of the catalyst and their pretreatment. Brønsted-type acidic sites are believed to be responsible for isopropanol dehydration, 3,3-dimethylbut-1-ene, cyclopropane and n-butene isomerization over the L.T. series mixed oxides. Similar sites are thought to be responsible for isopropanol dehydration, 3,3-dimethylbut-1-ene and cis but-2-ene isomerization over the H.T. series mixed oxides. However, Brønsted and Lewis-type sites may account for

cyclopropane and but-1-ene isomerization over the H.T. series mixed oxides.

A redox mechanism, involving the cations Sb^{5+} and Sn^{4+} found in the saturated solid solution of antimony tetroxide in stannic oxide, is thought to be responsible for the oxidative dehydrogenation of n-butenes to butadiene.

Acknowledgements

The research described in this thesis was carried out personally in the Department of Chemistry, University of Edinburgh, between October 1972 and October 1975.

I am very grateful to my supervisor Dr. D. Taylor for his encouragement and helpful guidance during the period of this research. I would also like to thank Professor C. Kemball, F.R.S., for the provision of laboratory facilities.

Thanks also goes to Mr. A. Anderson for maintenance of equipment, Mr. J. Broom for his glass blowing and Miss M. Fleming for typing this thesis. I would also like to thank my colleagues, too numerous to name, for making my three years so pleasant.

I acknowledge the award of a grant from the Science Research Council for the duration of this research project.

The following graduate courses were attended:-

Catalytic Club Seminars (1972-1975)

Fortran Computing

E.S.C.A.

Some General Aspects of Vibrational Spectroscopy

Differential Thermal Analysis (DTA) and Thermogravimetric Analysis (TGA)

Chemical Aspects of Oil Products Research

CHAPTER 1

General Introduction

1.1 In general, catalysed reactions can be divided into two main classes:-

i) Homogeneous catalysis, where both the catalyst and the reactants are in the same phase.

ii) Heterogeneous catalysis, where the catalytic reaction takes place at an interface between two phases.

This thesis is concerned only with heterogeneous catalytic reactions occurring at interfaces between solids and gases.

The first scientific observation of catalysis was reported at the end of the eighteenth century. Van Marum[1] discovered, in 1796, that alcohol was dehydrated by passage over copper. Then, following the deepened insight into chemistry, the number of catalytic reactions, known as such, rapidly increased. Kirchhoff[2], in 1812, studied the conversion of starch into dextrose and sugar by dilute mineral acids. Davy[3] and Döbereiner[4], between 1817 and 1823, investigated the glowing of metals in mixtures of combustible gases and air. An appraisal of these researches by Berzelius[5] led to their classification under the term catalysis.

A more comprehensive understanding of catalysis was introduced by Ostwald[6] in 1902, when he proposed that the rate of a reaction could be taken as a measure of catalytic activity. By correlating activity with a measurable quantity, he laid the foundations of the modern idea of catalysis.

During the nineteenth century, several theories were put forward to explain the action of heterogeneous catalysis.

The Intermediate Compound theory proposed that a reaction took place between the bulk solid and the reactant to give an intermediate. This intermediate then either decomposed or reacted further to produce the observed products. Although changes in the catalyst's surface were sometimes observed, it was difficult to prove the existence of these intermediates. Thus, the Intermediate Compound theory did not gain wide acceptance.

Faraday[7] proposed a theory of 'contact action', whereby physical forces of attraction between the catalyst and reactants brought increased reaction rates. This was due to the increased concentrations of reactants in the condensed layer. The specificity of catalytic reaction could not be explained by Faraday's theory, which only considered physical forces of attraction.

At the beginning of the twentieth century, specificity considerations led Sabatier[8] to postulate the existence of unstable surface compounds as intermediates in heterogeneous catalysis. Support for this concept was given by Langmuir's[9] work on adsorption. He found that metal surfaces adsorbed gases, and that, in many cases, the amount of adsorption increased with pressure to a constant maximum. Langmuir therefore suggested that adsorption on a solid surface involved short range attractions between surface and adsorbate. This resulted in bonds essentially chemical in nature, and limited in number by the 'sites' available for bonding on the surface.

Thus the process of adsorption, resulting in at least one of the gaseous reactants becoming attached to the surface, must occur if a heterogeneous catalytic reaction is to occur. Adsorption can be classified either as physical adsorption or chemisorption.

Physical Adsorption

The adsorbed molecule is held to the surface by weak Van der Waals' forces, of the type responsible for the cohesion in

liquids. The heat of physical adsorption is generally less than 20 kJ mol^{-1}. These values are usually found for heats of liquefaction and vaporization. Several adsorbed layers may be formed, and the rates of adsorption and desorption are rapid.

Chemisorption

This process involves the rearrangement of the electrons of the interacting gas and solid, resulting in the formation of chemical bonds. The heats of chemisorption are of the order of 80 to 200 kJ mol^{-1}. Thus rates of desorption are usually low. It is now generally accepted that chemisorbed species act as intermediates in heterogeneous catalytic reactions. However, for a catalytic reaction to occur, the strength of adsorption must be within certain limits. A reactant that is too strongly adsorbed will be difficult to remove and will poison the catalyst. On the other hand, a too weakly adsorbed reactant will not remain on the surface long enough to react.

Mechanism of Heterogeneous Catalysis

A catalytic reaction which takes place on a surface, can be broken down into five consecutive steps:-

(1) Diffusion of the reactant molecule to the surface.

(2) Chemisorption of at least one of the reactant species on the surface.

(3) Reaction of these adsorbed species, either among themselves, with physically adsorbed species, or with other molecules colliding with the surface.

(4) Desorption of the products.

(5) Diffusion of the products away from the surface.

The slowest of these processes determines the rate of the reaction. The processes of diffusion, as rate-controlling steps, arise more in the liquid phase and rarely affect reactions in low pressure

laboratory systems, unless the reaction is very fast. It can be determined, however, by measuring the rate at various temperatures, whether or not a reaction is diffusion controlled. If a straight line is obtained from an Arrhenius plot of greatly differing rates, then diffusion effects are unlikely to be important. Anyone of the steps (2), (3) and (4), which are chemical interactions, may be rate-determining.

Two main mechanisms have been put forward to explain the combination of reactants at the catalyst surface, these being the Langmuir-Hinshelwood[10][11] and Eley-Rideal[12][13] mechanisms.

In the Langmuir-Hinshelwood mechanism it is assumed that both reactant species are chemisorbed on adjacent sites on the catalyst. The rate of reaction is assumed to be determined by the reaction between the adsorbed molecules, and the adsorption and desorption processes are assumed to be in equilibrium. By this mechanism the hydrogen-deuterium exchange reaction on a metal would proceed thus:-

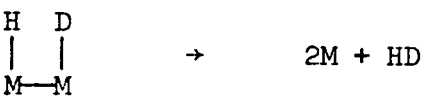

Most of the reactions to which Langmuir-Hinshelwood mechanisms have been applied take place at high temperatures, where it is reasonable to expect rapid adsorption and desorption. However, for low temperature reactions this may not be the case. Roberts[14], for example, found that although hydrogen adsorbed readily on tungsten at 193 K, its desorption was very slow, even at temperatures up to 673 K. This led Eley and Rideal to propose that only one species is chemisorbed and the second interacts with it, either directly from the gas phase, or from a

physically adsorbed layer. The hydrogen-deuterium exchange reaction would then proceed thus:-

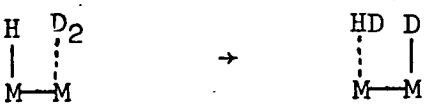

A full line represents chemisorption and a dotted line physical adsorption.

Catalytic Activity

Many ideas have been put forward to explain catalytic activity. Some of these are:- the electronic factor in catalysis, the Crystal Field theory and the Multiplet theory.

The Electronic Factor

The Boundary-Layer theory was postulated by Weisz[15]. The gas adsorbed is represented either as a donor or acceptor of electrons. The adsorbent is represented as a conventional semiconductor with a given concentration of ionised donor or acceptor centres. The ability of the adsorbent to participate in the chemisorption is determined by the height of the Fermi level. The theory was extended by Hauffe[16] to show the way that the height of the Fermi level could be used to influence reactions with well defined rate-determining steps. On the other hand, Wolkenstein's[17] theory introduced the concept of 'weak' and 'strong' bonding between the chemisorbed particle and semiconductor surface. In 'weak' bonding, the particle interacts with neither a hole nor an electron. The particle remains electrically neutral. When a free electron or hole participates in the bonding of the chemisorbed particle, a 'strong' n-(acceptor) bond or p-(donor) bond arises.

Attempts have been made to establish correlationships between catalytic activity and semiconductor type. Stone[18] noted that p-type oxides were best for the decomposition of nitrous oxide, while n-type oxides were the least effective. Additions of small quantities of altervalent ions, have been found to change the position of the Fermi level, consequently influencing the catalytic activity of a semiconductor. Winter[19] increased the 'p-typness' of nickel oxide by the addition of small quantities of lithium. In keeping with the observations made by Stone[18], the activity for nitrous oxide decomposition increased. However, the findings of Bielanski et al.,[20] studying doped nickel oxide, led them to suggest that the precise degree of semiconductivity of the metal oxide may have differed considerably in the bulk from that which prevailed at the surface.

Crystal Field Theory

This supposes that chemisorption on a surface transition metal cation increases the coordination number of the ion. This results in a change in the crystal field stabilization energy. Dowden and Wells[21] used the Crystal Field theory to explain the 'twin peak' activity pattern encountered for hydrogen-deuterium exchange over a series of transition metal oxides. They calculated the change in crystal field stabilization energy caused by an increase in coordination number, and concluded that the most catalytically active systems would have the configurations d^3, d^6 and d^8, since these showed the maximum changes. The minimum effect would be observed with the d^0, d^5 and d^{10} systems. As with the Boundary-Layer theory discrepancies have been observed, (Stone[18]).

Multiplet Theory of Balandin[22]

This supposes that only part of a molecule, named the 'index group', participates in a reaction and that only certain atoms of the catalyst possess the necessary configuration for the reaction. These

atoms are termed the 'multiplet'. During catalysis the 'index group' of a reactant molecule is superimposed on the 'active' atoms of the catalyst, thereby yielding an intermediate 'multiplet complex'. Within the 'multiplet complex', bond deformation and migration occurs.

There is no one general theory that can be used to explain all catalytic activity and selectivity.

1.2 Object of the Investigation

Previous investigations have revealed that catalysts based on tin-antimony oxides possess acidic[28][73] and oxidizing properties[23][73][92]. With these two aspects in mind, the object of the investigation was two-fold.

i) To gain an insight into the acidic properties of the catalysts by studying the dehydration of isopropanol and the isomerization of 3,3-dimethylbut-1-ene, cyclopropane and n-butenes.

ii) To increase the existing information about the oxidizing properties of the catalysts by investigating the oxidative dehydrogenation of n-butenes.

1.3 Structure of Tin-Antimony Mixed Oxides

The tin-antimony mixed oxides consist of one or more phases, depending on the Sn:Sb atomic ratio. X-ray data, electrical conductivity measurements and infra-red spectroscopy[23-26] have been used to obtain information about the phase composition of the mixed tin-antimony oxides.

Godin et al.,[23] Lazukin et al.,[24] and Wakabayashi et al.[25] found that the electrical conductivity of the mixed oxides increased

with increase in the atomic percentage of antimony. Godin et al.[23] attributed this to the substitution of Sb^{5+} ions for Sn^{4+} in the stannic oxide. Substitution by Sb^{5+} ions caused an equal number of Sn^{3+} ions to be created. The Sn^{3+} ions acted as electron donors which on ionization gave free electrons.

$$(Sn^{4+}_{1-2x}\ Sb^{5+}_{x}\ Sn^{3+}_{x})O_2^{2-} \rightleftharpoons (Sn^{4+}_{1-x}\ Sb^{5+}_{x})O_2^{2-} + xe^-$$

A similar explanation was put forward by Wakabayashi et al.[25]

Electrical conductivity[23-25] was found to increase until a certain critical value was reached, after which further addition of antimony oxide resulted in a decrease. This critical value is thought to be the solubility limit of antimony in stannic oxide. Godin et al.[23] and Wakabayashi et al.[25] gave it a value of approximately 5 atom % Sb, while Lazukin et al.[24] put it as high as 25 atom % Sb. However, according to Wakabayashi et al.[25] this value depended on the calcination temperature. They[25] reported that an increase in the calcination temperature of a catalyst from 1273 K to 1373 K may have increased the solubility limit to 25 atom % Sb. This value agrees with the one reported by Lazukin et al.[24] for a calcination temperature of 1323 K. Thus before the solubility limit is reached, the mixed oxide catalyst consists of a single phase, a solid solution of pentavalent, and also according to Lazukin et al.[24] trivalent antimony oxides, in stannic oxide. After this limit, there are two phases. One phase is a saturated solution of antimony oxide in stannic oxide, the other phase is antimony oxide. This latter phase was thought to be responsible for the decrease in electrical conductivity[23-25].

The antimony solubility limit in stannic oxide was set at 25 atom % Sb by Lazukin et al.[24] They showed that the fraction of the area occupied by the saturated solid solution remained approximately

constant for the mixed oxides with an antimony content of greater than 25 atom % Sb.

Roginskaya et al.,[26] using x-ray analysis and infra-red spectroscopy, carried out a comprehensive study of tin-antimony mixed oxides, which had been treated at a range of calcination temperatures. They observed an antimony trioxide phase, in a catalyst which had been heated at 1173 K. However, according to Simon and Theler[27], conversion to antimony trioxide takes place at the higher temperature of 1473 K. They[26] concluded that such conversion was due to the influence of a specific concentration of stannic oxide. Roginskaya et al.[26] also observed two additional phases, unnoticed by the other investigators[23-25]. One phase consisted of a solid solution of stannic oxide in antimony tetroxide, and the other phase was unidentifiable.

CHAPTER 2

2.1 Isomerization of 3,3-Dimethylbut-1-ene

To account for the isomerization of 3,3-dimethylbut-1-ene over alumina catalysts, Pines and Haag[29] proposed the following scheme:-

a)

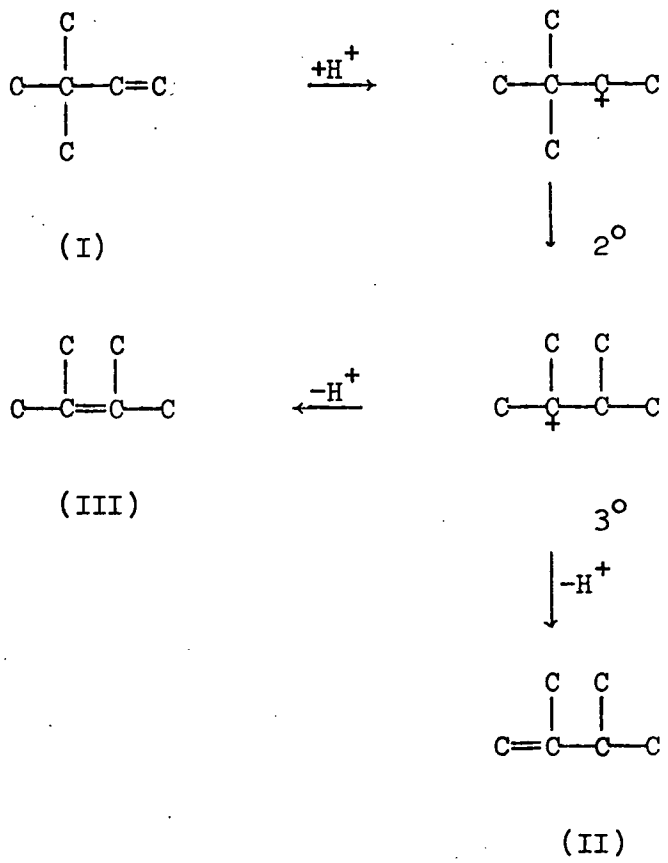

The initial formation of a secondary carbonium ion was followed by rearrangement to the more stable tertiary ion. The subsequent loss of a proton from this species, resulted in the formation of 2,3-dimethylbut-1-ene (II) or 2,3-dimethylbut-2-ene (III).

According to Pines and Haag[29], further rearrangement resulting in the formation of 2-methylpentenes, 3-methylpentene and n-hexenes proceeded as follows:-

b)

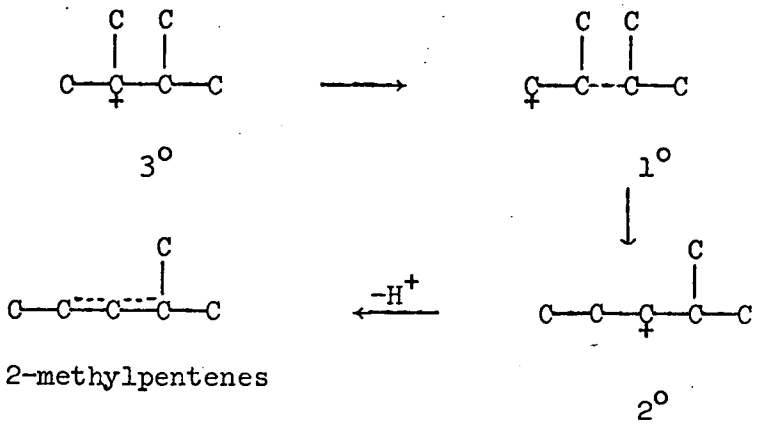

c)

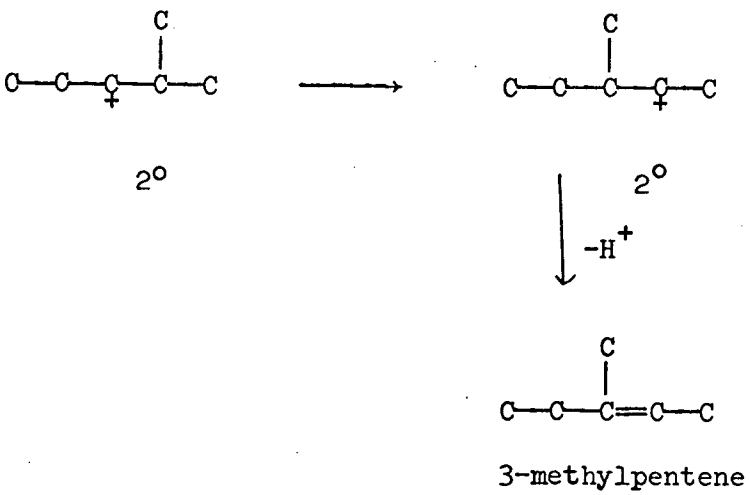

d)

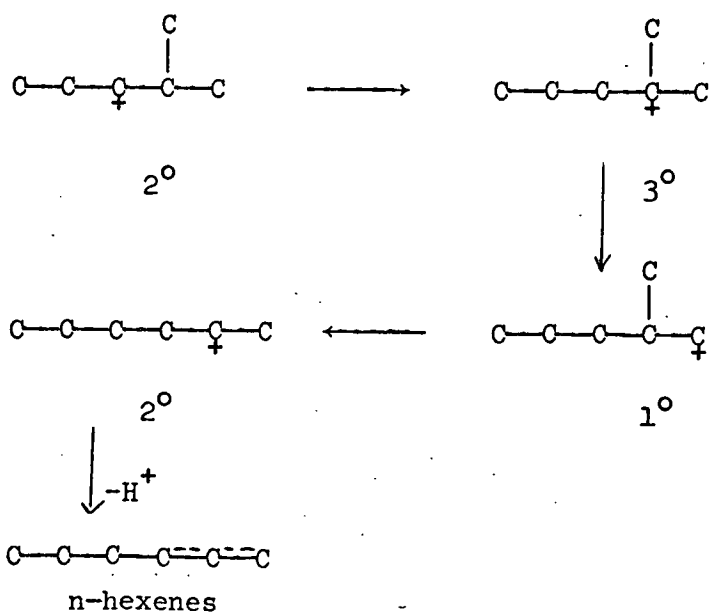

Of the many ways in which 3,3-dimethylbut-1-ene isomerization can take place, those implying secondary or tertiary carbonium ions will be favoured with respect to those implying primary carbonium ions. Thus, reaction b) will be slower than reaction a) or will require stronger acid sites, and similarly for reaction d) with respect to reaction a). Hence a careful analysis of reaction product distribution, and the exact determination of the total conversion, will permit the scale of acid strength and surface density of the sites to be determined.

The kinetic data obtained by Haag and Pines[30], indicated that the nature of the isomerization of 3,3-dimethylbut-1-ene was consecutive, i.e. a→b→c→d rather than parallel, over alumina catalysts. Such a reaction scheme required the regeneration of an olefin from a carbonium ion by the loss of a proton, to be faster than methyl migration. This would account for the observed initial formation of 2-methylpentenes, without the simultaneous production of detectable amounts of 3-methylpentene.

Isomerization and exchange studies have been carried out by Kemball et al.[31][32] over a range of zeolites. Their observations strongly supported the reaction mechanism proposed by Pines and Haag[28]. In the majority of cases, the only products detected were those of the 2,3-dimethylbutenes. To explain the exchange reaction of 3,3-dimethylbut-1-ene over magnesium oxide, a poor catalyst for the isomerization, Kemball et al.[31] invoked an allylic carbanion intermediate. Such a species could be formed by the loss of a proton from either 2,3-dimethylbut-1-ene or 2,3-dimethylbut-2-ene. It could not be formed directly from 3,3-dimethylbut-1-ene. Kemball et al.[32] also observed that the product ratio of 2,3-dimethylbut-2-ene to 2,3-dimethylbut-1-ene remained constant throughout the experiments and the isomers were formed in equilibrium proportions.

CHAPTER 3

3.1 Decomposition Mechanism for Alcohols

The decomposition of an alcohol can occur by either dehydration, resulting in an olefin and in some cases an ether, or by dehydrogenation giving rise to an aldehyde or a ketone.

There are three elimination mechanisms[33][34] by which dehydration can take place to form an olefin.

E_1 Elimination

The first step is rate-determining and involves ionisation of the substrate by loss of a hydroxyl ion.

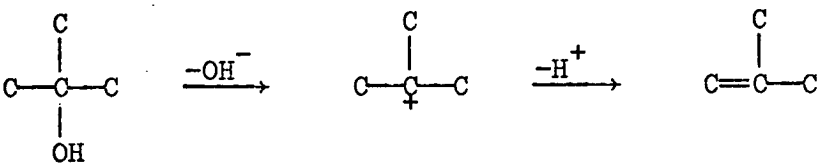

The rate of elimination depends only on the concentration of the substrate. This type of mechanism is expected where the substrate can yield a relatively stable carbonium ion.

E_2 Elimination

The elimination reaction consists of a one step, or 'concerted' mechanism where the base removes the β-hydrogen at the same time as the leaving hydroxyl departs from the α-carbon.

The elimination obeys second order kinetics; first order each in substrate and in base.

E_1cb Elimination

Like an E_2 elimination it depends on the presence of a base. It is a two stage process. The base removes the β-hydrogen to form a carbanion which after a significant length of time loses the hydroxyl group to give an olefin.

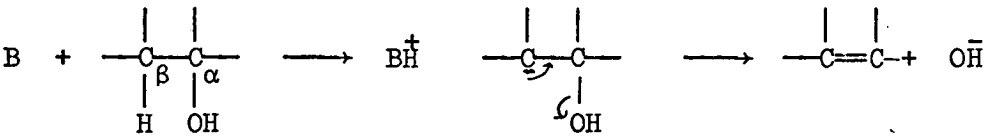

When it is possible to have two or more different β-eliminations, the selectivity towards each may be governed by either Saytzeff or Hofmann orientation rules[34]. Saytzeff elimination leads preferentially to the olefin carrying the larger number of alkyl groups. Hofmann elimination results in the olefin with the smaller number of alkyl groups. E_1 elimination takes place according to Saytzeff orientation rule, whereas E_2 elimination can take place according to both orientation rules. The extent to which Hofmann type elimination occurs depends on inductive, and to some extent steric effects.

The dehydration mechanism of alcohols over alumina catalysts has been reviewed by Pines and Manassen[35], and Knözinger[36]. Pines and Manassen[35] concluded that the mechanism for tertiary

alcohols could be interpreted by a carbonium ion intermediate, whereas secondary and primary alcohols were dehydrated according to a concerted mechanism.

The other product of dehydration is an ether. According to Knözinger[36] ether formation resulted from the reaction of surface alkoxide groups with molecularly adsorbed alcohol molecules. He believed that there were two routes by which ether formation could take place over alumina:-

i) The R-OH bond of the molecularly adsorbed alcohol and the RO-Al bond in the alkoxide group are broken.

ii) The RO-H bond in the alcohol molecule and the R-OAl bond in the alkoxide are broken. Such a mechanism can be represented as follows:-

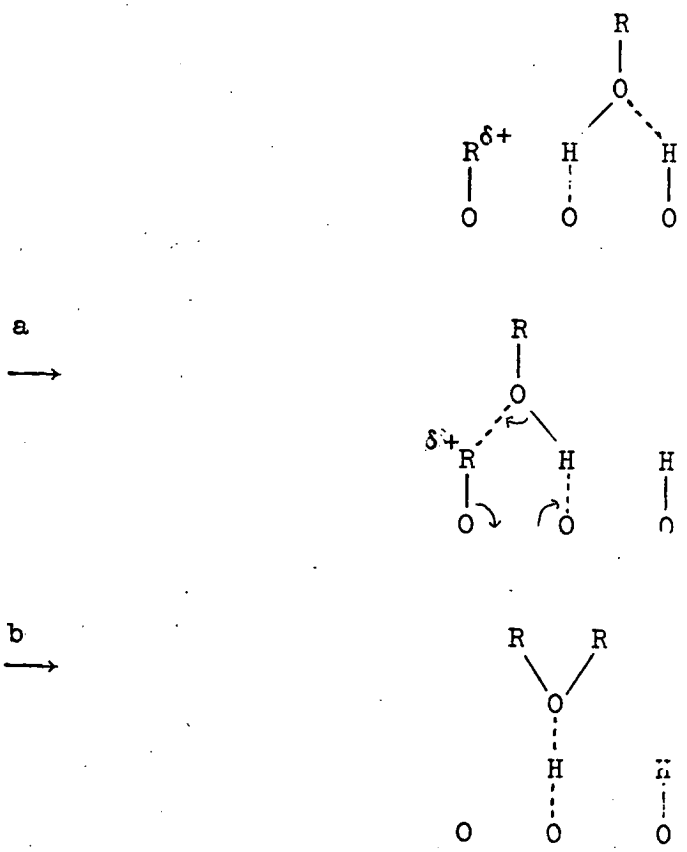

Knözinger[36] believed that the route ii) would be favoured on steric grounds, and the reverse step b→a could be used to represent the hydration of ethers. He also concluded that different intermediates would be required for the formation of ethers and olefins. However, Brey and Krieger[37] and Topchieva et al.[38] postulated a common intermediate, a carbonium ion[37] and an alkoxide[38].

From a series of investigations concerning the dehydration of alcohols to ethers over a variety of catalysts[39-44], it was concluded that ether formation took place through a concerted reaction between two alcohol molecules. One was adsorbed on an acidic site, the other on a basic site. Šimonik and Pines[41] postulated the following mechanism:-

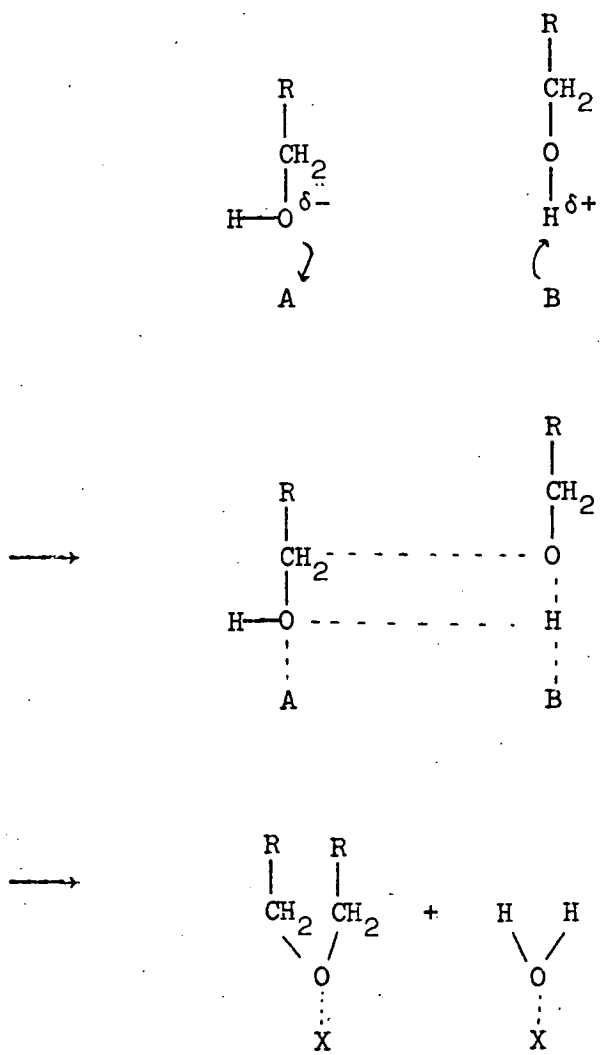

Within a series of alcohols, reactivity towards ether formation was found to be governed by steric effects. A comparison between primary and secondary alcohols by Licht et al.[43], revealed that primary alcohols were more reactive towards ether formation, and that retardation by water was greatest for secondary alcohols. In a later work by Licht et al.[44], they concluded that the differences between the secondary and primary alcohols were due to the higher basicity of the secondary alcohols.

Both Lewis and Brønsted-type acidity have been used to describe the mechanism for isopropanol dehydration. Gentry and Rudham[45] concluded that Brønsted-type acidity was responsible for dehydration over X zeolites, whereas Lewis-type acidity was postulated by Gentry et al.[46] to explain their observations on rutile.

Although Gentry et al.[46] were unable to explain the mechanism responsible for dehydrogenation, they were able to conclude that the sites for dehydration and dehydrogenation were different. Similar conclusions were drawn by Rajaram et al.[47] from a study of isopropanol decomposition on manganese molybdate and by Kibby and Hall[48] from their observations with a series of alcohols and hydroxapatite catalysts. Kibby and Hall[48] represented alcohol dehydrogenation as follows:-

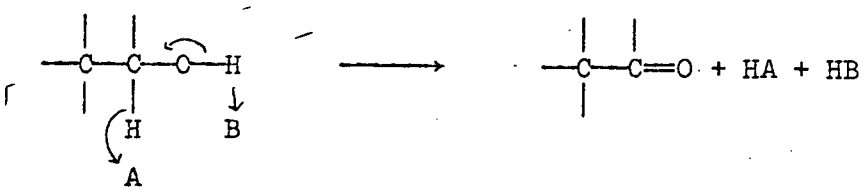

They[48] believed that dehydration and dehydrogenation took place by acid-base mechanisms. Rajaram et al.[47] concluded that the electronic factor was responsible for dehydrogenation.

There has been considerable controversy concerning dehydration and dehydrogenation of alcohols. In a study made by Schwab and Schwab-Agallidis[49], changes in selectivity towards dehydration or dehydrogenation were thought to be a function of heat treatment. This altered the texture of the catalyst. On flat surfaces dehydrogenation occurred, but in the pores of molecular dimensions, polarization on two sides of the molecule induced dehydration.

Batta et al.[50] studying the decomposition of isopropanol over zinc oxide, related its selectivity to the character of the bonds. They believed that the more ionic the character possessed by a catalyst oxide, then the more strongly dehydrogenating it would be. Whereas an increase in selectivity towards dehydration would arise the nearer the oxide approached a covalent character. Similar conclusions were drawn by McCaffrey et al.[51], from their observations of isopropanol decomposition over the first row transition metals.

Wolkenstein[17] and Hauffe[16] believed that selectivity was determined by the electronic factor. However, Wolkenstein[17] considered the initial step of isopropanol adsorption to be rate-determining for dehydrogenation. Hauffe[16] regarded the final step of the desorption of acetone to be rate-determining. According to Wolkenstein[17], isopropanol was adsorbed through the hydroxyl hydrogen for dehydrogenation and through the hydroxyl group as a whole for dehydration. Consequently, lowering the Fermi level retarded dehydrogenation but accelerated dehydration.

CHAPTER 4

Isomerization of Cyclopropane

4.1 Isomerization of cyclopropane results in the formation of propylene only, but alkylcyclopropanes give rise to a variety of products. The stability[52] of the reactive intermediate determines the product distribution. The order of stability for a carbonium ion and a radical is tertiary>secondary>primary. This is the order of instability for a carbanion.

4.2 The Structure of Cyclopropane

The bonding in cyclopropane is such that the ring atoms have more 'p' character than sp^3 hybridised carbon atoms. The angle between orbitals lies between that of a sp^3 hybrid (109^o 28') and that of a sp^2 hybrid carbon (90^o). The electrons of the carbon bonds are thus localised in bent or banana shaped bonds. The regions of high electron density lie outside the triangle formed by the carbon nuclei. Cyclopropane reacts readily with electrophilic reagents and it is relatively difficult to form a ring carbanion.

4.3 Metal Catalysts

Mass-spectroscopic studies of the metal catalysed deuterolysis of cyclopropane by Newham[53], revealed that adsorbed hydrocarbon radicals were formed as primary products. Newham[53] believed that such species would account for metal catalysed cyclopropane isomerization.

4.4 Oxide Catalysts

A variety of mechanisms have been put forward to explain 'acid'

catalysed cyclopropane isomerization. Roberts[54] invoked an n-propylcarbonium ion to account for cyclopropane isomerization over a range of acidic catalysts. He believed that the 'p' character of the carbon atoms facilitated proton attack.

Baird and Aboderin[55], studying the solvolysis of cyclopropane by deuterated sulphuric acid, postulated a cyclo-propylcarbonium ion. They represented it in two forms:-

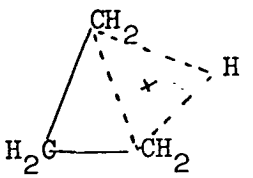

I

non-classical
hydrogen-bridged ion

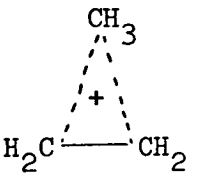

II

classical
carbon-carbon bridged ion

The non-classical ion was used to explain their data. They also suggested that the importance of non-classical ions (I) would be greatest in systems where the classical ions (II) occurred as unstable primary ions.

To explain the results of deuterated cyclopropane isomerization over silica-alumina, Larson et al.[56] proposed a bimolecular hydride transfer mechanism. Such a mechanism took place on Lewis-type acidic sites.

$$\text{Cyclo-}C_3H_6 \rightarrow \text{cyclo-}C_3H_5^+ + \text{Cat.-}\bar{H}$$

Transference of a hydride ion to either of the two 'non-carbonium carbons' resulted in the formation of propylene.

$$\text{cyclo-}C_3H_5^+ + \text{cyclo-}C_3D_6 \rightarrow \text{cyclo-}C_3D_5^+ + CH_2D\text{-}CH{=}CH_2$$

However, they did not exclude the possibility of a mechanism involving a cyclo-propylcarbonium ion. Such a mechanism would have

required Brønsted-type acidic sites.

To differentiate between the two mechanisms Hightower and Hall[57] studied the isomerization of deuterated alkylcyclopropanes over silica-alumina. The product spectrum enabled them to conclude that isomerization took place via a non-classical cyclo-propylcarbonium ion, similar to that postulated by Baird and Aboderin[55]. Analysis of the deuterium content of the products led them to conclude that the protonic sites were associated with carbonaceous residues. Bartley et al.[58], studying cyclopropane over a deuterated zeolite, also proposed a non-classical cyclo-propylcarbonium. They also introduced a further step involving an intramolecular hydrogen transfer. Flockhart et al.[59], studying a zeolite catalyst, concluded that cyclopropane isomerization took place on Brønsted-type acidic sites at low temperatures and on Lewis-type acidic sites at high temperatures.

CHAPTER 5

Isomerization of n-Butenes

5.1 The Adsorbed State of Olefins

In a review on the hydrogenation of olefins at metal surfaces, Bond and Wells[60] defined two basic kinds of adsorbed olefins 1) σ-di-adsorbed olefin 2) π-adsorbed olefin.

The σ-diadsorbed olefin involves rehybridization of the olefinic bond carbon atoms to sp^3 hydridization, followed by the formation of two σ-bonds between the carbons and the surface:-

$$RCH = CHR' + 2^* \rightarrow \begin{matrix} RCH - CHR' \\ | \quad | \\ * \quad * \end{matrix}$$

Two forms of the π-adsorbed olefin are possible, (i) involving the formation of a π-donor bond with the surface and retaining sp^2 hydridization,

$$\begin{matrix} RCH = CHR' \\ | \\ * \end{matrix}$$

and (ii), arising with olefins possessing one or more α-methylenic hydrogen atoms and involving a π-allyl species.

$$^* + RCH = CH\text{-}CH_2R' \rightarrow \begin{matrix} RCH\text{-}CH\text{-}CHR' \\ | \\ * \end{matrix}$$

The π-methyl allyl radical formed from a butene molecule can exist in <u>syn</u> and <u>anti</u> forms.

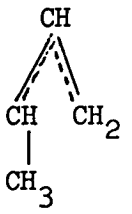

anti

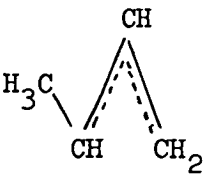

syn

Free rotation is prohibited with the π-allyl adsorbed species.

5.2 Isomerization Mechanism

Using the above types of adsorbed species, Bond and Wells[60] defined two possible mechanisms for olefin isomerization.

i) This involves either σ-adsorbed or π-adsorbed species, in which isomerization would be represented by addition of hydrogen followed by subsequent elimination.

Double-Bond Migration

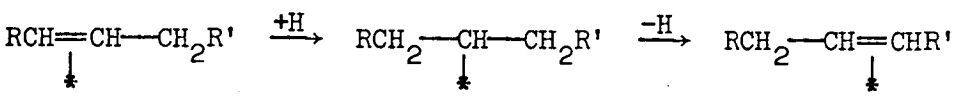

Cis-Trans Isomerization

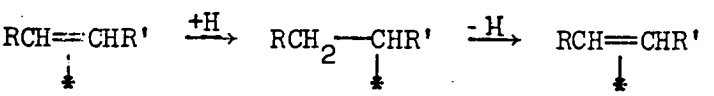

For double-bond migration and cis but-2-ene - trans but-2-ene isomerization there is a common, freely rotatable intermediate.

ii) This involves a π-allyl adsorbed species from which hydrogen is first eliminated and then replaced.

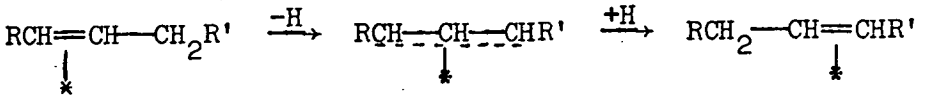

Free rotation is not possible with this intermediate and so cis but-2-ene - trans but-2-ene isomerization has to occur through the double bond shift as follows.

Cis But-2-ene - Trans But-2-ene Isomerization

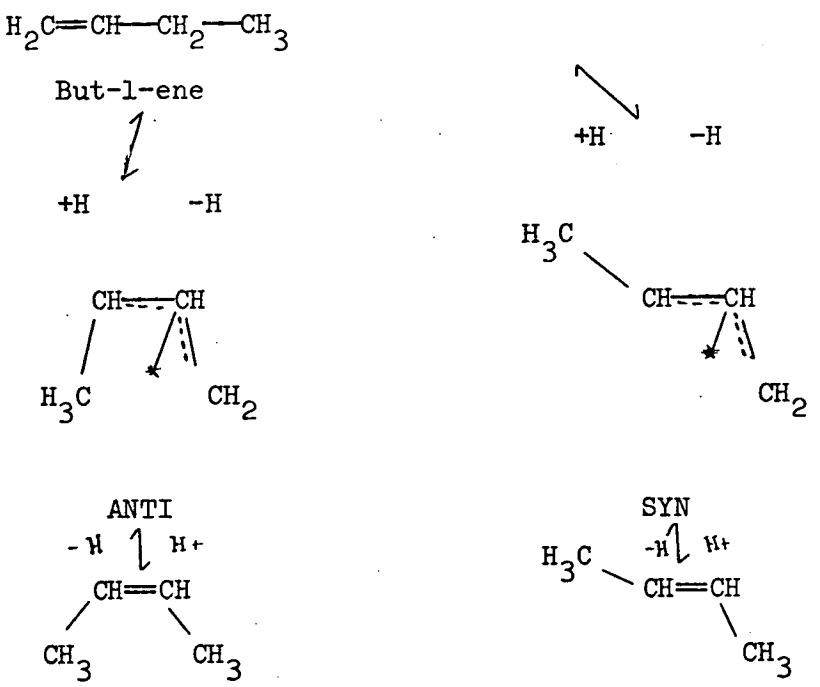

The initial product ratios obtained during double-bond migration and cis but-2-ene to trans but-2-ene interconversion have been used to obtain information about the basic and acidic properties of catalysts. However, there are circumstances in which such information will be inconclusive. For example, at any one time an n-butene reaction over a particular catalyst may be occurring by several different mechanisms, or under conditions where the surface reaction is fast compared to the desorption of the products, such

that the butenes may reach thermodynamic equilibrium on the surface before desorption takes place.

5.3 Acidic Catalysts

Early workers[61][62] studying the polymerization of olefins on phosphoric acid, postulated several theories, which could be used to explain the mechanism of double-bond migration in hydrocarbons. Ipatieff and Corson[61] believed that phosphoric acid added to the double-bond to form an ester intermediate, which then eliminated the acid in a different direction.

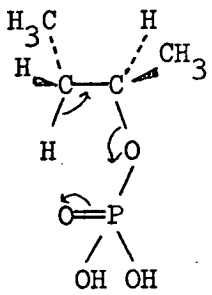

←TRANS

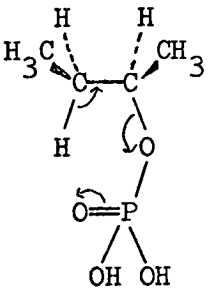

CIS →

A modified form of the mechanism put forward by Ipatieff and Corson[61], was later suggested by Farkas and Farkas[62]. However, Turkevich and Smith[63] could not verify such a mechanism due to the fact that they observed no exchange of ethylene with radioactive tritium phosphoric acid. They[63] put forward the 'Hydrogen Switch' mechanism i.e. a concerted mechanism in which an activated complex was formed between the olefin and acid. The acid acted both as a donor and an acceptor of hydrogen atoms. It can be represented with phosphoric acid as follows:-

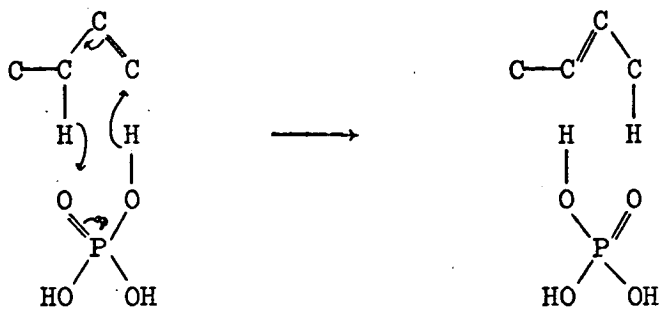

Turkevich and Smith[63] explained the failure of ethylene to exchange with phosphoric acid by the fact that ethylene does not have the three carbon atom system necessary for the 'Hydrogen Switch' mechanism. Haag and Pines[30], working with alumina, found that the 'Hydrogen Switch' mechanism could not be used to explain direct cis but-2-ene to trans but-2-ene interconversion. They proposed a common intermediate, the secondary butyl carbonium ion. Such an intermediate, was also suggested by Hightower and Hall[64] to explain an initial cis but-2-ene/trans but-2-ene product ratio of approximately 1.

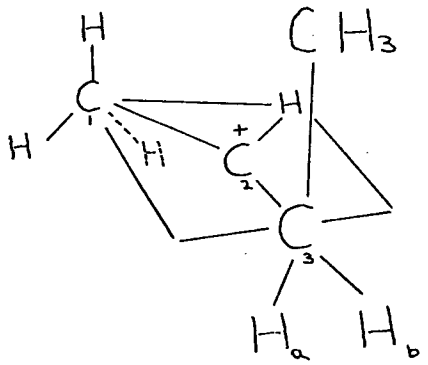

C_1, C_2, C_3 all lie in a plane parallel to the surface and free rotation about the C_2-C_3 bond is greatly inhibited. Loss of Ha or Hb, which are energetically similar, results in cis but-2-ene and trans but-2-ene respectively. The initial but-1-ene/but-2-ene product ratio obtained from isomerization of either but-2-enes, could only be explained by considering a combined statistical and energetic approach. This resulted in a theoretical ratio of 0.75.

To account for the observed initial cis but-2-ene/trans but-2-ene product ratiosof 2-4, Haag and Pines[30] suggested that the elimination of a proton from the secondary butyl carbonium ion proceeded through the rearrangement to a π-complex in a slow step, with a subsequent rapid loss of the proton.

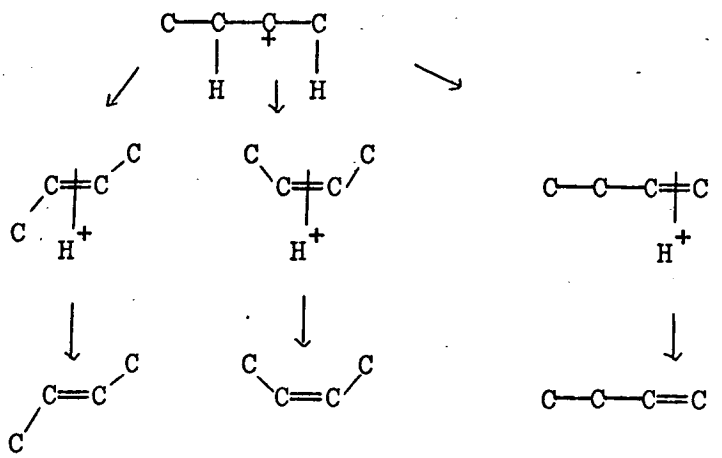

The energies of the π-complexes they believed were cis but-2-ene < trans but-2-ene = but-1-ene. This would account for the high initial cis but-2-ene/trans but-2-ene product ratios.

So in general, for a mechanism involving a secondary butyl carbonium ion:-

but-1-ene, will give an initial cis but-2-ene/trans but-2-ene product ratio ≥ 1

cis but-2-ene, will give an initial but-1-ene/trans but-2-ene product ratio ≤ 1

A butenyl (allylic) carbonium ion, resulting from hydride abstraction by a Lewis acid, was postulated by Leftin and Hermana[65]. As seen in Section 5.2, cis but-2-ene - trans but-2-ene isomerization occurring by an allylic intermediate, has to take place through a double-bond shift. Such a mechanism they believed would lead to high initial but-1-ene/but-2-ene product ratios for but-2-ene isomerization.

5.4 Basic Catalysts

According to Pines and Schaap[66], in the presence of strong basic catalysts, mono-olefins underwent a reversible double-bond shift by a chain mechanism. Such a mechanism involved allylic carbanion

intermediates. In contrast to acid catalysed isomerization, no rearrangement of the carbon skeleton was observed.

Abstraction of an allylic proton resulted in a resonance-stabilized intermediate.

$$B^-Na^+ + RCH_2{-}CH{=}CH_2 \longrightarrow BH + RCH^-{-}CH{=}CH_2 \; (Na^+) \leftrightarrow RCH{=}CH{-}CH_2^- \; (Na^+)$$

In the presence of additional olefin, exchange of metal for an allylic proton took place, resulting in the isomerized olefin and more of the basic intermediate.

$$RCH{=}CH{-}CH_2^- \; (Na^+) + RCH_2{-}CH{=}CH_2 \longrightarrow RCH{=}CH{-}CH_3 + RCH^-{-}CH{=}CH_2 \; (Na^+)$$

Haag and Pines[67], studying a range of basic catalysts, observed the rapid conversion of but-1-ene to cis but-2-ene. To account for this, they concluded that either the cis butenyl carbanion was reacting rapidly, or it was present in greater concentrations as a result of an additional stabilized structure.

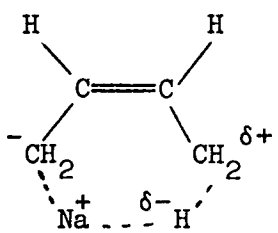

The latter interpretation was favoured.

Foster and Cvetanovic[68], studying the reactions of n-butenes over a series of basic catalysts, also observed a rapid conversion of but-1-ene to cis but-2-ene. They attributed this to the lack of free rotation in the carbanion intermediate.

So in general, for a mechanism involving an allylic carbanion intermediate:-

but-1-ene, will give an initial cis but-2-ene/trans but-2-ene product ratio > 1

cis but-2-ene, will give an initial but-1-ene/trans but-2-ene product ratio > 1

5.5 Metal Catalysts

Bond and Wells[60] studied n-butene isomerization on various metals supported on alumina and postulated a mechanism involving a secondary butyl radical intermediate.

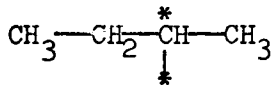

As free rotation about the carbon-metal bond was possible, then both positional and geometric isomerization could occur through the same intermediate.

The secondary butyl radical can be adsorbed in a variety of conformations, which are important in predicting initial product ratios. Considering the metal atom to which the olefin is attached as equivalent to another methyl, the following conformations are important.

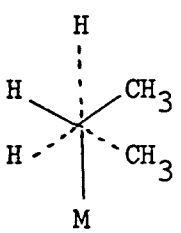

I

Cis But-2-ene

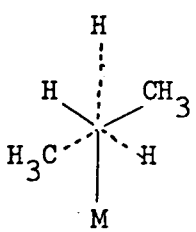

II

Trans But-2-ene

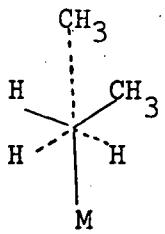

III

Mixture of Cis but-2-ene + Trans but-2-ene

Conformations II and III have similar energies, while I has a slightly higher value. Thus at low temperatures, I will not contribute much to the products and the initial trans but-2-ene/cis but-2-ene product ratio from but-1-ene will be >1 at low temperatures, tending to 1 at higher temperatures

5.6 Isomerization of n-Butenes over Tin-Antimony Mixed Oxide Catalysts

Previous investigations of n-butene reactions, have been carried out under conditions, where considerable amounts of butadiene formation as well as n-butene isomerization have been observed. For this thesis, n-butene isomerization studies were carried out under conditions in which butadiene formation was minimal.

Trifirò et al.[69], observed that the tin-antimony mixed oxides had a much higher isomerization activity than stannic oxide. On the other hand, antimony tetroxide was found to be practically inactive. They attributed the high activity of the mixed oxides, to the increase in concentration of tin with a valence lower than four. Such a species was formed on the addition of antimony tetroxide to form the tin-antimony mixed oxides.

Takte and Rooney[70] investigated the effect of the addition of trace amounts of sulphide to stannic oxide on but-1-ene isomerization. They concluded that but-1-ene isomerization proceeded via the formation of 1-methyl-allyl radicals at paramagnetic centres. Such centres, were believed to be low valence states of tin, formed on the addition of sulphide. However, Kemball et al.[71] failed to establish any correlation between paramagnetic centres and but-1-ene isomerization over stannic oxide. They observed, unlike Trifirò et al.[69], that isomerization took place readily over stannic oxide.

Kemball et al.[71] also noted exclusive cis but-2-ene to trans but-2-ene isomerization, when cis but-2-ene was reacted over stannic oxide. To account for this, an intramolecular mechanism involving a secondary butyl carbonium ion was invoked. The initial cis but-2-ene/trans but-2-ene product ratios from but-1-ene were shown by Kemball et al.[71] to be in the range 1.2-1.5. On the other hand, Trifirò et al.[69] reported a value of 3.

Alieva et al.[72], studying the tin-antimony mixed oxide (atomic ratio Sn:Sb = 4:1), noted that the addition of alkali metals decreased the activity for but-1-ene isomerization activity. They attributed this to the neutralization of Lewis-type acidic sites. Similar explanations were put forward by Sala and Trifirò[73], to account for the inhibiting effect of water on isomerization. Sala and Trifirò[73], also observed that the method of preparation of the mixed oxides influenced their isomerizing activity.

CHAPTER 6

Oxidation

6.1 Introduction to Oxidation

Hydrocarbon derivatives containing oxygen and other hetero-atoms are important intermediates in the petrochemical industry. Consequently, a great deal of effort has been expended in attempts to develop selective oxidation catalysts. According to Voge[74], a proper description of heterogeneous catalytic oxidation must treat several different problems simultaneously:-

i) The characterization of the solid surface in its reactive state.

ii) Identification of the oxygen and other species on the surface and the reactions undergone by each.

iii) The step involved in the reaction path.

iv) The structures and energies of the intermediates.

In spite of exhaustive studies on the selective oxidation of hydrocarbons, according to Hucknall[75], only a few general rules have emerged. He believed that all selective oxidation catalysts were composed of at least two oxide components, one responsible for activity and the other for selectivity. Hucknall concluded that there was insufficient evidence to say whether both cations took part in the surface process, or whether the role of activating component served only to modify the oxygen-metal bond in the base catalyst. He put forward the following facts, which he believed could be accepted as universal for the allylic oxidation of olefins, such as propylene and n-butenes:-

a) The first step in the reaction involves the dissociative chemisorption of the olefin with the abstraction of an α-hydrogen.

b) This first step is rate-determining.

c) In many cases, the rate of formation of reaction products is equal to the rate of the reduction of the catalyst in the absence of gaseous oxygen, thus favouring the theory of Mars and Van Krevelen[76].

The allylic intermediate, formed as a result of step a) can be attached to the surface by a π-bond or by a σ-bond. According to Adams[77], the reactivities of the olefins are related to the types of allylic hydrogens. Thus, the rates follow the order:-

tertiary>secondary>primary

The theory of Mars and Van Krevelen[76], favoured by step c) basically envisaged that the catalytic oxidation of hydrocarbons proceeded via the following steps:-

(1) Reaction between hydrocarbon and the oxide to give products and a partially reduced catalyst.

(2) Reoxidation of the reduced catalyst with gaseous oxygen to restore the catalyst to its original state.

In such a scheme the oxygen serves only to reoxidize the catalyst. This was unlike the idea used by Adams[77] to explain the oxidative dehydrogenation of but-1-ene to butadiene over bismuth-molybdate. He believed that there was an initial adsorption of oxygen on the catalyst surface, before the reaction commenced. However, the observations of Sachtler and De Boer[78] were consistent with the theory of Mars and Van Krevelen[76]. Sachtler and De Boer noted that the selectivity and activity for propylene oxidation over a bismuth-molybdate catalyst, could be related to the

strength of the metal-oxygen bond.

According to Hucknall[75] only in the case of one catalyst, bismuth-molybdate, has a complete picture of oxidation catalysis emerged. Useful information about the oxidation mechanism of other systems, has been obtained by comparing them with bismuth-molybdate.

6.2 Propylene Oxidation with Tin-Antimony Oxide Catalysts

Belousov and Gershingorina[79], studied the oxidation reactions of propylene over antimony oxides, containing the cation in various valence states. Generally, the oxidation products were carbon oxides, water, aldehydes (acrolein, acetaldehyde and propionaldehyde) and acids (acetic and acrylic). The product spectrum and selectivity depended strongly upon the valence state of the cation.

Lazukin et al.[24] and Crozat and Germain[80] reported that stannic oxide, although more active than antimony tetroxide, was much less selective towards the formation of aldehydes. Similarly, Wakabayashi et al.[81], studying stannic oxide and antimony pentoxide calcined at 1273 K, observed that pure stannic oxide yielded mainly carbon dioxide and carbon monoxide, but that antimony pentoxide produced only trace amounts of product.

Seiyama et al.[82] and Fattore et al.[83] studying propylene oxidation in the presence and absence of gaseous oxygen respectively, classified the oxides according to product formation. Seiyama et al.[82] regarded antimony tetroxide as an acrolein former and stannic oxide as a benzene or 1,5-hexadiene former. They[82] believed that the difference in product formation was due to the electronegativity of the metal ion. However, antimony tetroxide was found to be selective for 1,5-hexadiene formation by Fattore et al.[83]. They believed that oxidation with antimony tetroxide was due only to surface oxygen, but oxygen diffusion

from the bulk to the surface was thought to take place with stannic oxide.

There is considerable support for the view that a redox mechanism operates with the tin-antimony mixed oxides. However, there are varying ideas as to the nature of the cations involved.

Godin et al.[23], by the use of isotopic labelled propylene, studied acrolein formation over a range of tin-antimony mixed oxides and concluded that a π-allyl species was involved. They postulated a redox mechanism, similar to the one proposed by Batist et al.[84] for bismuth-molybdate catalysts.

$$C_3H_6 + A.V. + O^{2-} \rightarrow C_3H_5^- + OH^- \quad) \quad (1)$$
$$Sb^{5+} + C_3H_5^- \rightarrow (C_3H_5....Sb)^{4+} \quad)$$

$$(C_3H_5....Sb)^{4+} + 2O^{2-} \rightarrow C_3H_4O + Sb^{3+} + OH^- + 2e + 2A.V. \quad (2)$$

$$2OH^- \rightarrow O^{2-} + A.V. + H_2O \quad (3)$$

$$\tfrac{1}{2}O_2 + Sb^{3+} + A.V. \rightarrow O^{2-} + Sb^{5+} \quad (4)$$

$$\tfrac{1}{2}O_2 + 2e + A.V. \rightarrow O^{2-} \quad (5)$$

$(C_3H_5....Sb)^{4+}$ represents an allyl anion π-bonded to Sb^{5+} and A.V. is an anion vacancy.

The site of propylene oxidation was believed to be an Sb^{5+} ion surrounded by oxygen ions in octahedral coordination. Reaction (2) was probably a two step process, with hydrogen abstraction from the allyl anion, before introduction of the oxygen atom. The possibility that both cations participate in the redox mechanism over bismuth-molybdate was proposed by Batist et al.[84] and also by Peacock et al.[85]. A similar mechanism for tin-antimony mixed oxides was postulated by Crozat and Germain[80]. They[80] believed that the roles of the tin and antimony cationswere analogous to those of the bismuth and molybdenum cations, respectively. The following mechanism was put forward:-

$$CH_3—CH=CH_2 \rightarrow CH_2—CH—CH_2$$
$$\downarrow \qquad\qquad \downarrow$$
$$O^{2-}Sb^{5+} \rightarrow O^{-}HSb^{5+} + e$$
$$Sn^{4+} + e \rightarrow Sn^{3+}$$
$$2O^{-}H \rightarrow O^{2-} + H_2O$$

In accordance with Godin et al.[23] the Sb^{5+} cations were the centres for the adsorption of propylene. The cations Sn^{4+}, Sn^{3+} were the centres for the adsorption and activation of the oxygen. Reoxidization of the catalyst occurred at the tin cations.

$$Sn^{3+} \rightarrow Sn^{4+} + e$$
$$\tfrac{1}{2}O_2 + e \rightarrow O^{-}$$
$$O^{-} + e \rightarrow O^{2-}$$

Wakabayashi et al.[25] also believed that the antimony cations may have been the centres for propylene adsorption. They concluded that the formation of acrolein involved O^{-} species formed from oxygen and carbon dioxide formation was associated with lattice oxygen, (O^{2-} species).

Godin et al.[23], Lazukin et al.[24], Wakabayashi et al.[25], all noted that the selectivity for acrolein formation remained fairly constant, if a saturated solid solution of antimony oxide in stannic oxide was present. Lazukin et al.[24] believed that the catalytic properties of the tin-antimony mixed oxides were determined by the saturated solid solution. Calculations carried out by Lazukin et al.[24] led them to conclude that the saturated solid solution occupied a constant fraction of the tin-antimony mixed oxide area.

6.3 Oxidative Dehydrogenation of n-Butenes with Tin-Antimony Oxide Catalysts

A number of investigators have observed that n-butene isomerization tends to accompany n-butene dehydrogenation over tin-antimony oxide catalysts.

Sekushova et al.[86] noted that stannic oxide and antimony tetroxide were very unreactive for the oxidative dehydrogenation of C_4:C_5 olefin mixtures. Antimony tetroxide was found to be less active than stannic oxide. Trifirò et al.[69] reported that antimony tetroxide was less active but more selective than stannic oxide. On the other hand, Sala and Trifirò[73], studying a range of antimony oxides, observed that only antimony pentoxide was active and that stannic oxide showed very little activity. They[73] attributed the oxidizing properties of stannic oxide to the presence of free electrons. The oxidizing properties of antimony pentoxide were thought to be due to the presence of antimony-oxygen double bonds and/or surface defects.

Trimm and Gabbay[87], studying a tin-antimony mixed oxide, (atomic ratio Sn:Sb = 1:4), proposed the following mechanism:

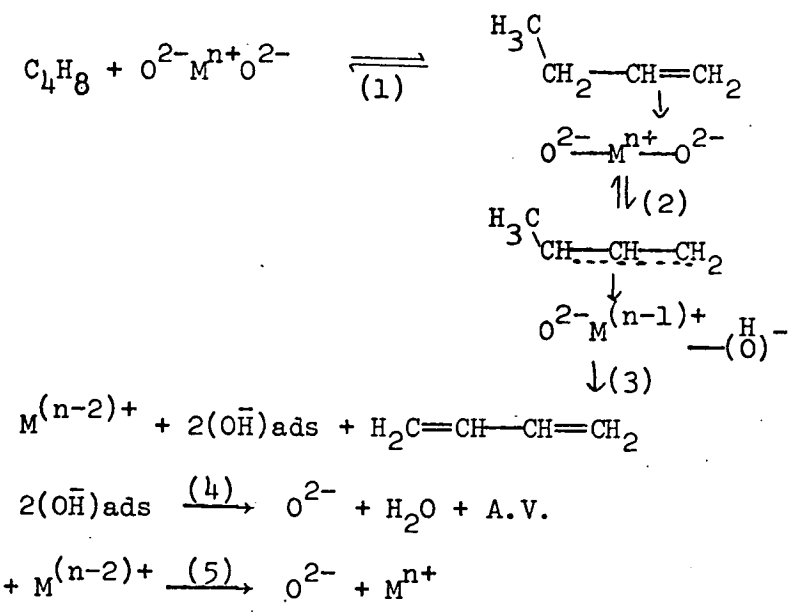

Trimm and Gabbay[87] believed that step (2) was the rate-determining one and that the reaction took place primarily over the Sn^{4+} ions. However, the possibility that the antimony oxides may have been involved in the abstraction of allylic hydrogens was not excluded.

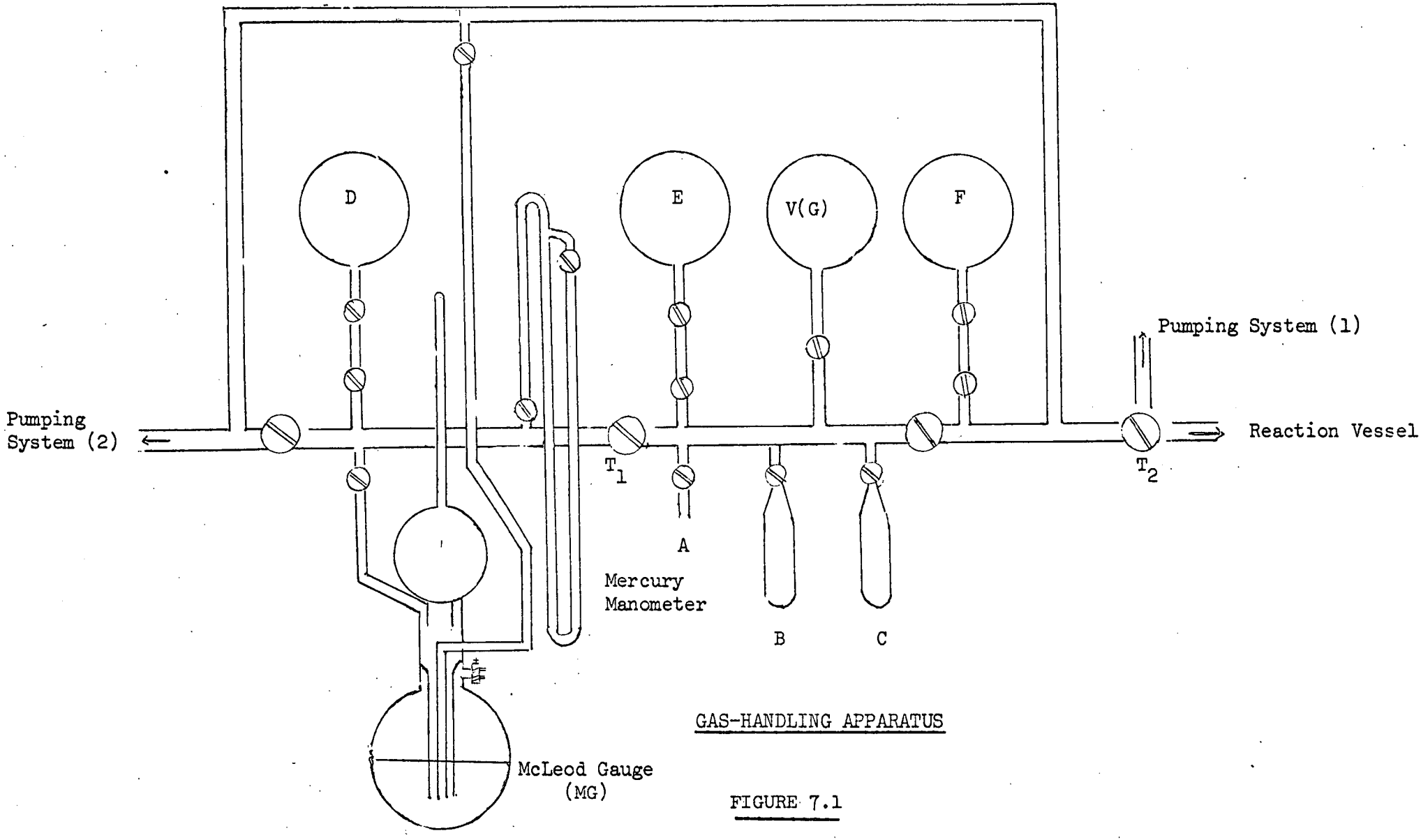

GAS-HANDLING APPARATUS

FIGURE 7.1

CHAPTER 7

Experimental

The apparatus used to study reactions on tin-antimony oxides consisted of a gas-handling apparatus, demontable reaction vessel, and a gas chromatography analysis system.

7.1 Gas-Handling Apparatus

A diagram of the gas-handling apparatus is shown in Figure 7.1. The line was constructed throughout of "Pyrex" glass. All the ground glass joints and taps were lubricated with "Apiezon L" high vacuum grease. Evacuation of the apparatus to a pressure of 133 $\mu N\ m^{-2}$ (10^{-6} Torr) was obtained by two pumping systems. Each system consisted of an electrically heated mercury diffusion pump, backed by a two stage "Edwards Speedivac" rotary pump. Mercury contamination from the former was prevented by an adjacent liquid nitrogen cooled trap. One system (1) was used exclusively for pumping the reaction vessel, while the other system (2) pumped the remainder of the apparatus. High vacuum pressure measurements were made with the McLeod gauge 'MG', the calibration and operation of which have been described by Leck[88]. Retention of a pressure of 133 $\mu N\ m^{-2}$ (10^{-6} Torr), during evacuation, was ensured by regular maintenance of the rotary pumps, cleaning of the cold traps and avoidance of 'streaking' in the tap grease. All the reagents were introduced into the gas-handling apparatus at A. Gaseous reactants were stored in bulbs D, E and F, and liquid reactants in demontable

sample vessels at B and C. Purification of each reactant was carried out before storage.

7.2 Purification Procedure

Purification and storage of the reactants was only attempted when the McLeod gauge indicated a pressure of 133 μN m^{-2} (10^{-6} Torr) in the gas-handling apparatus. The procedure involved the degassing of the reactant sample by a repeated cycle of freezing, pumping and thawing with the aid of liquid nitrogen cooled traps at B and C. On the final distillation step, only the middle third of the frozen reactant sample was used for storage purposes. The other two thirds were released to the pumps. This ensured the highest possible purity for the reactant sample. This procedure was also carried out with the reagents used to obtain the relative sensitivity factors (Section 7.8). At the start of each experiment the reagents were further purified by a single cycle of freezing, pumping and thawing.

7.3 Volume Calibrations

Successive expansions into the evacuated, uncalibrated sections of the gas-handling apparatus of volume Vi were made from a bulb of known volume V(G), filled with a measured pressure of gas P. The reduced pressure Pi obtained on each expansion step was measured by the mercury manometer. Boyle's Law ($PV = Pi(Vi+V)$) was then applied in each case to calculate the unknown volume. The values obtained in this way at 298 K were:-

dosing volume T_1 to T_2 = 1.06×10^{-4} m^3

reaction volume + reaction vessel 1 = 2.69×10^{-4} m^3

reaction volume + reaction vessel 2 = 2.76×10^{-4} m^3

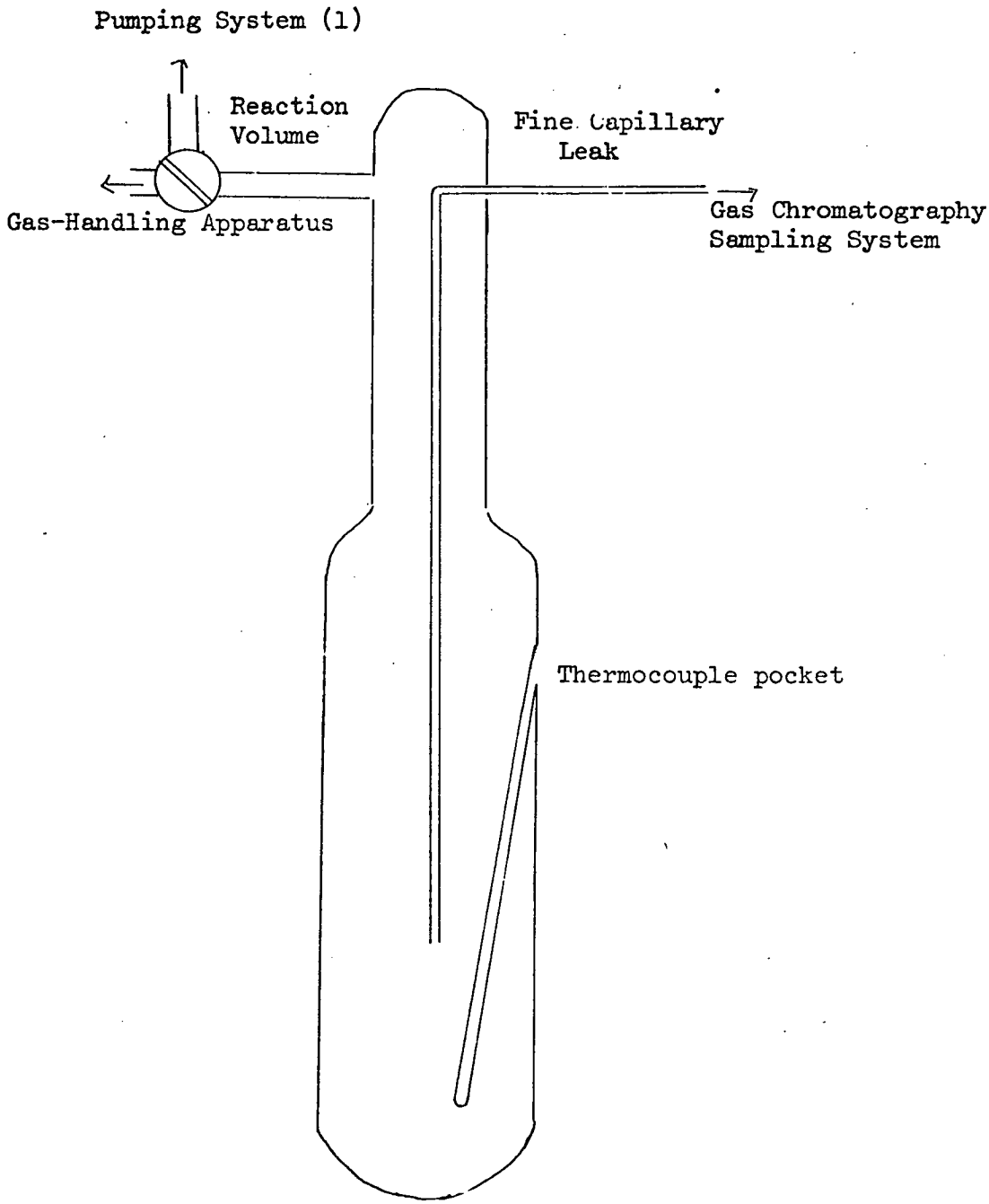

REACTION VESSEL

FIGURE 7.2

Unless otherwise stated reaction vessel 1 was used for all the reactions carried out in Chapter 8 and reaction vessel 2 was employed for the reactions given in Chapter 9 and Chapter 11.

7.4 Reaction Vessel

The reaction vessel shown in Figure 7.2, was made of "Pyrex" glass. The cone of the reaction vessel was attached to the gas-handling apparatus at a B24 water-cooled socket by means of a "Viton" o-ring. The 'greaseless' connection and the water-cooled socket ensured that grease contamination of the sample was minimized. A short side arm, sealed to the B24 socket, connected one side of the reaction vessel to a three-way ground glass T-tap. One limb of this tap connected with the gas-handling apparatus, the other limb with the pumping system. The other side of the reaction vessel was connected to the gas chromatography sampling system, by means of a 0.5 mm bore capillary tube which passed through the B24 socket and terminated in the centre of the reaction vessel.

Heat was supplied externally to the reaction vessel by a close-fitting electric furnace. The furnace temperature was kept to within $\pm$0.5 K of the desired value by a "Eurotherm" proportional controller and a chromel-alumel thermocouple. The temperature of the sample was monitored with a second thermocouple and a digital voltmeter. One junction of the thermocouple was located in the thermocouple well of the reaction vessel, Figure 7.2, and the other junction in ice at 273 K. The digital voltmeter readings were converted to temperatures by use of a chromel-alumel thermocouple calibration chart[89].

SAMPLING SYSTEM

FIGURE 7.3

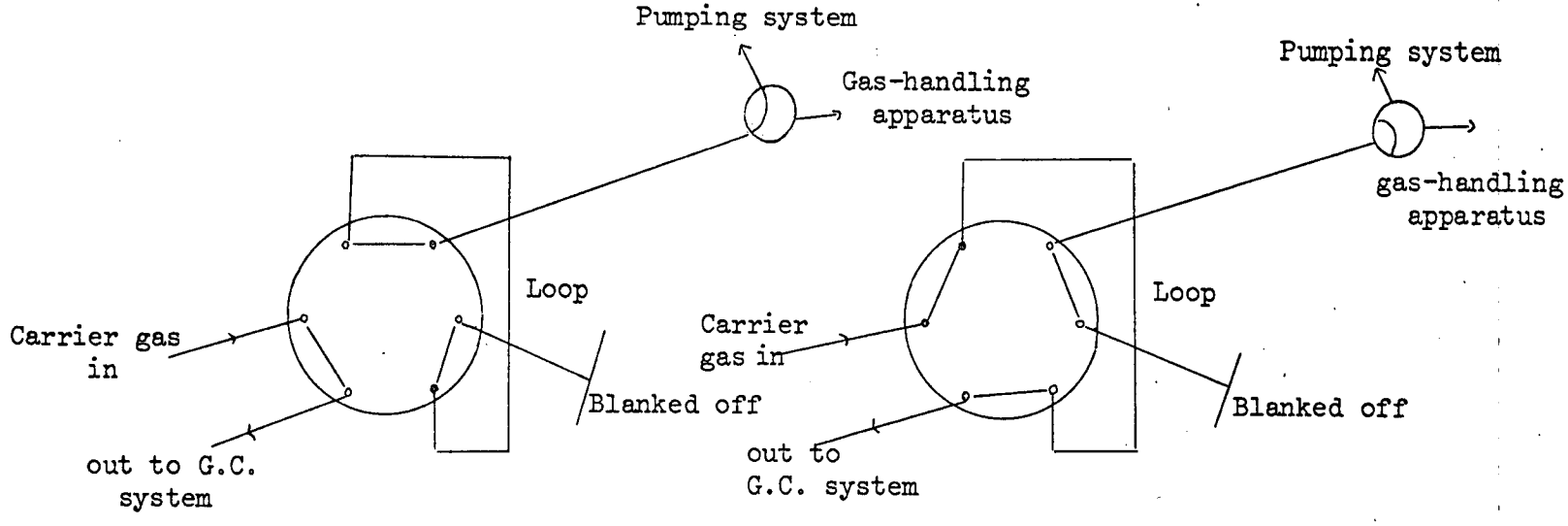

POSITION 1

POSITION 2

7.5 Experimental Procedure

At the end of the outgassing period, a pressure of 133 μN m^{-2} (10^{-6} Torr) was obtained in the gas-handling apparatus and reaction vessel. After purification, the pressure of reactant required to give the desired pressure in the reaction vessel was admitted to the dosing volume (T_1 to T_2). With the temperature of the reaction vessel at the required value, tap T_2 was opened for a period of 10 seconds to allow the reactant to expand into the reaction vessel. At the end of 10 seconds, tap T_2 was immediately closed, in order to isolate the reaction vessel from the gas-handling apparatus and timing of the reaction commenced.

7.6 Gas Chromatography Sampling System

A diagram of the gas chromatography sampling system is shown in Figure 7.3. The steps involved in the sampling procedure were as follows:-

i) Before taking a sample, the three-way Y-tap and the sampling valve (position 1) were set such that the loop could be evacuated by the pumping system.

ii) The three-way Y-tap was turned through 120° to link the reaction vessel and the loop for a period of 10 seconds. The first sample of the gas phase was discarded, by turning the three-way Y-tap back through 120°. This procedure was adopted to ensure that the gas phase in the connecting capillary was, as nearly as possible, representative of the gas phase in the reaction vessel. After a period of 10 seconds, the sampling procedure was repeated.

iii) The three-way Y-tap was then closed by turning it approximately 60^{o} to a neutral position. At the same time, the sampling valve was rotated to position 2, in order to seal the loop from the gas-handling apparatus and link it to the carrier gas supply. It was kept in position 2 for a period of 30 seconds, to allow the contents of the loop to be flushed by the carrier gas into the gas chromatography column.

iv) Finally, both the three-way Y-tap and the sampling valve were returned to their original positions to allow re-evacuation of the sampling system in readiness for the next sample.

Calibrations at 298 K, showed that each sample resulted in the removal of 0.5% of the reaction vessel's contents.

7.7 Gas Chromatography Detection System

The gas phase sample was flushed by nitrogen carrier gas into a "Perkin-Elmer F11" gas chromatograph. The chromatograph employed the appropriate packed column to enable separation of each component in the sample mixture. Type and operating conditions of the columns will be described at the beginning of the appropriate sections.

The whole effluent from the column was passed through a "Perkin-Elmer" flame ionization detector. The detector flame was fed by hydrogen and air at pressures of 120 kN m^{-2} and 170 kN m^{-2}, respectively. The ionization current produced by combustion of each hydrocarbon was amplified and displayed in peak form on a "Servoscribe" potentiometric recorder. The recorder was coupled

in parallel with a "Hewlett Packard" digital integrator. This model simultaneously provided a printed output of the hydrocarbon peak area and the retention time at which the maximum peak height appeared on the recorder. Product identification was achieved by comparing sample retention times with those of known samples.

7.8 Relative Sensitivity Factors

To determine the relative sensitivities of the chromatograph to a reactant and its products, a sample from the reaction vessel containing the species in equal pressures, was passed through the chromatograph. The integrated peak areas produced were noted. Setting the sensitivity factor of the reactant to unity, the relative sensitivities of the products were obtained by division of the reactant's integrated peak area with the product's peak area.

7.9 Treatment of Experimental Results

Two conditions had to be satisfied before a series of results was considered valid.

i) A blank run with the reactant, in the absence of the catalyst, must have been carried out. The standard experimental procedure for the reactant was used and a gas phase sample analysed. The walls of the reaction vessel had no catalytic activity, if only the reactant was detected.

ii) Catalysts which showed no activity, were only considered to be inactive if, on repeating the experiment with a fresh sample, no product formation was seen during a period of 4 hr.

For each sample, obtained during an experiment, the integrated peak areas of the products were multiplied by the appropriate relative sensitivity factors.

All the reactions carried out for this thesis appeared not to conform very closely to either zero order or first order kinetics. All the reactions took place in two stages, an initial 'fast' stage S_1 and a subsequent 'slower' stage S_2. Percentage composition versus time plots, were used throughout to give an indication of catalytic activity. This was obtained by measuring either the rate of disappearance of the reactant or the rate of appearance of the product, during stages S_1 and S_2, by drawing the best straight line through the relevant points. Typical examples are given in Figures 8.1 and 8.2. The rate values, with their appropriate subscripts, were represented by R_1 and R_2 corresponding to S_1 and S_2. Unless otherwise stated the units of R_1 and R_2 are 10^{-3} % min^{-1} m^{-2}. Two similar activity patterns could be obtained by plotting the values of R_1 or R_2, found for any given reaction, against catalyst composition. Thus, only R_1 values are used in the construction of activity patterns.

Great care had to be taken in the choice of the experimental conditions, to ensure maximum reliability. The conditions had to be such that sufficient number of samples could be taken during stages S_1 and S_2. An indication of the reproducibility in the rate values was obtained from repeat experiments.

Selectivity for product formation, at given times during stages S_1 and S_2, was obtained by dividing the percentage composition of the product by the percentage composition of reactant used. The values are represented by Se_1 and Se_2, in units of %.

The values of R_1 and R_2 at various temperatures were found and the values of $\log_{10} R_1$ or $\log_{10} R_2$ plotted against 10^3 K/T in order to obtain the activation energy (E) from the Arrhenius equation,

$$\log_{10} R_{1,2} = \log_{10} A - E / 2.303 RT.$$

7.10 Catalysts

All the catalysts used in this work were supplied by the B.P. Co. Ltd. They were prepared and analysed by the following procedures.

The materials used in the catalyst preparations were "Fry"s pure powdered tin and pure powdered antimony from "Associated Lead". All the reagents used in the preparations were of 'Analar' grade. A representative number of tin-antimony catalysts were prepared by taking different proportions from two large batches of precipitated tin oxide and antimony oxide. Each composition was then thoroughly mixed, washed, dried, pelleted and heat treated.

Preparation of Stannic Oxide

1.450 kg of "Fry"s pure powdered tin was added over a period of 50 minutes to a mixture of 5.46 dm^3 HNO_3 and 18.32 dm^3 water at 373 K, while stirring. The mixture was maintained at 373 K for a further 30 minutes then cooled. The white gelatinous precipitate of tin oxide was filtered off and thoroughly washed with distilled water, prior to storage under water.

Preparation of Antimony Oxide

692.2 g of pure powdered antimony ("Associated Lead") was added over a period of 50 minutes to 2.85 dm^3 HNO_3 at 373 K, while

stirring. The mixture was maintained at 373 K for a further 30 minutes and was then cooled. The pale yellow precipitate of antimony oxide was filtered off and thoroughly washed with distilled water, prior to storage under water.

Preparation of Tin-Antimony Mixed Oxides

Various proportions of the above two wet precipitates were taken to give the required mixtures. The combined precipitates were thoroughly mixed in the form of a slurry, filtered off, washed with 3 dm^3 distilled water, dried overnight at 383 K and finally ground so as to pass a 100 mesh sieve.

Pelleting

Each composition was mixed with 1% w./w. graphite ("Avarc Pure Flake No. 3") as a lubricant before pelleting.

Heat Treatment

The pellets were then treated in air at 1123 K in stainless steel baskets. The heat treatment programme consisted of a temperature rise from room temperature to 1123 K at a rate of 20 K hr^{-1} followed by a heat soak at 1123 K for 16 hr. After that time the pellets were slowly cooled to room temperature.

Analysis

X-ray fluorescence analysis, for tin and antimony, was carried out on samples of the heat treated pellets. Debye-Scherrer X-ray powder photographs showed that the heat treated samples were heterogeneous, and consisted of:- SnO_2, αSb_2O_4, and minor amounts of βSb_2O_4.

Surface Area

Surface areas, of the heat treated catalysts, were measured by the standard BET method[90] using nitrogen as adsorbate.

The analysis and surface area results of the catalysts used, are shown in Table 7.1.

TABLE 7.1

X-ray fluorescence analysis of H.Tr. pellets Cat.Comp./Atom % Sb	Surface area/$m^2\ g^{-1}$	Colour
0	4.2	white
3.3	9.9	blue-grey
6.13	12.2	blue-grey
6.2	16.4	blue-grey
7.4	18.1	blue-grey
8.7	17.9	dark blue-grey
19.6	20.8	dark grey
26.8	18.4	grey
49.5	12.5	light grey
75.0	7.0	light grey
100	0.9	white

Atom % Sb = atomic ratio $\frac{Sb}{Sb+Sn}$ x 100

H.Tr. = heat treated

Cat.Comp. = catalyst composition.

7.11 Pretreatment of Catalysts

A fresh finely grounded sample was used for each experiment. Two different methods for pretreating the samples were used.

A) The Low Temperature (L.T.) Series

Accurately weighed samples, of ∿0.2 g for the tin-antimony mixed oxides and ∿0.5 g for stannic oxide and antimony tetroxide, were outgassed for 5 hr at a temperature of 293 K.

B) The High Temperature (H.T.) Series

Accurately weighed samples, of ∿0.2 g for the tin-antimony mixed oxides and ∿0.5 g for stannic oxide and antimony tetroxide, were outgassed for 16 hr at a temperature of 698 K.

At the end of the outgassing period, the sample was isolated from the pumping system at a pressure of 133 $\mu N\ m^{-2}$ (10^{-6} Torr). The reactant was then admitted into the reaction vessel, as described in Section 7.5. The pressure and number of molecules present in the reaction vessel will be stated in the appropriate sections.

Chemicals

The source and purity of reactants, and reagents used in the determination of sensitivity factors or for pretreatment experiments, are given in Tables 7.2, 7.3 and 7.4, respectively.

TABLE 7.2

Reactants	Source	Purity
3,3-dimethylbut-1-ene	Koch-Light	purum
isopropanol	Fluka	purum
cyclopropane	British Oxygen Co.	99.5%
but-1-ene	Cambrian Chemicals Ltd.	99.5%
cis but-2-ene	Cambrian Chemicals Ltd.	99.5%
trans but-2-ene	Cambrian Chemicals Ltd.	99.5%

TABLE 7.3

Reagents	Source	Purity
2,3-dimethylbut-1-ene	Fluka	purum
2,3-dimethylbut-2-ene	Fluka	purum
di-isopropyl ether	Fisons	research grade
acetone	A.H. Baird	research grade
propylene	Cambrian Chemicals Ltd.	99.5%
butadiene	Cambrian Chemicals Ltd.	99.5%

TABLE 7.4

Reagents	Source	Purity
pyridine	B.D.H. Chemicals Ltd.	analar
2,6-dimethylpyridine	B.D.H. Chemicals Ltd.	analar

CHAPTER 8

Isomerization of 3,3-Dimethylbut-1-ene

8.1 Chromatographic Column

Separation of the products formed during 3,3-dimethylbut-1-ene isomerization, was carried out using a "Perkin-Elmer" stainless steel column. The column, of length 2 m and internal diameter 3 mm, was packed with 35% propylene carbonate on 'Chromosorb P'. Good separation of products and reactant was achieved by operating the column at a temperature of 293 K and a nitrogen carrier gas pressure of 40 kN m^{-2}. The following retention times, measured according to Section 7.7, were obtained:-

3,3-dimethylbut-1-ene = 2.0 min

2,3-dimethylbut-1-ene = 5.1 min

2,3-dimethylbut-2-ene = 8.0 min.

8.2 Relative Sensitivity Factors

Measured according to Section 7.8

3,3-dimethylbut-1-ene = 1.0

2,3-dimethylbut-1-ene = 0.8

2,3-dimethylbut-2-ene = 0.8.

8.3 Experimental Procedure

The two methods of pretreating the catalysts were carried out as described in Section 7.11, with a modification in the pretreatment of the H.T. series. A weight of ∿1 g, for the tin-antimony mixed oxides, was used instead of ∿0.2 g. At the end of the outgassing period, the

3,3-DIMETHYLBUT-1-ENE ISOMERIZATION

373 K

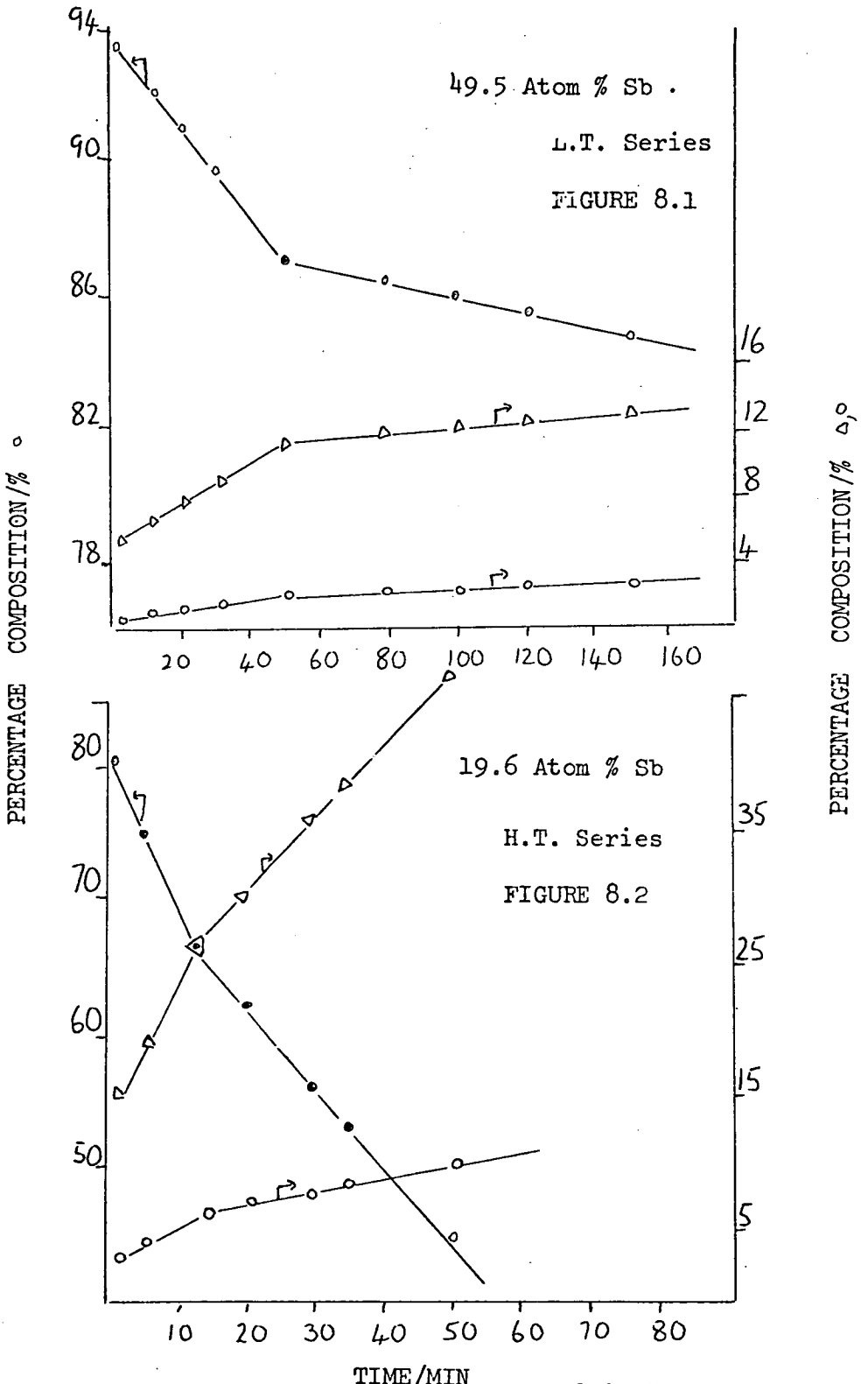

∘ 3,3-DIMETHYLBUT-1-ENE

△ 2,3-DIMETHYLBUT-2-ENE

∘ 2,3-DIMETHYLBUT-1-ENE

sample was isolated from the pumping system at a pressure of 133 μN m^{-2} (10^{-6} Torr). With the reaction vessel at a temperature of 373 K, 3,3-dimethylbut-1-ene was admitted by expansion to give a pressure of 1.60 kN m^{-2} (12 Torr). This was equivalent to 8.37×10^{19} molecules. Standard experimental procedure was then carried out.

8.4 Results

Figures 8.1 and 8.2 illustrate typical plots of percentage composition versus time, for the L.T. and the H.T. series, respectively. The only products formed were 2,3-dimethylbut-1-ene and 2,3-dimethylbut-2-ene. In all cases, there was preferential formation of 2,3-dimethylbut-2-ene and the selectivity remained effectively constant throughout stages S_1 and S_2. The selectivities are presented in Tables 8.1 and 8.2.

TABLE 8.1

L.T. Series Outgassed at 293 K for 5 hr

Reaction Temperature 373 K

Cat.Comp./ Atom % Sb	Se_1/% at 10 min		Se_2/% at 50 min	
	I	II	I	II
8.7	18	82	17	83
19.6	16	84	17	83
26.8	18	82	17	83
49.5	18	82	15	85
75.0	18	82	14	86

TABLE 8.2

H.T. Series Outgassed at 698 K for 16 hr

Reaction Temperature 373 K

Cat.Comp./ Atom % Sb	Se_1/% at 10 min		Se_2/% at 50 min	
	I	II	I	II
8.2	16	84	17	83
19.6	20	80	18	82
26.8	17	83	17	83
49.5	18	82	17	83
75.0	22	78	18	82

I = 2,3-dimethylbut-1-ene

II = 2,3-dimethylbut-2-ene

The rates of disappearance R_1 and R_2 for 3,3-dimethylbut-1-ene are presented in Tables 8.3 and 8.4

TABLE 8.3

L.T. Series Outgassed at 293 K for 5 hr

Reaction Temperature 373 K

Cat.Comp./ Atom % Sb	$R_1/10^{-3}$ % min^{-1} m^{-2}	$R_2/10^{-3}$ % min^{-1} m^{-2}
0	0	0
6.2	0	0
8.7	16	2.6
19.6	21	8.1
26.8	51	11
49.5	57	13
75.0	50	11
100	0	0

TABLE 8.4

H.T. Series Outgassed at 698 K for 16 hr

Reaction Temperature 373 K

Cat.Comp./ Atom % Sb	$R_1/10^{-3}$ % min m^{-2}	$R_2/10^{-3}$ % min^{-1} m^{-2}
0	0	0
6.2	0	0
8.7	18	5.8
19.6	64	15
26.8	190	62
49.5	145	39
75.0	159	43
100	0	0

For both the L.T. series and the H.T. series, no activity was observed with stannic oxide, antimony tetroxide and the 6.2 atom % Sb mixed oxide. Further experiments, in which the reaction temperature was increased, during the runs, from 373 K to 573 K were carried out for all three catalysts. Increasing the temperature did not result in any product formation.

Repeat experiments indicated an average difference of 5% in the rate values. Results of repeat experiments are presented in Table 8.5.

3,3-DIMETHYLBUT-1-ENE ISOMERIZATION ACTIVITY PATTERNS
373 K

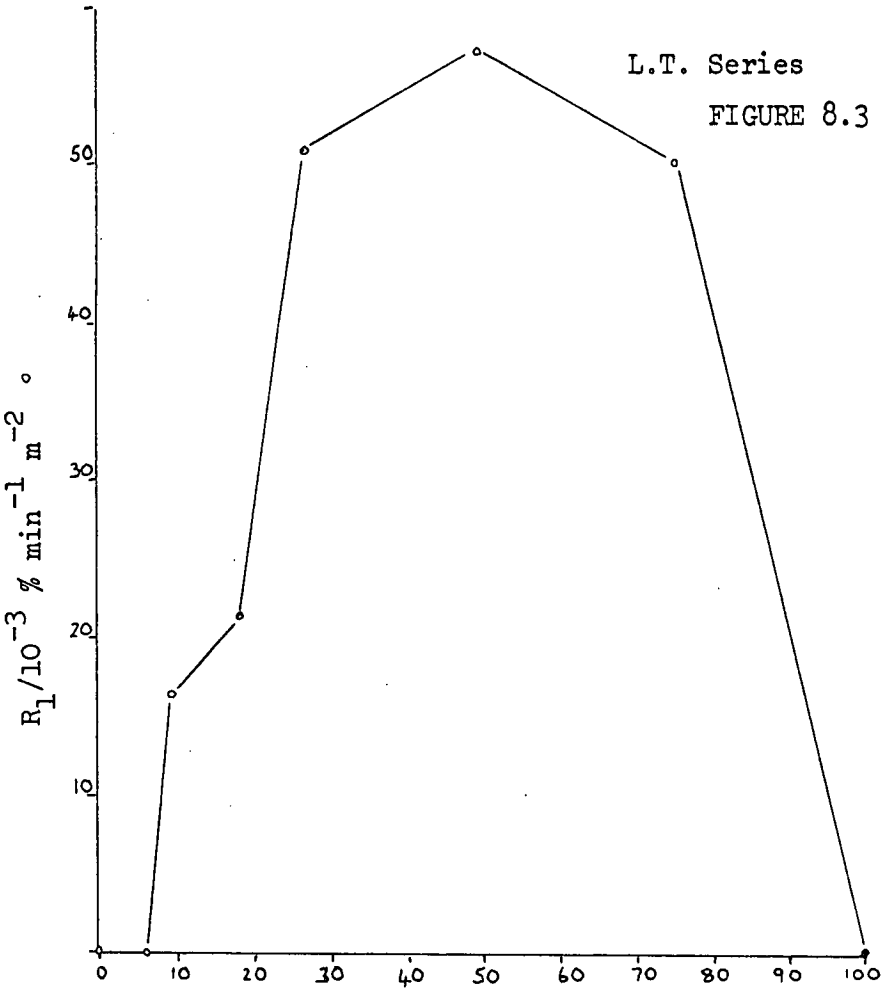

FIGURE 8.3

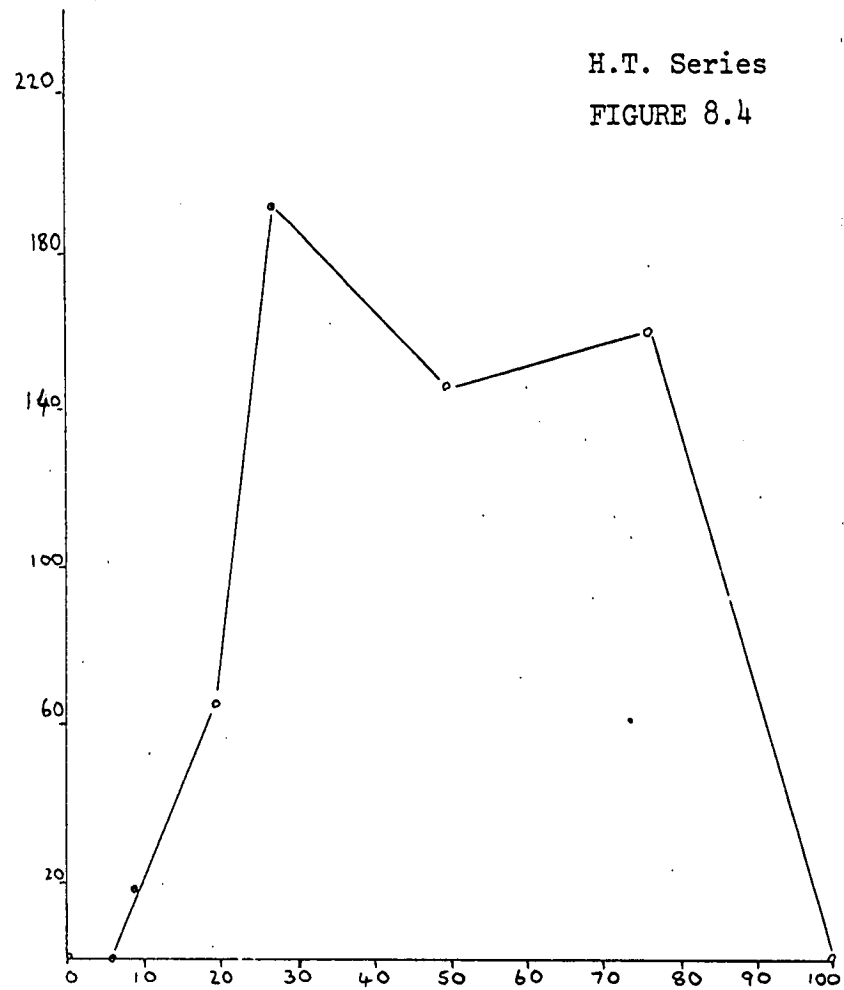

FIGURE 8.4

CAT.COMP./ATOM % Sb

TABLE 8.5

H.T. Series Outgassed at 698 K for 16 hr

Reaction Temperature 373 K

Cat.Comp./ Atom % Sb	$R_1/10^{-3}$ % min^{-1} m^{-2}	$R_2/10^{-3}$ % min^{-1} m^{-2}
19.6*	64	15
19.6	60	14
19.6	64	14

Values* quoted in Table 8.4

Changes of greater than ±5% in the activity patterns were considered significant. The activity patterns, illustrated in Figures 8.3 and 8.4, for the L.T. and H.T. series respectively, were found to differ. Maximum activity was observed with the 49.5 atom % Sb and 26.8 atom % Sb mixed oxides for the L.T. and H.T. series, respectively. Both series displayed similar trends in the catalyst composition region of 8.7 atom % Sb to 26.8 atom % Sb. In this region, an increase in the antimony content resulted in an increase in activity. Two different trends were observed for the catalyst composition region of 26.8 atom % Sb to 75.0 atom % Sb. No decrease in the activity of the L.T. series was seen until the catalyst composition of 75.0 atom % Sb. The 49.5 atom % Sb mixed oxide of the H.T. series, was found to be less active than the 26.8 atom % Sb and 75.0 atom % Sb mixed oxides.

An experiment was carried out using a 49.5 atom % Sb mixed oxide sample of ∿0.2 g, which had been pretreated according to the H.T. method. The rate values obtained are presented in Table 8.6.

3,3-DIMETHYLBUT-1-ENE ISOMERIZATION
ARRHENIUS PLOTS

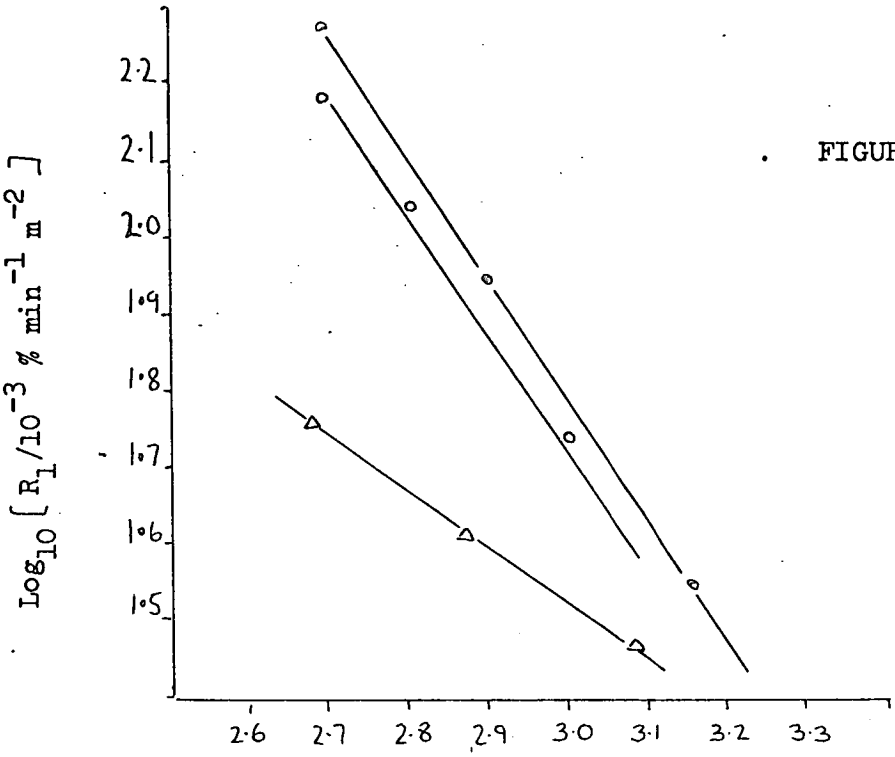

FIGURE 8.5

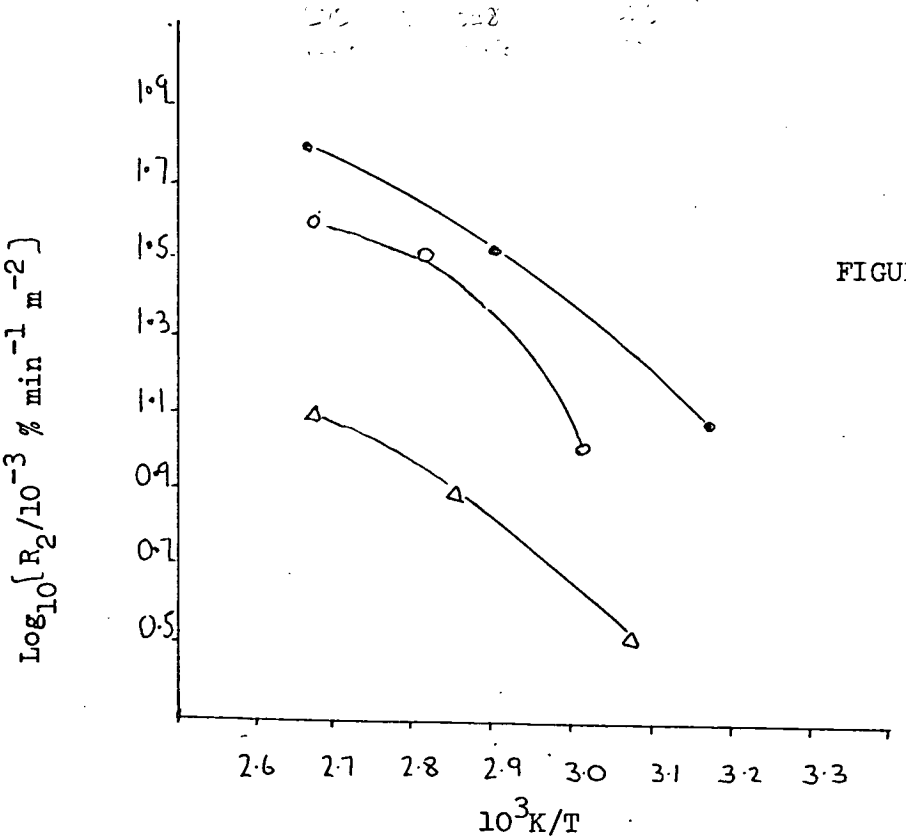

FIGURE 8.6

L.T. Series

△ 49.5 Atom % Sb

H.T. Series

○ 26.8 Atom % Sb
○ 75.0 Atom % Sb

TABLE 8.6

H.T. Series Outgassed at 698 K for 16 hr

Reaction Temperature 373 K

Cat.Comp./ Atom % Sb	$R_1/10^{-3}$ % min^{-1} m^{-2}	$R_2/10^{-3}$ % min^{-1} m^{-2}
49.5*	145	39
49.5	147	40

Values* quoted in Table 8.4 for the ∿1 g sample

The values for the ∿0.2 sample were not significantly different than those of the 1 g sample.

Arrhenius plots, obtained using R_1 and R_2, are shown in Figures 8.5 and 8.6. Values for activation energies and frequency factors could be estimated only from Arrhenius plots in which R_1 values had been used. These values, and the estimated error in them, are given in Tables 8.7 and 8.8.

Arrhenius Parameters

TABLE 8.7

L.T. Series Outgassed at 273 K for 5 hr

Cat.Comp./ Atom % Sb	E/kJ mol^{-1}	$\log_{10}$ ($A/10^{-3}$ % min^{-1} m^{-2})
49.5	15±2	3.8±0.5

TABLE 8.8

H.T. Series Outgassed at 698 K for 16 hr

Cat.Comp./ Atom % Sb	E/kJ mol^{-1}	$\log_{10}$ ($A/10^{-3}$ % min^{-1} m^{-2})
26.8	30±2	6.5±0.4
75.0	27±2	6.0±0.4

R_2 values did not give straight line plots. The smaller activation energy was found for the sample pretreated according to the L.T. method.

8.5 Treatment with Sodium Acetate Solution

The effect of different concentrations of sodium acetate solutions on two mixed oxides of the H.T. series was studied.

Prior to outgassing, ∿1 g samples of the 19.6 atom % Sb and 26.8 atom % Sb mixed oxides were treated with equal quantities of either 1% (w./w.) sodium acetate solution or 10% (w./w.) sodium acetate solution. At the end of a period of 60 min., the samples were filtered off and then thoroughly washed with four equal proportions of distilled water. The standard H.T. pretreatment method was then carried out. Values for R_1, R_2 and Se_1, Se_2 are shown in Tables 8.9 and 8.10, respectively.

Sodium Acetate Treated Catalysts

H.T. Series Outgassed at 698 K for 16 hr

Reaction Temperature 373 K

TABLE 8.9

Cat.Comp./ Atom % Sb	$R_1/10^{-3}$ % min^{-1} m^{-2}	$R_2/10^{-3}$ % min^{-1} m^{-2}
19.6*	64	15
19.6[a]	60	12
19.6[b]	38	7.3
26.8*	190	62
26.8[b]	22	4.3

TABLE 8.10

Cat.Comp./ Atom % Sb	Se_1/% at 10 min		Se_2/% at 50 min	
	I	II	I	II
19.6*	20	80	18	82
19.6[a]	16	84	17	83
19.6[b]	19	81	18	82
26.8*	17	83	17	83
26.8[b]	19	81	18	82

*Values for untreated mixed oxides, Tables 8.2 and 8.4

I = 2,3-dimethylbut-1-ene

II = 2,3-dimethylbut-2-ene

a = 1% (w./w.) sodium acetate solution

b = 10% (w./w.) sodium acetate solution

Treatment reduced the values of R_1 and R_2, but did not significantly alter those of Se_1 and Se_2. A 10% (w./w.) sodium acetate solution had a greater retarding effect on the more active 26.8 atom % Sb mixed oxide than on the less active 19.6 atom % Sb mixed oxide.

Decomposition of Isopropanol

8.6 Chromatographic Column

Separation of the products formed during the dehydration and dehydrogenation of isopropanol, was carried out using a "Perkin-Elmer" stainless steel column. The column, of length 2 m and internal diameter 3 mm, was packed with 28% carbowax 1500 on 'Chromosorb W' AW/DMCS. Good separation of products and reactant was obtained by operating the column at a temperature of 338 K and a nitrogen carrier gas pressure of 100 kN m^{-2}. The following retention times, measured according to Section 7.7, were obtained:-

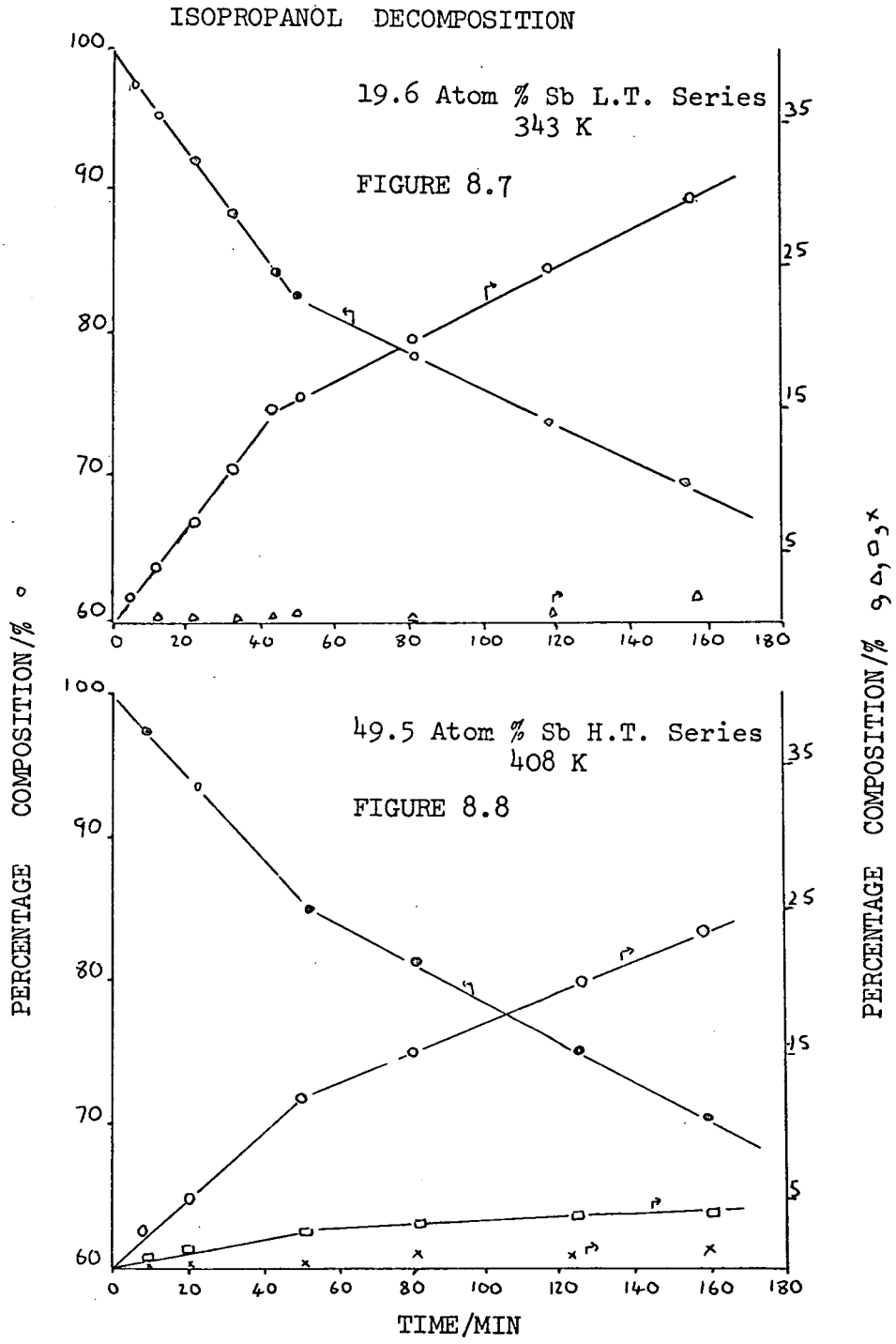
ISOPROPANOL DECOMPOSITION
19.6 Atom % Sb L.T. Series
343 K
FIGURE 8.7
49.5 Atom % Sb H.T. Series
408 K
FIGURE 8.8
PERCENTAGE COMPOSITION/% o
PERCENTAGE COMPOSITION/% δ, Δ, □, ×
TIME/MIN
δ Isopropanol
o Propylene
Δ Acetone+Di-isopropyl ether
□ Acetone
× Di-isopropyl ether

propylene = 0.5 min

di-isopropyl ether = 2.0 min

acetone = 4.0 min

isopropanol = 6.5 min

8.7 Relative Sensitivity Factors

Measured according to Section 7.8

isopropanol = 1.0

propylene = 1.09

di-isopropyl ether = 0.43

acetone = 1.13.

8.8 Experimental Procedure

The samples were pretreated according to the two methods described in Section 7.11. At the end of the outgassing period, the sample was isolated from the pumping system at a pressure of 133 μN m^{-2} (10^{-6} Torr). Once the reaction vessel was at the desired reaction temperature, isopropanol was admitted by expansion to give a pressure of 0.67 kN m^{-2} (5 Torr). This was equivalent to 3.80×10^{19} molecules, at a temperature of 343 K, for the L.T. series. For the H.T. series, the isopropanol pressure was equivalent to 3.20×10^{19} molecules at 408 K. The standard experimental procedure was then carried out.

8.9 Results

Products resulting from dehydration and dehydrogenation of isopropanol were observed. Dehydration resulted in the formation of propylene and di-isopropyl ether, and dehydrogenation led to the formation of acetone. Examples of typical percentage composition versus time plots are illustrated, for both series, in Figures 8.7

and 8.8. Such plots were used to obtain values for the rates of appearance of propylene R_{1P}, R_{2P} and the rates of appearance of acetone R_{1A}, R_{2A}. As di-isopropyl ether was formed in small amounts, it was not possible to obtain values for its rates of appearance.

Selectivity towards dehydrogenation and dehydration was found to vary with the percentage composition of the catalysts and with the method of pretreatment. This is illustrated in Tables 8.11 and 8.12.

TABLE 8.11

L.T. Series Outgassed at 293 K for 5 hr

Reaction Temperature 343 K

Cat.Comp./ Atom % Sb	Se_1/% at 10 min			Se_2/% at 50 min		
	P	A	DE	P	A	DE
7.4	100.0			89.5		10.5
8.7	87.5		12.5	90.5		9.5
19.6	97.7	0.2	2.1	96.0	0.6	3.4
26.8	90.1	2.2	7.7	94.6	0.5	4.9
49.5	93.5	2.6	3.9	95.3	0.9	3.8
75.0	96.2	0.3	3.5	95.8	0.7	3.5

TABLE 8.12

H.T. Series Outgassed at 698 K for 16 hr

Reaction Temperature 408 K

Cat.Comp./ Atom % Sb	Se_1/% at 10 min			Se_2/% at 50 min		
	P	A	DE	P	A	DE
0	9.8	90.2		6.9	93.1	
6.13	8.5	90.1	1.4	6.1	93.1	0.8
8.7	54.0	43.7	2.3	52.7	44.7	2.6
19.6	87.2	11.2	1.6	86.0	12.3	1.7
26.8	87.0	10.6	2.4	92.8	5.7	1.5
49.5	80.4	15.3	4.3	83.2	12.5	4.3
75.0	100.0			82.5	16.1	1.4

P = propylene

A = acetone

DE = di-isopropyl ether

The L.T. series was found to be very selective for propylene formation. Acetone, in trace amounts, was observed for the 19.6 atom % Sb, 26.8 atom % Sb, 49.5 atom % Sb and 75.0 atom % Sb mixed oxides. Slightly higher selectivity for di-isopropyl ether formation than for acetone formation was found. The selectivity never exceeded 12.5% and remained in general, for most of the mixed oxides, in the region of 2% to 5%. Except for the 7.4 atom % Sb mixed oxide, for which di-isopropyl ether formation occurred only during stage S_2, selectivity did not alter significantly with time.

The mixed oxides of the H.T. series were found to be more selective for acetone formation than the corresponding ones of the

L.T. series. Stannic oxide and the 6.13 atom % Sb mixed oxide were particularly selective, and a further increase in the antimony content resulted in a decrease in selectivity. Acetone selectivity for the 19.6 atom % Sb, 26.8 atom % Sb and 49.5 atom % Sb mixed oxides was found to be similar. Unlike the L.T. series, selectivity for acetone formation was greater than for di-isopropyl ether formation. Selectivity did not alter significantly with time, except for the 75.0 atom % Sb mixed oxide. This was due to the fact that acetone and di-isopropyl ether formation occurred only during stage S_2.

The rates of appearance of propylene, R_{1P} and R_{2P}, for both series are presented in Tables 8.13 and 8.14.

TABLE 8.13

L.T. Series Outgassed at 293 K for 5 hr

Reaction Temperature 343 K

Cat.Comp./ Atom % Sb	$R_{1P}/10^{-3}$ % min^{-1} m^{-2}	$R_{2P}/10^{-3}$ % min^{-1} m^{-2}
0	0	0
7.4	8.7	3.4
8.7	32	19
19.6	100	34
26.8	142	58
49.5	205	69
75.0	137	59
100	0	0

ISOPROPANOL DEHYDRATION ACTIVITY PATTERNS

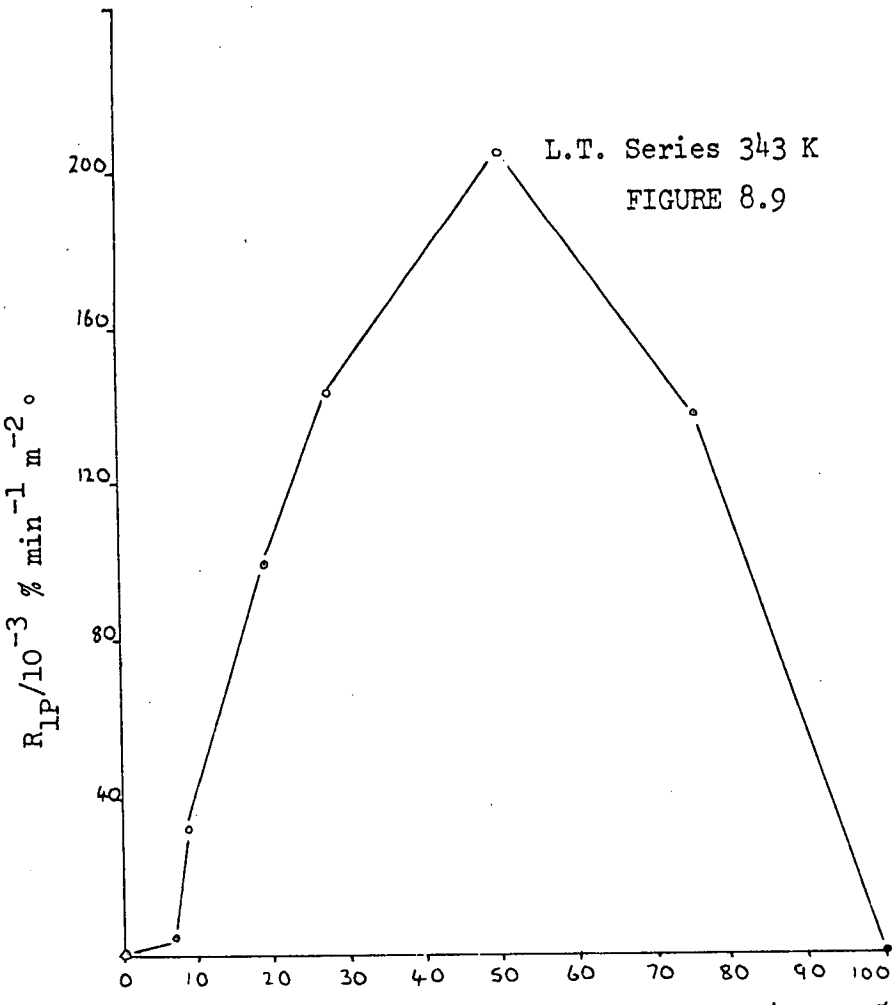

L.T. Series 343 K

FIGURE 8.9

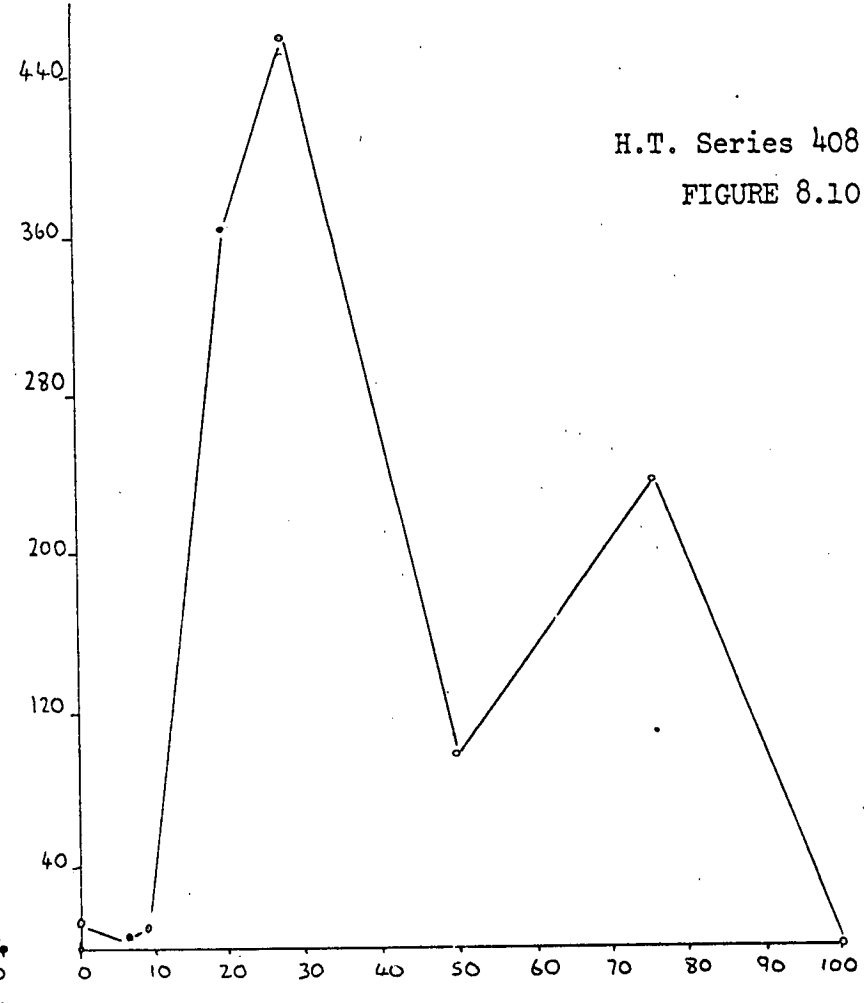

H.T. Series 408 K

FIGURE 8.10

TABLE 8.14

H.T. Series Outgassed at 698 K for 16 hr

Reaction Temperature 408 K

Cat.Comp./ Atom % Sb	$R_{1P}/10^{-3}$ % min^{-1} m^{-2}	$R_{2P}/10^{-3}$ % min^{-1} m^{-2}
0	12	2.6
6.13	7.0	2.0
8.7	9.2	2.4
19.6	367	107
26.8	460	179
49.5	99	49
75.0	238	92
100.0	0	0

The most suitable reaction temperatures were 343 K for the L.T. series and 408 K for the H.T. series. Isopropanol reacted very rapidly at 408 K over the mixed oxides of the L.T. series.

For example, the percentage of propylene, after 15 min. of reaction, was 92% for the 26.8 atom % Sb mixed oxide. The selectivities for the products formed at 10 min. were:- propylene 95.2%, acetone 4.0% and di-isopropyl ether 0.8%. These values are not significantly different from those quoted in Table 8.11, for the 26.8 atom % Sb mixed oxide of the L.T. series.

Activity patterns for propylene formation, for both series, are presented in Figures 8.9 and 8.10. Maximum propylene activity for the L.T. and H.T. series was found with the 49.5 atom % Sb and 26.8 atom % Sb mixed oxides, respectively. Figures 8.9 and 8.10 illustrate the different trends in the activity patterns for the two series. Activity increased in the catalyst composition region of 7.4 atom % Sb to

49.5 atom % Sb for the L.T. series. Increasing the antimony content further to give 75.0 atom % Sb resulted in a reduction in activity. For the H.T. series, activity increased in the catalyst composition region of 6.13 atom % Sb to 26.8 atom % Sb. Unlike the L.T. series, an increase in antimony content to give 49.5 atom % Sb resulted in a decrease in activity. The latter mixed oxide was also less active than the 75.0 atom % Sb mixed oxide for propylene formation. Antimony tetroxide was inactive for both series, but stannic oxide showed activity for the H.T. series.

The rates of acetone appearance, R_{1A}, R_{2A}, are presented in Table 8.15 for the H.T. series. Such values could not be measured for the mixed oxides of the L.T. series, as acetone was formed in trace amounts only.

TABLE 8.15

H.T. Series Outgassed at 698 K for 16 hr

Reaction Temperature 408 K

Cat.Comp./ Atom % Sb	$R_{1A}/10^{-3}$ % min^{-1} m^{-2}	$R_{2A}/10^{-3}$ % min^{-1} m^{-2}
0	147	63
6.13	91	25
8.7	55	19
19.6	45	16
26.8	21	6.8
49.5	18	4.8
75.0	0	15
100	0	0

Greater activity for acetone formation than for propylene formation was observed for stannic oxide, the 6.13 atom % Sb and 8.7 atom % Sb mixed oxides. The remainder of the mixed oxides exhibited a greater activity for propylene formation. Increasing the antimony content resulted in a decrease in acetone formation. An exception to this trend was displayed by the 75.0 atom % Sb mixed oxide, which formed acetone only during stage S_2.

An indication of the experimental reproducibility was obtained by repeat experiments. Values found for the rates of propylene and acetone appearance are given in Tables 8.16 and 8.17, respectively.

H.T. Series Outgassed at 698 K for 16 hr

Reaction Temperature 408 K

TABLE 8.16

Cat.Comp./ Atom % Sb	$R_{1P}/10^{-3}$ % min^{-1} m^{-2}	$R_{2P}/10^{-3}$ % min^{-1} m^{-2}
8.7*	9.2	2.4
8.7	8.6	2.2
26.8*	460	179
26.8	423	163

TABLE 8.17

Cat.Comp./ Atom % Sb	$R_{1A}/10^{-3}$ % min^{-1} m^{-2}	$R_{2A}/10^{-3}$ % min^{-1} m^{-2}
8.7*	55	19
8.7	50	17
26.8*	21	6.8
26.8	21	7.5

Values* quoted in Tables 8.14 and 8.15

R_{1P}, R_{2P} = rate of appearance of propylene

R_{1A}, R_{2A} = rate of appearance of acetone

Tables 8.16 and 8.17, indicate that the average difference in the rate values of R_{1P}, R_{2P} and R_{1A}, R_{2A} was 8%. Changes of greater than $\pm$8% in the activity patterns were considered to be significant.

8.10 Pyridine Treated Catalysts

The effect of pyridine on two mixed oxides of the H.T. series was examined.

After outgassing, pyridine was expanded into the reaction vessel, at a temperature of 408 K, to give pressures of 0.13 kN m^{-2} (1 Torr) or 0.40 kN m^{-2} (3 Torr). The pyridine pressure was equivalent to 0.62×10^{19} molecules or 1.91×10^{19} molecules. At the end of a period of 30 min., the reaction vessel was evacuated for a period of 30 min., at 408 K. Standard experimental procedure was then carried out. The rates and selectivities for product formation are presented in Tables 8.18, 8.19 and 8.20.

Pyridine Treated Catalysts

H.T. Series Outgassed at 698 K for 16 hr

Reaction Temperature 408 K

TABLE 8.18

Cat.Comp./ Atom % Sb	$R_{1P}/10^{-3}$ % min^{-1} m^{-2}	$R_{2P}/10^{-3}$ % min^{-1} m^{-2}
6.13*	7.0	2.0
6.13[a]	0	0
26.8*	460	179
26.8[a]	299	129
26.8[b]	8.4	3.6

TABLE 8.19

Cat.Comp./ Atom % Sb	$R_{1A}/10^{-3}$ % min^{-1} m^{-2}	$R_{2A}/10^{-3}$ % min^{-1} m^{-2}
6.13*	91	25
6.13[a]	9.0	4.3
26.8*	21	6.8
26.8[a]	22	7.2
26.8[b]	6.5	2.8

TABLE 8.20

Cat.Comp./ Atom % Sb	Se_1/% at 10 min			Se_2/% at 50 min		
	P	A	DE	P	A	DE
6.13*	8.5	90.1	1.4	6.1	93.1	0.8
6.13[a]		100			100	
26.8*	87.0	10.6	2.4	92.8	5.7	1.5
26.8[a]	86.8	11.7	1.5	87.8	9.5	2.7
26.8[b]	62.5	37.5		63.0	37.0	

Values* for untreated catalysts quoted in Tables 8.12, 8.14 and 8.15

R_{1P}, R_{2P} = rate of appearance of propylene

R_{1A}, R_{2A} = rate of appearance of acetone

a = 0.13 kN m^{-2} (1 Torr) pyridine

b = 0.40 kN m^{-2} (3 Torr) pyridine

P = propylene

A = acetone

DE = di-isopropyl ether

Tables 8.18 and 8.19, illustrate the appreciable effect pyridine treatment had on product formation. No propylene formation was observed for the 6.13 atom % Sb mixed oxide, which had been treated with a pyridine pressure of 0.13 kN m^{-2} (1 Torr). The rates of acetone appearance were much lower than the corresponding ones obtained with the untreated 6.13 atom % Sb mixed oxide. The effect of such treatment on the 26.8 atom % Sb mixed oxide was to reduce the rate values of propylene appearance by an average of 32%. No significant change was detected in the rate values for acetone appearance. Treating the 26.8 atom % Sb

mixed oxide with a pyridine pressure of 0.40 kN m^{-2} (3 Torr) led to significant reductions in propylene and acetone formation. The effect of pyridine treatment on selectivity is shown in Table 8.20. Treatment of the 6.13 atom % Sb mixed oxide with a pyridine pressure of 0.13 kN m^{-2} (1 Torr) resulted in 100% selectivity for acetone formation. Treating the 26.8 atom % Sb mixed oxide with a pyridine pressure of 0.13 kN m^{-2} (1 Torr) did not significantly alter its selectivity. However, when the pyridine pressure was increased to 0.40 kN m^{-2} (3 Torr) a decrease in propylene selectivity was observed.

Isomerization of Cyclopropane

8.11 Chromatographic Column

Separation of propylene, formed as a result of cyclopropane isomerization, and cyclopropane was carried out using the column described in Section 8.1. Good separation of the product and reactant was achieved by operating the column at a temperature of 303 K and a nitrogen carrier gas pressure of 50 kN m^{-2}. The following retention times, measured according to Section 7.7, were obtained:-

propylene = 3.0 min

cyclopropane = 4.0 min

8.12 Relative Sensitivity Factors

Measured according to Section 7.8

cyclopropane = 1.0

propylene = 1.1

8.13 Experimental Procedure

The pretreatment of the L.T. and H.T. series was carried out as described in Section 7.11. At the end of the outgassing period

CYCLOPROPANE ISOMERIZATION 411 K

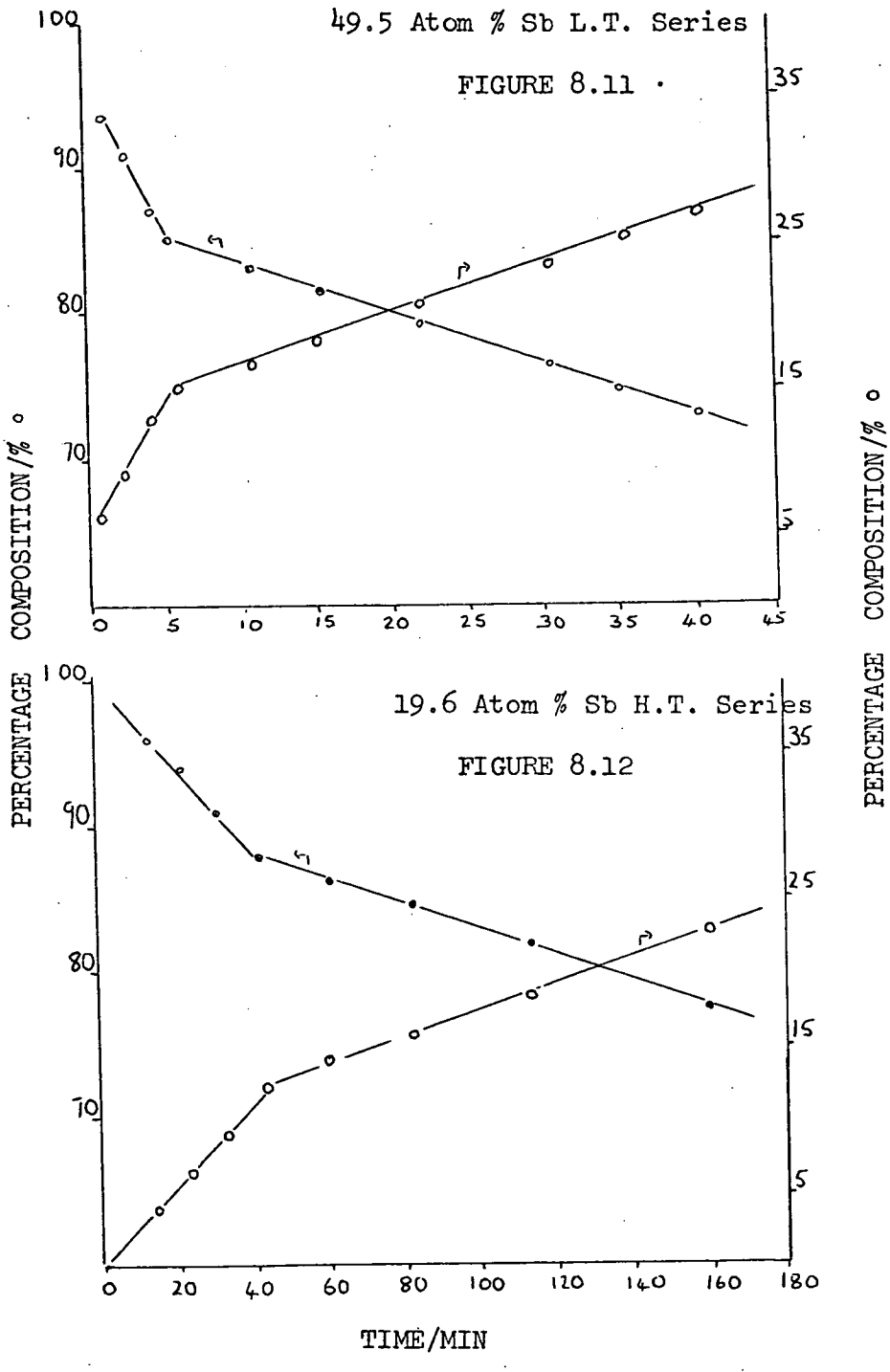

the sample was isolated from the pumping system at a pressure of 133 $\mu N\ m^{-2}$ (10^{-6} Torr). Cyclopropane was admitted by expansion into the reaction vessel, at 411 K, to give a pressure of 1.60 $kN\ m^{-2}$ (12 Torr). This was equivalent to 7.56×10^{19} molecules. Standard experimental procedure was then carried out.

8.14 Results

Figures 8.11 and 8.12 illustrate the typical plots of percentage composition versus time used to obtain values for the rates of disappearance of cyclopropane, R_{1CP} and R_{2CP}. These values are given in Tables 8.21 and 8.22.

TABLE 8.21

L.T. Series Outgassed at 293 K for 5 hr

Reaction Temperature 411 K

Cat. Comp./ Atom % Sb	$R_{1CP}/10^{-3}$ % min^{-1} m^{-2}	$R_{2CP}/10^{-3}$ % min^{-1} m^{-2}
0	0	0
8.7	206	15
19.6	403	50
26.8	528	82
49.5	796	159
75.0	287	102
100	0	0

CYCLOPROPANE ISOMERIZATION ACTIVITY PATTERNS

411 K

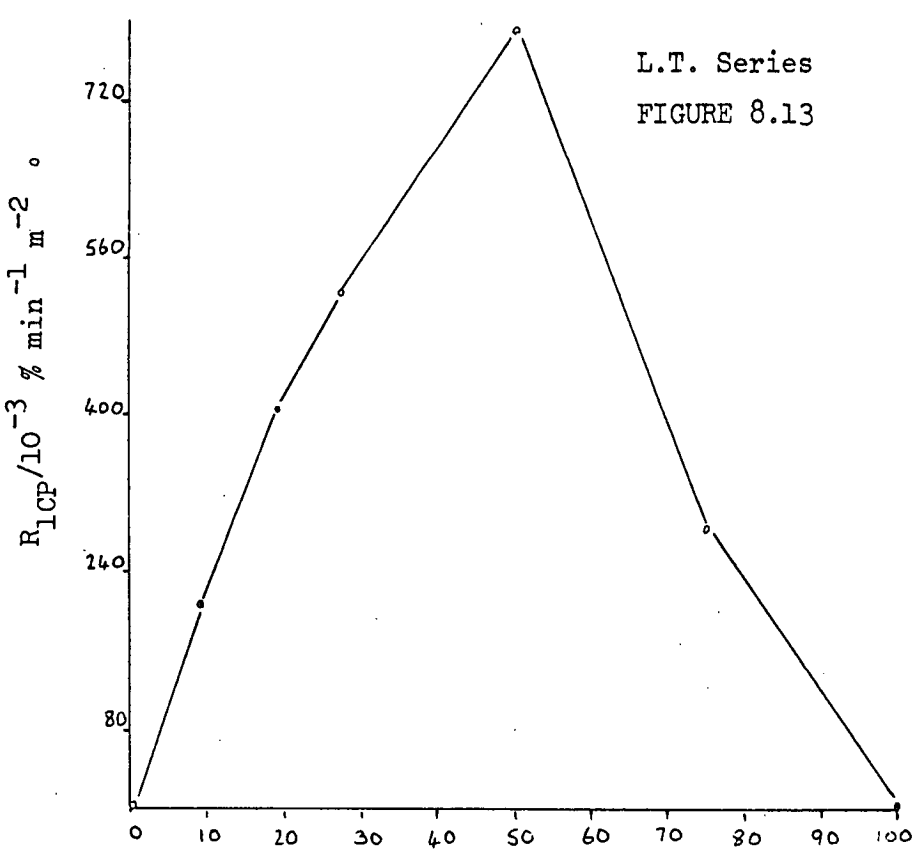

L.T. Series

FIGURE 8.13

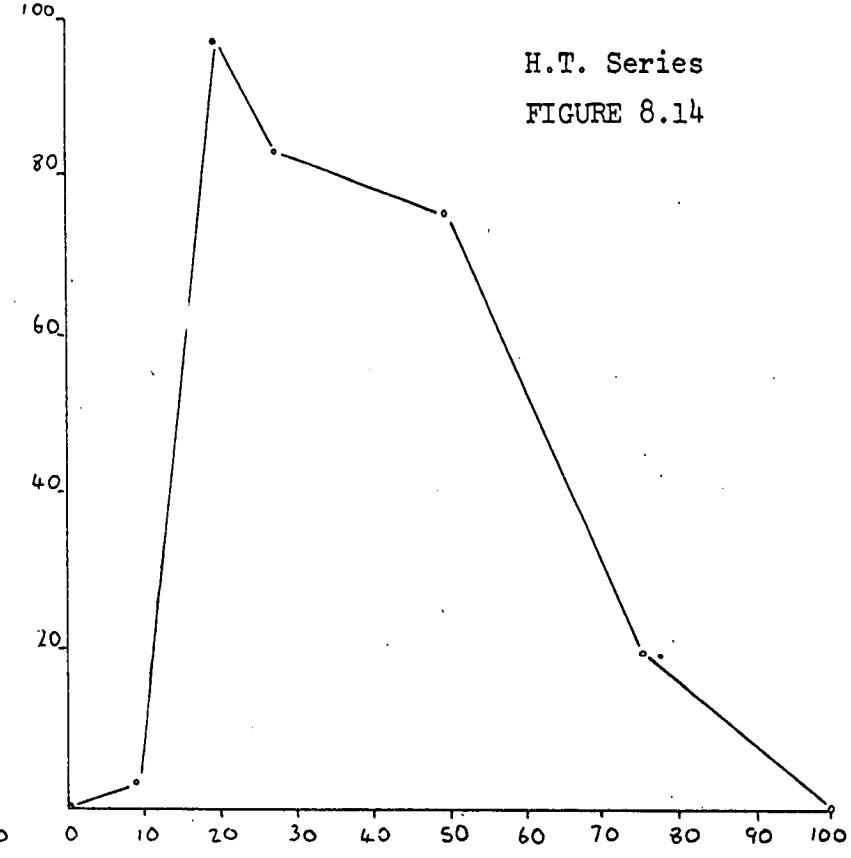

H.T. Series

FIGURE 8.14

CAT.COMP./ATOM % Sb

TABLE 8.22

H.T. Series Outgassed at 698 K for 16 hr

Reaction Temperature 411 K

Cat. Comp./ Atom % Sb	$R_{1CP}/10^{-3}$ % min^{-1} m^{-2}	$R_{2CP}/10^{-3}$ % min^{-1} m^{-2}
0	0	0
8.7	1.8	0.2
19.6	97	36
26.8	83	29
49.5	75	17
75.0	19	6.8
100	0	0

The only product detected was propylene. Stannic oxide and antimony tetroxide, pretreated according to both methods, showed no activity. The mixed oxides of the L.T. series were more active than the corresponding ones of the H.T. series. The activity patterns for both series are displayed in Figures 8.13 and 8.14. The 49.5 atom % Sb and 19.6 atom % Sb mixed oxides displayed the greatest activity for the L.T. and H.T. series, respectively. In both series, an increase in the antimony content from 8.7 atom % Sb to 19.6 atom % Sb resulted in an increase in activity. The H.T. series showed a decrease in activity, with increasing antimony content, for the catalyst composition region of 19.6 atom % Sb to 75.0 atom % Sb. This trend was observed with the L.T. series when the antimony content was increased from 49.5 atom % Sb to 75.0 atom % Sb.

A repeat experiment gave an indication of the reproducibility in the rate values. These are presented in Table 8.23.

TABLE 8.23

H.T. Series Outgassed at 698 K for 16 hr

Reaction Temperature 411 K

Cat.Comp./ Atom % Sb	$R_{1CP}/10^{-3}$ % min^{-1} m^{-2}	$R_{2CP}/10^{-3}$ % min^{-1} m^{-2}
19.6*	97	36
19.6	89	33

Values* quoted in Table 8.22

The average difference in the rate values was 8%. Changes of greater than ±8% in the activity patterns were regarded as significant.

Increasing the reaction temperature above 411 K led to a decrease in the rate values for the H.T. series. This is illustrated by the values quoted in Table 8.24.

TABLE 8.24

H.T. Series Outgassed at 698 K for 16 hr

Cat. Comp./ Atom % Sb	R.T./K	$R_{1CP}/10^{-3}$ % min^{-1} m^{-2}	$R_{2CP}/10^{-3}$ % min^{-1} m^{-2}
26.8*	411	83	29
26.8	473	78	30
26.8	498	37	13
75.0*	411	19	6.8
75.0	443	0	0
75.0	443	0	0

Values* quoted in Table 8.22

R.T. = reaction temperature

CYCLOPROPANE ISOMERIZATION

ARRHENIUS PLOTS

FIGURE 8.15

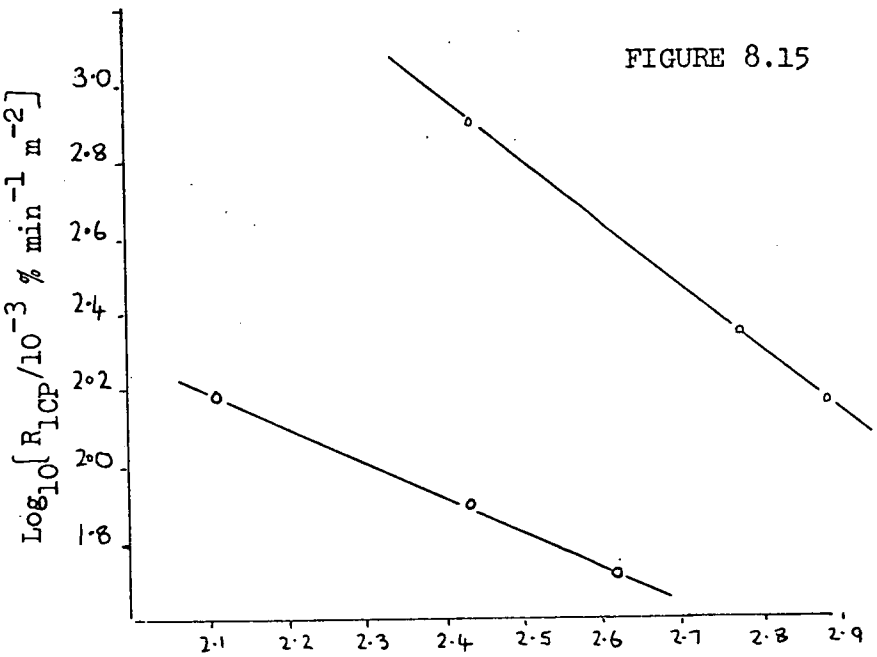

FIGURE 8.16

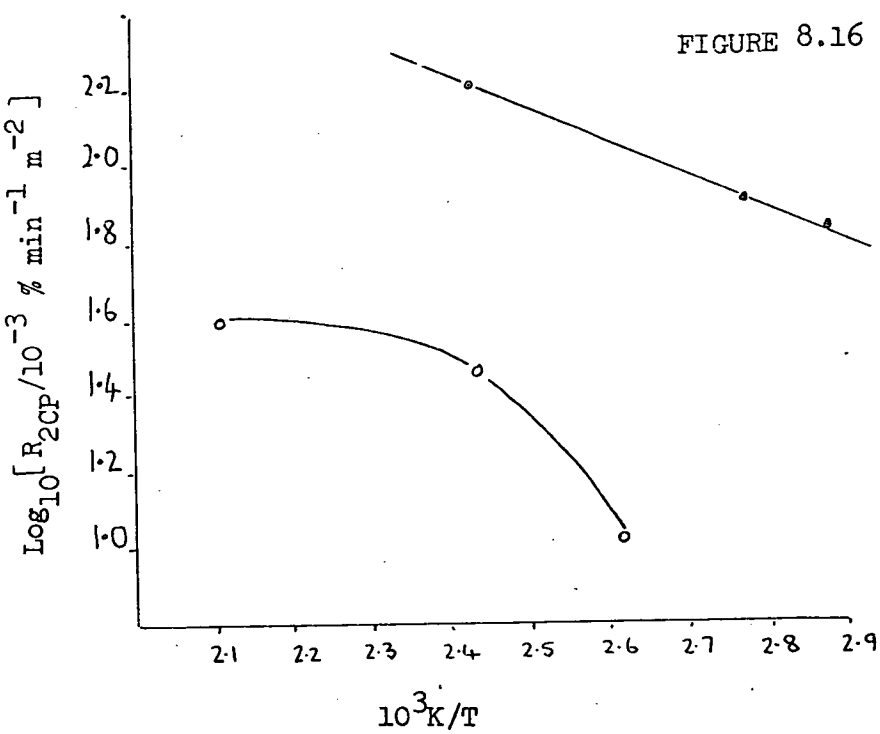

o 49.5 Atom % Sb L.T. Series

o 26.8 Atom % Sb H.T. Series

This imposed restrictions upon the study of the H.T. series. The reaction temperature of 411 K was found to be the most suitable one for both series. The Arrhenius plots for the H.T. series were obtained by using R_{1CP} and R_{2CP} values for temperatures lower than 411 K. Examples of the Arrhenius plots, obtained with mixed oxides from both series, are given in Figures 8.15 and 8.16. Straight line plots were achieved by using either R_{1CP}, or R_{2CP} values for the 49.5 atom % Sb mixed oxide of the L.T. series. Such a plot for the 26.8 atom % Sb mixed oxide, pretreated according to the H.T. method, was only obtained using the R_{1CP} value. The Arrhenius parameters estimated from Figures 8.15 and 8.16, are presented in Tables 8.25 and 8.26.

Arrhenius Parameters

L.T. Series Outgassed at 293 K for 5 hr

TABLE 8.25

Cat.Comp./ Atom % Sb	R	E/kJ mol^{-1}	$\log_{10}$ ($A/10^{-3}$ % min^{-1} m^{-2})
49.5	R_{1CP}	32±4	7.0±0.9
49.5	R_{2CP}	16±3	4.3±0.8

H.T. Series Outgassed at 698 K for 16 hr

TABLE 8.26

Cat.Comp./ Atom % Sb	R	E/kJ mol^{-1}	$\log_{10}$ ($A/10^{-3}$ % min^{-1} m^{-2})
26.8	R_{1CP}	18±3	4.2±0.5

R = rate value used for Arrhenius plot

The more active 49.5 atom % Sb mixed oxide had a larger activation energy than the less active 26.8 atom % Sb mixed oxide. However, for stage S_2, the activation energy was approximately the same as the stage S_1 value for the 26.8 atom % Sb mixed oxide.

8.15 Infra-red Spectroscopy Investigation

Preliminary investigations were carried out using the 8.7 atom % Sb and 49.5 atom % Sb mixed oxides. Samples, weighing ~0.3 g, were pressed into 30 mm diameter discs at about 1.5×10^{18} N m^{-2}, in a stainless steel die. The discs were then mounted in a brass sample holder, centred in a cylindrical "Pyrex" cell with potassium bromide windows. The apparatus and the operating conditions of the "Perkin Elmer 225" infra-red spectrophotometer have been described by Howe et al.[91] No transmission was observed with either of the two samples. Consequently, an investigation of the spectra of adsorbed pyridine on the tin-antimony mixed oxides could not be carried out.

8.16 Summary

Except for one case, stannic oxide and antimony tetroxide showed no activity. The only example of activity was the decomposition of isopropanol by stannic oxide, which had been pretreated according to the H.T. method.

Activity was found to depend on the catalyst composition and on the pretreatment method. Isopropanol decomposition and cyclopropane isomerization took place more readily with the mixed oxides of the L.T. series than the corresponding ones of the H.T. series. For 3,3-dimethylbut-1-ene isomerization, the mixed oxides of the H.T. series displayed the greatest activity. The pretreatment method had the greatest effect on the isopropanol decomposition. The catalysts

pretreated according to the L.T. method showed the greatest selectivity for dehydration.

Similar activity patterns, with maximum activity at the 49.5 atom % Sb mixed oxide, were observed for all three reactions over the mixed oxides of the L.T. series. This is illustrated by Figures 8.3, 8.9 and 8.13. Except for the catalyst compositions of 0 atom % Sb and ~6 atom % Sb, similar activity patterns for 3,3-dimethylbut-1-ene isomerization and propylene formation from isopropanol were observed for the H.T. series. Maximum activity for both reactions occurred with the 26.8 atom % Sb mixed oxide. The most active catalyst for cyclopropane isomerization was the 19.6 atom % Sb mixed oxide. The activity patterns, for the three reactions over the H.T. series, are displayed by Figures 8.4, 8.10 and 8.14.

CHAPTER 9

Isomerization of But-1-ene

9.1 Chromatographic Column

Separation of the products formed during but-1-ene isomerization was carried out using a stainless steel column. The column, of length 3 m and internal diameter 3 mm, was packed with 28% bis-2-methoxyethyladipate on 'Chromosorb P'. Good separation of products and reactant was achieved by operating the column at a temperature of 298 K and a nitrogen carrier gas pressure of 40 kN m^{-2}. The following retention times, measured according to Section 7.7, were obtained:-

but-1-ene	=	1.0 min
trans but-2-ene	=	3.5 min
cis but-2-ene	=	5.0 min.

9.2 Relative Sensitivity Factors

Measured according to Section 7.8

but-1-ene	=	1.0
trans but-2-ene	=	1.3
cis but-2-ene	=	1.3

9.3 Experimental Procedure

Pretreatment of the two catalyst series studied, was carried out as described in Section 7.11. At the end of the outgassing period, the sample was isolated from the pumping system at a pressure of 133 μN m^{-2} (10^{-6} Torr). With the reaction vessel

BUT-1-ENE ISOMERIZATION 293 K

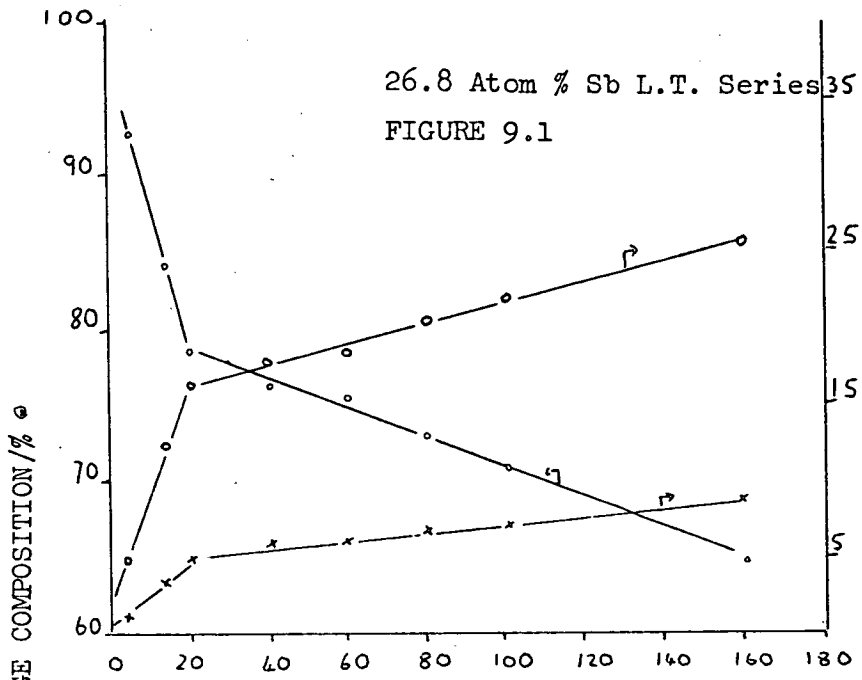

26.8 Atom % Sb L.T. Series
FIGURE 9.1

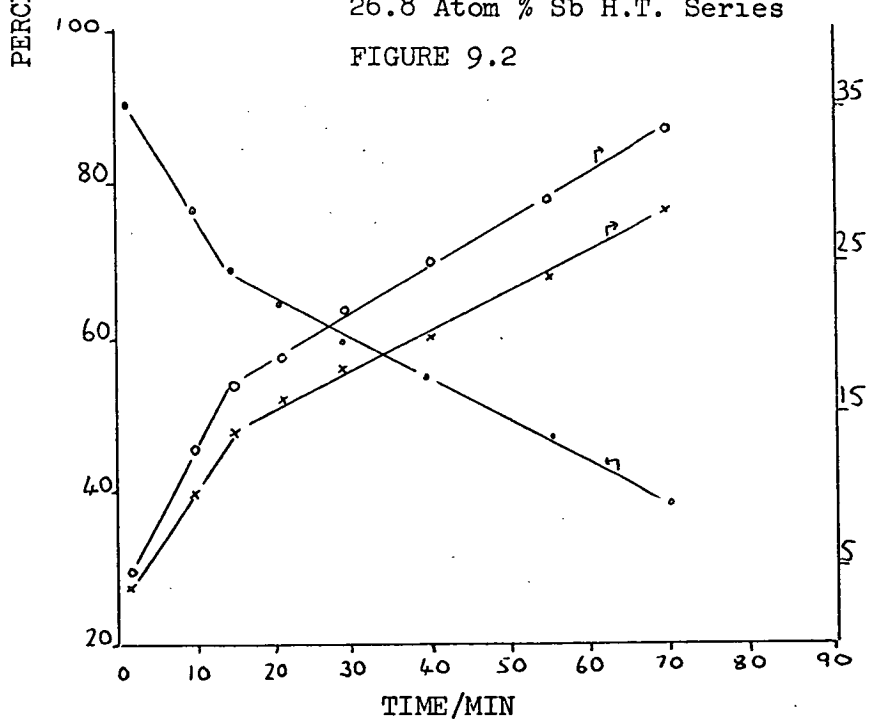

26.8 Atom % Sb H.T. Series
FIGURE 9.2

∘ BUT-1-ENE o CIS BUT-2-ENE

× TRANS BUT-2-ENE

at a temperature of 293 K, but-1-ene was admitted by expansion to give a pressure of 1.46 kN m^{-2} (11 Torr). This was equivalent to 9.97×10^{19} molecules.

9.4 Results

But-1-ene isomerization resulted in the formation of trans but-2-ene and cis but-2-ene. Butadiene was detected in trace amounts only. As the percentage of butadiene never exceeded 0.3%, its rate of formation was not measured. Figures 9.1 and 9.2, illustrate typical percentage composition versus time plots, for the L.T. and H.T. series, respectively. Such plots were used to obtain values for the rates of disappearance, R_{1b} and R_{2b}, of but-1-ene. Initial product ratios of cis but-2-ene/trans but-2-ene were obtained from stage S_1. The values for the rates of disappearance of but-1-ene are presented in Tables 9.1 and 9.2.

TABLE 9.1

L.T. Series Outgassed at 293 K for 5 hr

Reaction Temperature 293 K

Cat. Comp./ Atom % Sb	$R_{1b}/10^{-3}$ % min^{-1} m^{-2}	$R_{2b}/10^{-3}$ % min^{-1} m^{-2}	initial cis/trans
0	0	0	-
7.4	35	8	3.5
8.7	71	17	4.0
19.6	103	23	3.4
26.8	247	41	3.2
49.5	269	76	3.3
75.0	146	17	3.0
100	0	0	-

TABLE 9.2

H.T. Series Outgassed at 698 K for 16 hr

Reaction Temperature 293 K

Cat.Comp./ Atom % Sb	$R_{1b}/10^{-3}$ % min^{-1} m^{-2}	$R_{2b}/10^{-3}$ % min^{-1} m^{-2}	initial cis/trans
0	0	0	-
7.4	210	190	1.2
8.7	280	210	1.1
19.6	923	462	1.0
26.8	470	140	1.2
49.5	0	0	-
75.0	0	0	-
100	0	0	-

For both series, no activity was observed for stannic oxide and antimony tetroxide. The 49.5 atom % Sb and the 75.0 atom % Sb mixed oxides, pretreated according to the H.T. method, showed no activity until the reaction temperature was raised to 318 K. Values for R_{1b} and R_{2b}, at 318 K, are presented in Table 9.3

TABLE 9.3

H.T. Series Outgassed at 698 K for 16 hr

Reaction Temperature 318 K

Cat.Comp./ Atom % Sb	$R_{1b}/10^{-3}$ % min^{-1} m^{-2}	$R_{2b}/10^{-3}$% min^{-1} m^{-2}	initial cis/trans
49.5	145	78	1.4
75.0	45	19	1.4

BUT-1-ENE ISOMERIZATION ACTIVITY PATTERNS

∘ 293 K × 318 K

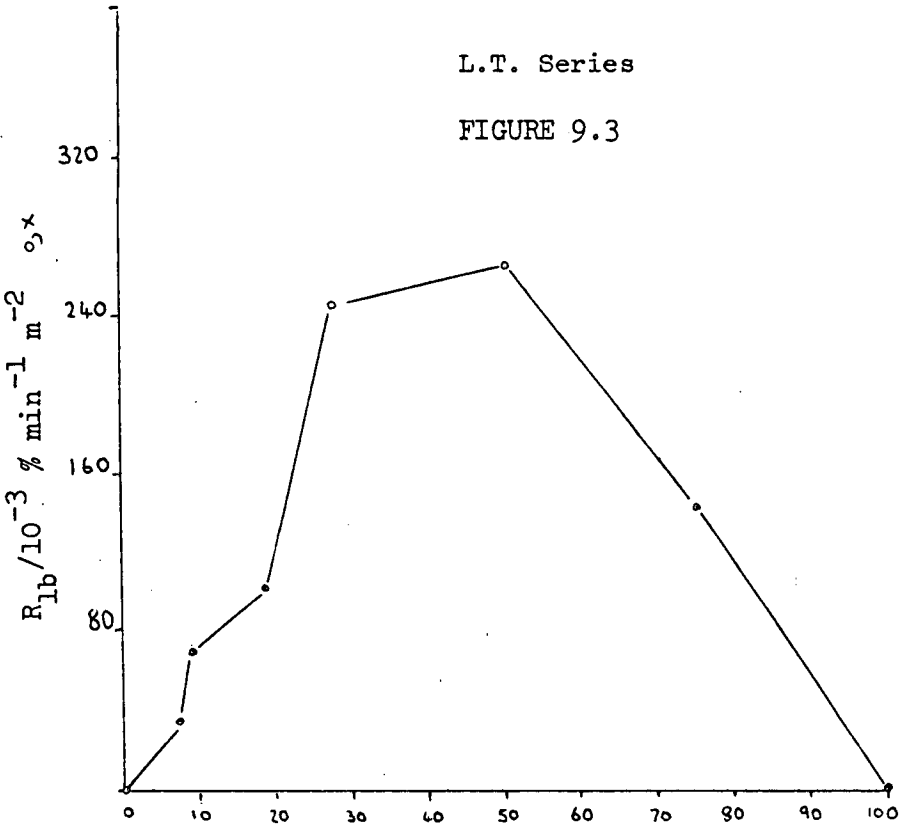

FIGURE 9.3

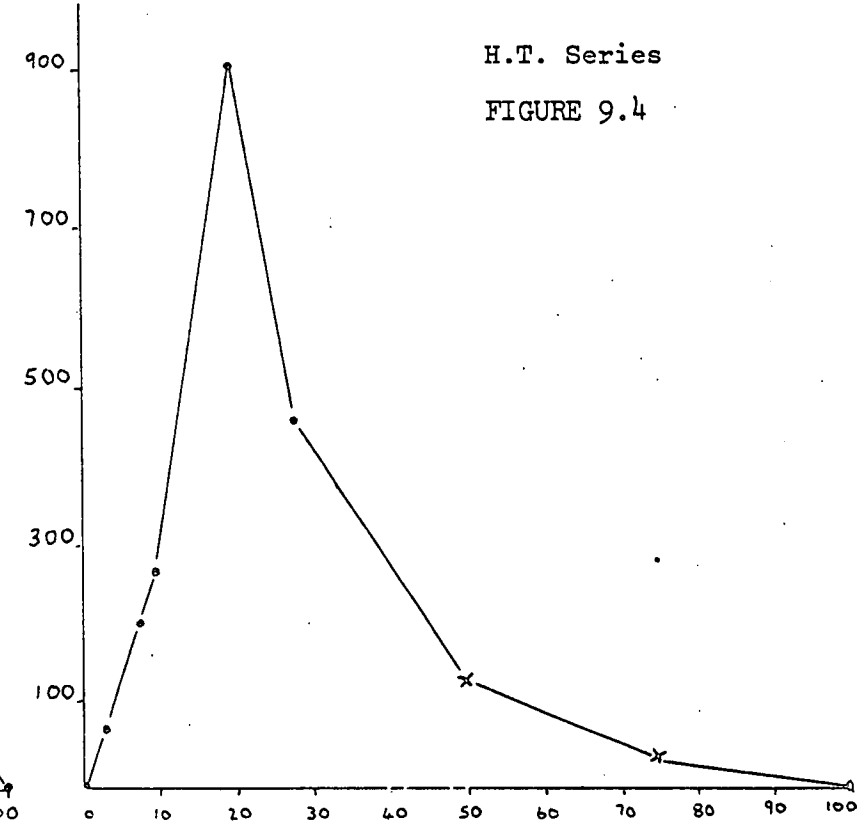

FIGURE 9.4

CAT.COMP./ATOM % Sb

Most of the mixed oxides of the H.T. series, with the exception of the two quoted in Table 9.3, were more active than the corresponding ones of the L.T. series. The largest initial cis but-2-ene/trans but-2-ene product ratios were obtained for the mixed oxides of the L.T. series.

The activity patterns, for both series, are presented in Figures 9.3 and 9.4. Maximum activity for the L.T. and H.T. series was observed with the 49.5 atom % Sb and 19.6 atom % Sb mixed oxides, respectively. For the catalyst composition region of 7.4 atom % Sb to 19.6 atom % Sb, increasing the antimony content resulted in an increase in activity, for both series. In the L.T. series, this trend continued until a catalyst composition of 49.5 atom % Sb. After this composition, activity decreased with increasing antimony content. For the H.T. series, rates increased until the catalysts contained more than 19.6 atom % Sb. Increasing the antimony content further, resulted in a decrease in activity.

An indication of the reproducibility in the rate values is given in Tables 9.4 and 9.5. The average difference in the rate values was 4%. Changes in the activity patterns of greater than $\pm 4\%$ were regarded as significant.

TABLE 9.4

L.T. Series Outgassed at 293 K for 5 hr

Reaction Temperature 293 K

Cat.Comp./ Atom % Sb	$R_{1b}/10^{-3}$ % min^{-1} m^{-2}	$R_{2b}/10^{-3}$ % min^{-1} m^{-2}	initial cis/trans
8.7*	71	17	4.0
8.7	69	16	3.9
19.6*	103	23	3.4
19.6	97	22	3.2
49.5*	269	76	3.3
49.5	260	72	3.4

TABLE 9.5

H.T. Series Outgassed at 698 K for 16 hr

Reaction Temperature 293 K

Cat.Comp./ Atom % Sb	$R_{1b}/10^{-3}$ % min^{-1} m^{2}	$R_{2b}/10^{-3}$ % min^{-1} m^{-2}	initial cis/trans
7.4*	210	190	1.2
7.4	203	188	1.1

* values quoted in Tables 9.1 and 9.2

BUT-1-ENE ISOMERIZATION

ARRHENIUS PLOTS

FIGURE 9.5

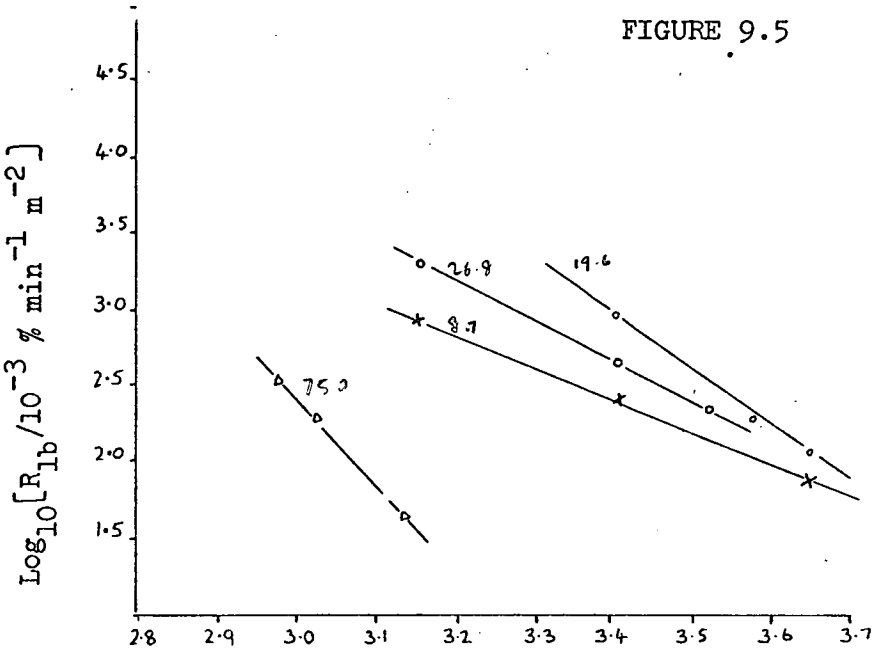

FIGURE 9.6

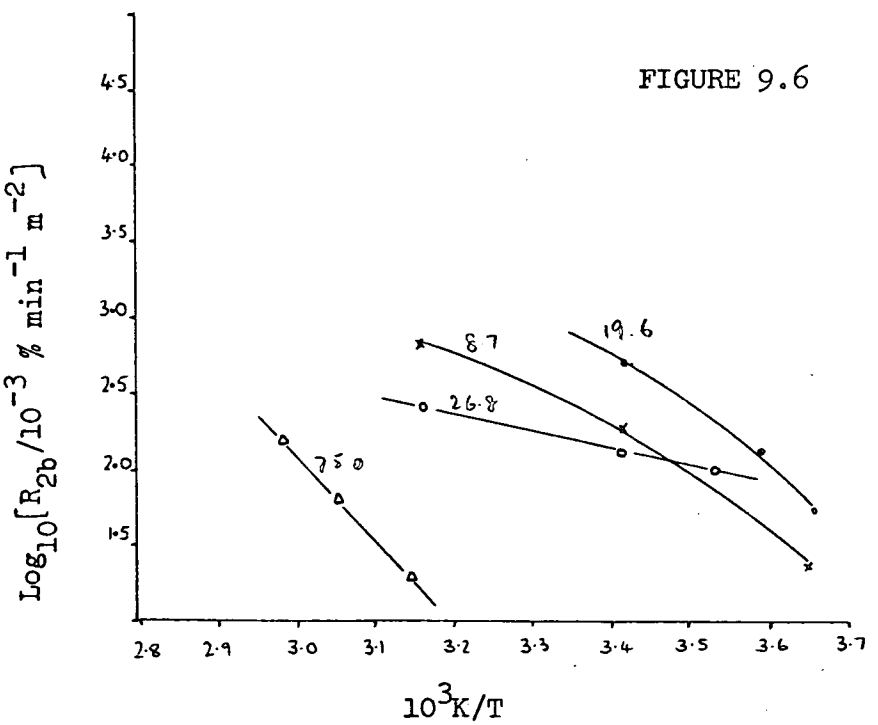

x 8.7 Atom % Sb
o 19.6 Atom % Sb
o 26.8 Atom % Sb
△ 75.0 Atom % Sb

Arrhenius plots, obtained by using R_{1b} and R_{2b} values, for the H.T. series are presented in Figures 9.5 and 9.6. Only for the 26.8 atom % Sb and 75.0 atom % Sb mixed oxides were straight line plots obtained with R_{2b} values. Values for the Arrhenius parameters and the estimated errors in their values are given in Table 9.6.

Arrhenius Parameters

TABLE 9.6

H.T. Series Outgassed at 698 K for 16 hr

Cat.Comp./ Atom % Sb	R	E/kJ mol^{-1}	$\log_{10}$ ($A/10^{-3}$ % min^{-1} m^{-2})
8.7	R_{1b}	44±2	10.3±0.5
19.6	R_{1b}	68±4	15.0±0.9
26.8	R_{1b}	50±2	11.5±0.5
	R_{2b}	25±1	6.5±0.3
75.0	R_{1b}	120±5	21.2±0.9
	R_{2b}	106±5	18.7±0.9

R = rate value used for Arrhenius plot.

The 75.0 atom % Sb mixed oxide had a significantly larger activation energy than the mixed oxides of lower antimony content.

9.5 2,6-Dimethylpyridine Treated Catalysts

Two samples of the 19.6 atom % Sb mixed oxide were pretreated according to the L.T. and H.T. method. The effect of treatment with

2,6-dimethylpyridine on their activity was investigated. After outgassing the catalyst, 2,6-dimethylpyridine was expanded into the reaction vessel. The temperature of the reaction vessel was 293 K for the L.T. series sample and 698 K for the H.T. series sample. The pressure of 2,6-dimethylpyridine was 0.13 kN m^{-2} (1 Torr). This was equivalent to 0.89×10^{19} molecules for the L.T. series sample and 0.37×10^{19} molecules for the H.T. series sample. The 2,6-dimethylpyridine was left in contact with the samples for a period of 60 min. During this time the H.T. series sample was allowed to cool to 293 K. This was followed by an evacuation period of 10 min. Standard experimental procedure was then carried out. The resulting reductions in the rate values are illustrated by Tables 9.7 and 9.8.

2,6-Dimethylpyridine Treated Catalysts

TABLE 9.7

L.T. Series Outgassed at 293 K for 5 hr

Reaction Temperature 293 K

Cat.Comp./ Atom % Sb	$R_{1b}/10^{-3}$ % min^{-1} m^{-2}	$R_{2b}/10^{-3}$ % min^{-1} m^{-2}	initial cis/trans
19.6*	103	23	3.4
19.6	28	13	3.2

TABLE 9.8

H.T. Series Outgassed at 698 K for 16 hr

Reaction Temperature 293 K

Cat.Comp./ Atom % Sb	$R_{1b}/10^{-3}$ % min^{-1} m^{-2}	$R_{2b}/10^{-3}$ % min^{-1} m^{-2}	initial cis/trans
19.6*	923	462	1.0
19.6	42	15	1.0

* values for untreated catalysts quoted in Tables 9.1 and 9.2.

The activity of the H.T. series sample, pretreated with the smaller amount of 2,6-dimethylpyridine, was reduced to the greater extent.

9.6 The Effect of Pressure on Activity

Samples of the 8.7 atom % Sb mixed oxide were pretreated according to the H.T. method. The experimental procedure was carried out as described in Section 9.3. The effect on activity of different but-1-ene pressures was investigated. The pressures of but-1-ene used were, 0.80 kN m^{-2} (6 Torr), 2.13 kN m^{-2} (16 Torr) and 2.66 kN m^{-2} (20 Torr). These were equivalent to 5.46×10^{19} molecules, 14.6×10^{19} molecules, and 18.2×10^{19} molecules, at a temperature of 293 K. In order that comparisons between the rates obtained for different but-1-ene pressures can be made, the rates

are given in units of molecules min^{-1} m^{-2}.

8.7 atom % Sb Mixed Oxide

TABLE 9.9

H.T. Series Outgassed at 698 K for 16 hr

Reaction Temperature 293 K

but-1-ene/ 10^{19} molecules	$R_{1b}/10^{16}$ molecules min^{-1} m^{-2}	$R_{2b}/10^{16}$ molecules min^{-1} m^{-2}	initial cis/trans
5.46	35.5	30.0	1.0
9.97*	27.9	20.9	1.1
14.6	23.5	19.0	1.0
18.2	11.2	7.6	1.1

* values for the 8.7 atom % Sb mixed oxide obtained from Table 9.2

Increasing the but-1-ene pressure resulted in a decrease in activity. The rate values obtained with a but-1-ene pressure of 2.66 kN m^{-2} (20 Torr), for a few selected mixed oxides, are presented in Table 9.10.

TABLE 9.10

H.T. Series Outgassed at 698 K for 16 hr

Reaction Temperature 293 K

Cat.Comp./ Atom % Sb		$R_{1b}/10^{-3}$% min^{-1} m^{-2}	$R_{2b}/10^{-3}$ % min^{-1} m^{-2}	initial cis/trans
3.3		18	12	1.5
6.2		51	26	1.5
8.7	280	62	47	1.1
19.6	923	134	100	1.1
26.8	470	85	52	1.4

Maximum activity was observed with the 19.6 atom % Sb mixed oxide. This was also shown by the H.T. series, quoted in Table 9.2, for a but-1-ene pressure of 1.46 kN m^{-2} (11 Torr). Repeat experiments, presented in Table 9.11, gave an indication of the reproducibility in the rate values. The average difference between the rate values was 5%.

TABLE 9.11

H.T. Series Outgassed at 698 K for 16 hr

Reaction Temperature 293 K

Cat. Comp./ Atom % Sb	$R_{1b}/10^{-3}$ % min^{-1} m^{-2}	$R_{2b}/10^{-3}$ % min^{-1} m^{-2}	initial cis/trans
6.2*	51	26	1.5
6.2	49	24	1.5
8.7*	62	47	1.1
8.7	58	47	1.0

* values given in Table 9.10

9.7 Butadiene Treated Catalysts

The catalyst studied was the 8.7 atom % Sb mixed oxide. It was pretreated according to the H.T. method. The amount of butadiene detected for a but-1-ene reaction at 293 K was approximately 0.2%. Increasing the reaction temperature to 393 K, resulted in approximately 1%. An investigation of the effect on activity of treatment with different butadiene pressures was carried out. Butadiene was expanded into the reaction vessel at 293 K. At the end of a period of 30 min., the reaction vessel was evacuated for

BUTADIENE TREATED 8.7 Atom % Sb
H.T. Series Mixed Oxide

FIGURE 9.7

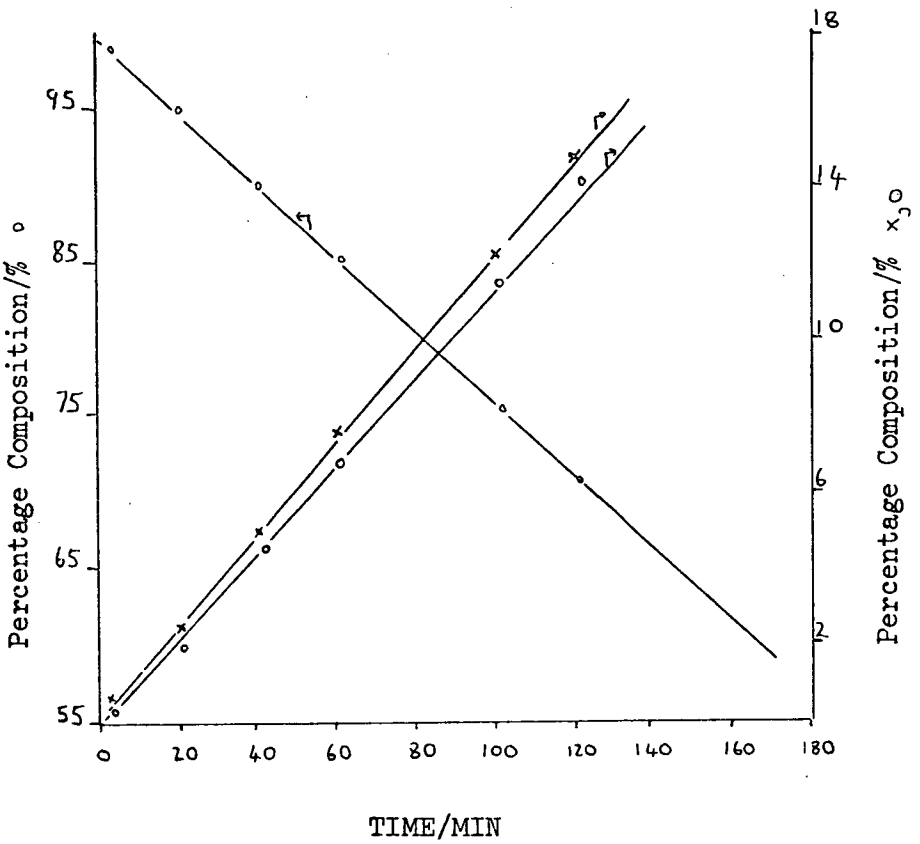

o BUT-1-ENE

× CIS BUT-2-ENE

o TRANS BUT-2-ENE

a period of 10 min. Standard experimental procedure was then carried out. The pressures of butadiene used were, 0.27 kN m^{-2} (2 Torr), 0.53 kN m^{-2} (4 Torr) and 1.33 kN m^{-2} (10 Torr). These pressures were equivalent to 1.84×10^{19} molecules, 3.68×10^{19} molecules and 9.08×10^{19} molecules, respectively. A but-1-ene pressure of 2.13 kN m^{-2} (16 Torr) equivalent to 14.6×10^{19} molecules, was used for all the experiments. The rates obtained, after treatment with different pressures of butadiene, are given in Table 9.12.

TABLE 9.12

8.7 atom % Sb

H.T. Series Outgassed at 698 K for 16 hr

Reaction Temperature 293 K

Pressure Butadiene / kN m^{-2}	$R_{1b}/10^{-3}$ % min^{-1} m^{-2}	$R_{2b}/10^{-3}$ % min^{-1} m^{-2}	initial cis/trans
-	162*	131	1.0
0.27	75	-	1.1
0.53	0	0	-
1.33	0	0	-

* values for untreated catalyst

Treatment with a butadiene pressure of 0.53 kN m^{-2} (4 Torr) or 1.33 kN m^{-2} (10 Torr) completely destroyed the activity of the 8.7 atom % Sb mixed oxide. For the sample treated with 0.27 kN m^{-2} (2 Torr) a departure from the standard percentage composition versus time plot was observed. This is shown in Figure 9.7. The rate of disappearance of but-1-ene was represented by a single

CIS BUT-2-ENE ISOMERIZATION 293 K

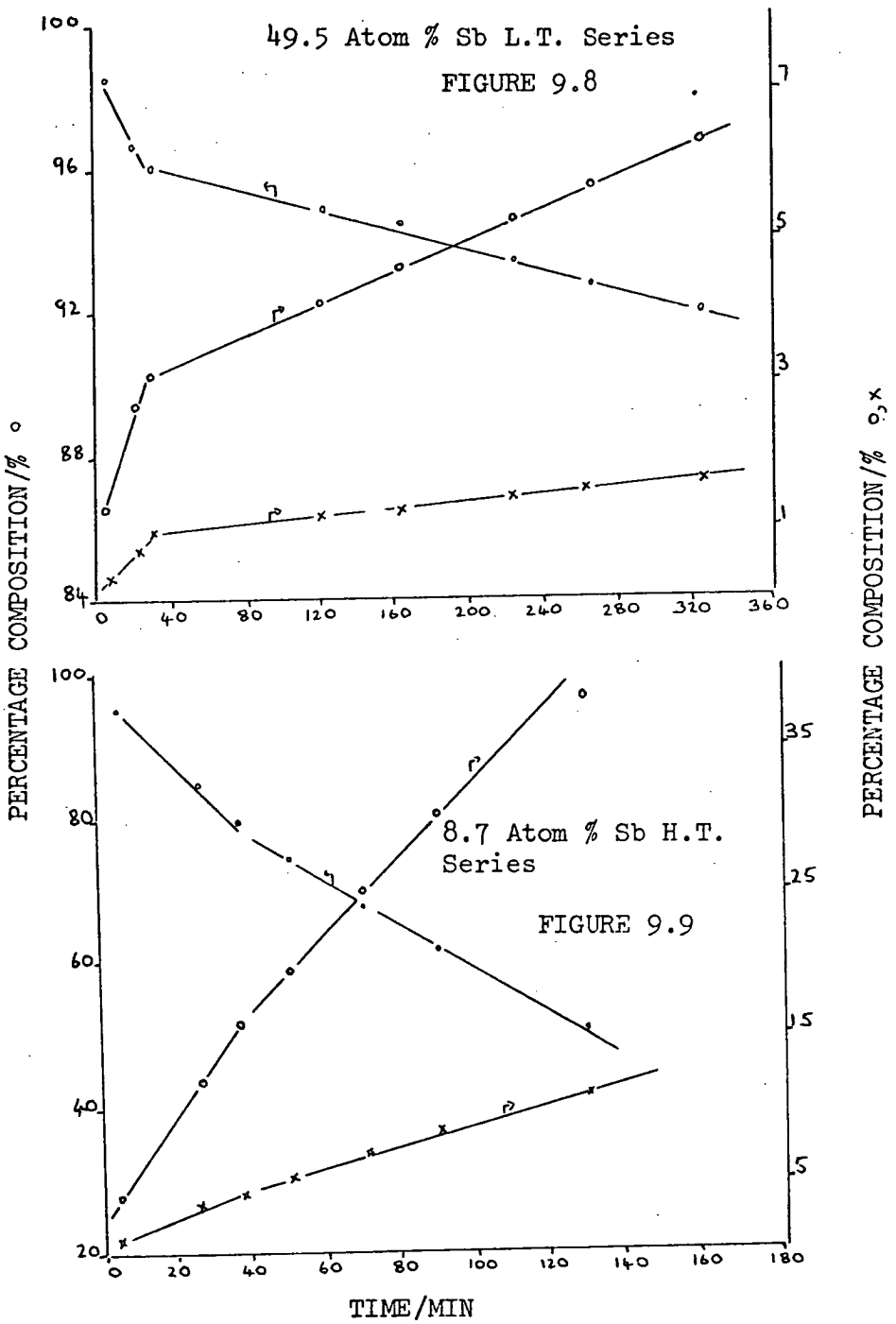

CIS BUT-2-ENE ISOMERIZATION
323 K

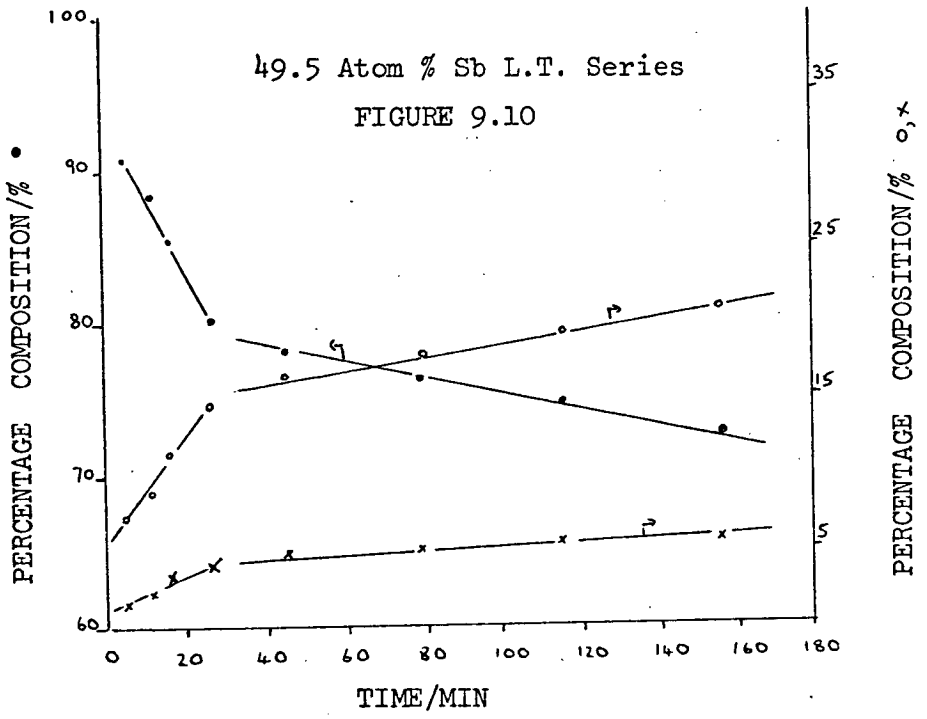

straight line plot. The value for the rate of disappearance of but-1-ene is presented under the R_{1b} column in Table 9.12.

Isomerization of Cis But-2-ene

9.8 Experimental Procedure

The chromatographic column and sensitivity factors have been described in Sections 9.1 and 9.2. Reaction temperatures of 293 K and 323 K were used for the L.T. series. For the H.T. series, the reaction temperature was 293 K. A cis but-2-ene pressure of 1.46 kN m^{-2} (11 Torr) was used. This was equivalent to 9.97×10^{19} molecules and 9.04×10^{19} molecules, at temperatures of 293 K and 323 K, respectively. Standard experimental procedure was carried out.

9.9 Results

Cis but-2-ene isomerization resulted in the formation of trans but-2-ene and but-1-ene. Standard percentage composition versus time plots are given in Figures 9.8, 9.9 and 9.10. The values for the rates of disappearance of cis but-2-ene, R_{1C} and R_{2C}, are presented in Tables 9.13, 9.14 and 9.15. Initial product ratios of trans but-2-ene/but-1-ene were obtained from stage S_1.

TABLE 9.13

L.T. Series Outgassed at 293 K for 5 hr

Reaction Temperature 293 K

Cat.Comp./ Atom % Sb	$R_{1C}/10^{-3}$ % min^{-1} m^{-2}	$R_{2C}/10^{-3}$ % min^{-1} m^{-2}	initial trans/ but-1-ene
0	0	0	-
8.7	6.9	1.1	3.5
19.6	17	1.5	5.2
26.8	24	2.6	3.7
49.5	41	5.5	4.1
75.0	12	3.0	4.2
100	0	0	-

TABLE 9.14

H.T. Series Outgassed at 698 K for 16 hr

Reaction Temperature 293 K

Cat.Comp./ Atom % Sb	$R_{1C}/10^{-3}$ % min^{-1} m^{-2}	$R_{2C}/10^{-3}$ % min^{-1} m^{-2}	initial trans/ but-1-ene
0	0	0	-
6.13	57	35	3.1
7.4	99	66	2.9
8.7	100	67	3.6
19.6	24	13	3.9
26.8	19	4	3.8
49.5	0	0	-
75.0	0	0	-
100	0	0	-

CIS BUT-2-ENE ISOMERIZATION ACTIVITY PATTERNS
293 K

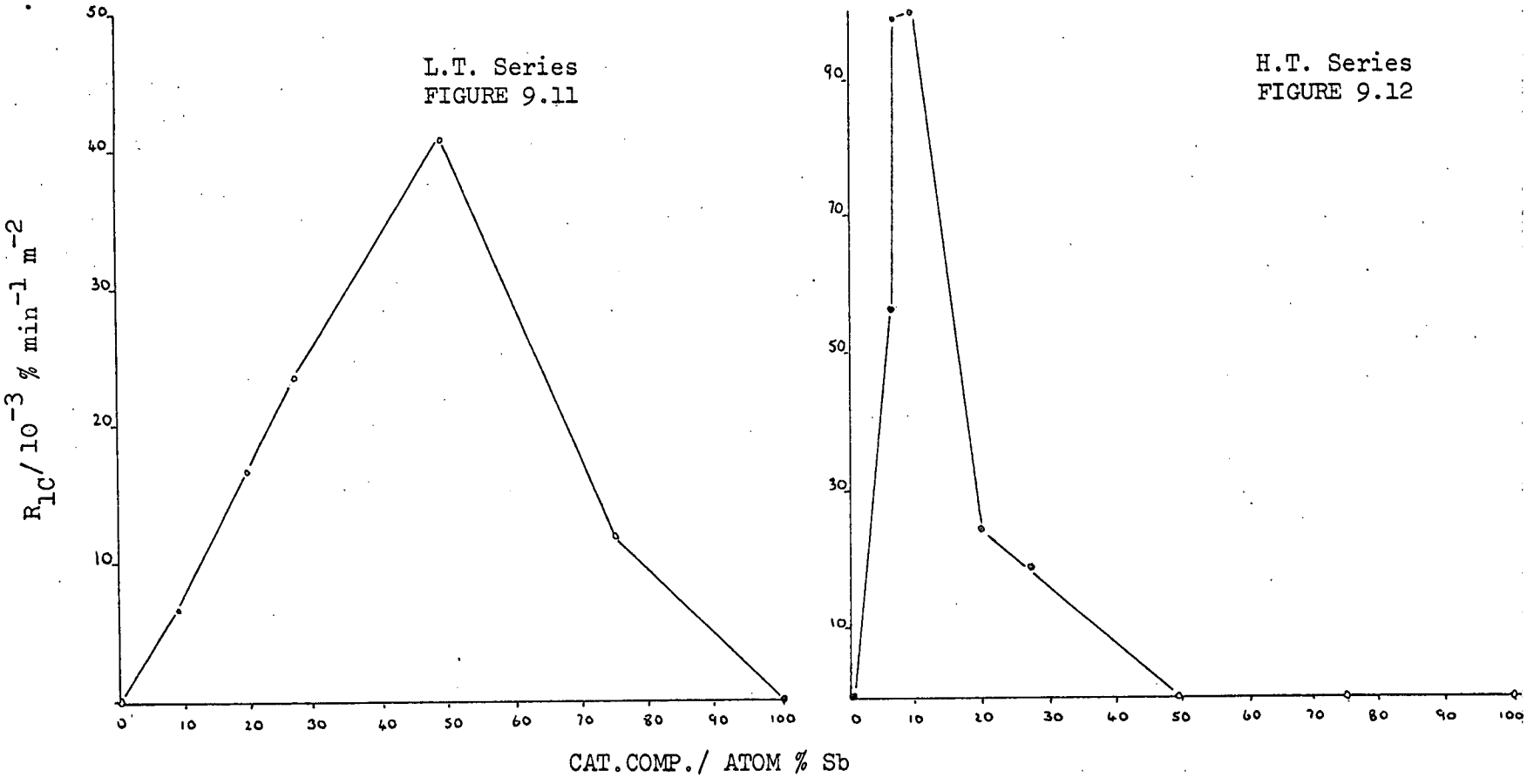

TABLE 9.15

L.T. Series Outgassed at 293 K for 5 hr

Reaction Temperature 323 K

Cat.Comp./ Atom % Sb	$R_{1C}/10^{-3}$ % min^{-1} m^{-2}	$R_{2C}/10^{-3}$ % min^{-1} m^{-2}	initial trans/ but-1-ene
8.7	28	4	2.3
19.6	98	15	3.6
26.8	120	19	3.2
49.5	292	25	3.6
75.0	50	15	2.8

For both series, stannic oxide and antimony tetroxide exhibited no activity. The 49.5 atom % Sb and 75.0 atom % Sb mixed oxides, pretreated according to the H.T. method, were also inactive at 293 K. Activity patterns for both series, at 293 K, are shown in Figures 9.11 and 9.12. Maximum activity was observed with the 49.5 atom % Sb mixed oxide of the L.T. series. Approximately the same maximum activity was found for the 7.4 atom % Sb and 8.7 atom % Sb mixed oxides of the H.T. series. Increasing activity with increasing antimony content was observed for the catalyst composition region of 8.7 atom % Sb to 49.5 atom % Sb for the L.T. series. In the H.T. series, all the mixed oxides, having more than 8.7 atom % Sb, showed a decrease in activity with increasing antimony content.

The initial product ratios indicated that all the mixed oxides formed trans but-2-ene preferentially. Increasing the reaction temperature to 323 K, for the L.T. series, led to no significant decrease

in the initial product ratios. The increase in the reaction temperature did not alter the activity pattern.

Tables 9.16 and 9.17 give an indication of the reproducibility in the rate values for both series. The average difference in the rate values for repeat experiments was 7%. Changes of greater than ±7% in the activity patterns were regarded as significant.

TABLE 9.16

L.T. Series Outgassed at 293 K for 5 hr

Reaction Temperature 293 K

Cat.Comp./ Atom % Sb	$R_{1C}/10^{-3}$ % $min^{-1}\ m^{-2}$	$R_{2C}/10^{-3}$ % $min^{-1}\ m^{-2}$	initial trans/ but-1-ene
8.7*	6.9	1.1	3.5
8.7	6.3	1.0	4.0

TABLE 9.17

H.T. Series Outgassed at 698 K for 16 hr

Reaction Temperature 293 K

Cat.Comp./ Atom % Sb	$R_{1C}/10^{-3}$ % $min^{-1}\ m^{-2}$	$R_{2C}/10^{-3}$ % $min^{-1}\ m^{-2}$	initial trans/ but-1-ene
8.7*	100	67	3.6
8.7	96	64	3.9

* values quoted in Tables 9.13 and 9.14.

9.10 2,6-Dimethylpyridine Treated Catalysts

A study was made of the effect of 2,6-dimethylpyridine on the 49.5 atom % Sb and 8.7 atom % Sb mixed oxides. These mixed oxides were pretreated according to the L.T. and H.T. method, respectively. The experimental procedure was similar to the one described in Section 9.5. The pressure of 2,6-dimethylpyridine used was 0.13 kN m^{-2} (1 Torr). This was equivalent to 0.89×10^{19} molecules for the L.T. series and 0.37×10^{19} molecules for the H.T. series. The effect of such treatment on the values of R_{1C} and R_{2C}, is illustrated by Tables 9.18 and 9.19.

2,6-Dimethylpyridine Treated Catalysts

TABLE 9.18

L.T. Series Outgassed at 293 K for 5 hr

Reaction Temperature 293 K

Cat. Comp./ Atom % Sb	$R_{1C}/10^{-3}$ % min^{-1} m^{-2}	$R_{2C}/10^{-3}$ % min^{-1} m^{-2}	initial trans/ but-1-ene
49.5*	41	5.5	4.1
49.5	17	2.6	4.2

TABLE 9.19

H.T. Series Outgassed at 698 K for 16 hr

Reaction Temperature 293 K

Cat.Comp./ Atom % Sb	$R_{1C}/10^{-3}$ % min^{-1} m^{-2}	$R_{2C}/10^{-3}$ % min^{-1} m^{-2}	initial trans/ but-1-ene
8.7*	100	67	3.6
8.7	81	49	3.8

* values for untreated catalysts quoted in Tables 9.13 and 9.14.

Treatment with 2,6-dimethylpyridine resulted in a decrease in activity for both series.

9.11 Summary

Stannic oxide and antimony tetroxide, pretreated according to both methods, were inactive for but-1-ene and cis but-2-ene isomerization.

Similar activity patterns, with maximum activity at the 49.5 atom % Sb mixed oxide, were found for isopropanol dehydration, but-1-ene, cis but-2-ene, 3,3-dimethylbut-1-ene and cyclopropane isomerization, with the L.T. series. This is illustrated by Figures 8.3, 8.9, 8.13, 9.3 and 9.11.

Two different activity patterns were noted for but-1-ene and cis but-2-ene isomerization with the H.T. series. The activity pattern for but-1-ene isomerization, Figure 9.4, was like the one obtained for cyclopropane isomerization, Figure 8.14. Maximum activity occurred with the 19.6 atom % Sb mixed oxide. Maximum activity for cis but-2-ene isomerization, Figure 9.12, was seen with the 7.4 atom % Sb and 8.7 atom % Sb mixed oxides.

CHAPTER 10

Discussion

The data presented in Chapters 8 and 9 (and a later Chapter 11) did not allow an unambiguous decision to be made between zero and first order kinetics, for any of the reactions investigated. Since the primary objectives of the work were to establish activity patterns as a function of catalyst composition and to obtain information about the nature of the active sites, rather than to establish detailed kinetics, it seemed best to treat both of the S_1 and S_2 stages as effectively zero order. It must also be pointed out that when the stages were treated as first order processes, the activity patterns which were obtained did not differ significantly from those reported.

Deactivation of the catalyst during the course of an experiment was observed with all the reactions investigated. Sala and Trifiro[73] and Christie[92] have also encountered this phenomenon. Christie[92], studying propylene oxidation with tin-antimony mixed oxides from the same source as the ones used for this thesis, observed that deactivation occurred after approximately 60% of the reaction was completed. In contrast to Christie's observations, the results obtained for this thesis indicated that deactivation took place at a much earlier stage. It was generally found that before the onset of the S_2 stage between 15% to 30% of the reaction had taken place. In some cases, extrapolation of the percentage composition line back to zero time did not pass through the 100% point. This would seem to indicate that some particularly active sites had been deactivated before the onset of stage S_1.

Sala and Trifirò[73], investigating the oxidative dehydrogenation of but-1-ene, observed deactivation only with an antimony oxide sample. Deactivation did not occur with stannic oxide and the tin-antimony mixed oxides.

In spite of the deactivation phenomenon, adequate reproducibility could be achieved if particular care was taken with the choice of the experimental conditions. This was an important factor, as the activity patterns for the different reactions played a major role in deciding the nature of the active sites.

Isomerization of 3,3-Dimethylbut-1-ene

Information on the acidic properties of tin-antimony oxide catalysts is limited. Hughes et al.[28] and Christie[92], using catalysts from the same source as the ones studied for this thesis, postulated carbonium ion mechanisms for propylene/D_2O and isobutene/D_2O exchange, respectively. The former reaction, however, involved an allylic intermediate if the catalysts were pretreated with propylene. Sala and Trifirò[73], studying the oxidative dehydrogenation of n-butenes, concluded that Lewis-type acidic sites were responsible for the isomerization which occurred concurrently with the dehydrogenation.

The isomerization of 3,3-dimethylbut-1-ene, believed to proceed only by a carbonium ion mechanism, was used as a test reaction to investigate the acidity of the tin-antimony oxide catalysts. As discussed earlier in Section 2.1, evidence for such a reaction scheme was obtained by Haag and Pines[29][30] and also by Kemball et al.[31][32] in a later investigation. It is worth while emphasising the important features of the reaction scheme. The first step is the addition of a proton to form a secondary carbonium ion, which rearranges to the more

stable tertiary ion. Such a mechanism can take place over a catalyst which has hydroxyl groups capable of displaying Brønsted-type acidity.

The activity patterns, illustrated in Figures 8.3 and 8.4, clearly show that only the tin-antimony mixed oxides are capable of displaying Brønsted-type acidity, at 373 K. The individual oxides and the 6.2 atom % Sb mixed oxide were inactive in the temperature range of 373 K to 573 K.

The inactivity of the 6.2 atom % Sb mixed oxide is surprising as other reactions (to be discussed later) revealed that it is capable of showing acidic properties. The retarding effect on activity of pretreatment with sodium acetate, shown in Table 8.9, is consistent with the views of Roca et al.[93] They believed that Na^+ ions exchange with protons and poison Brønsted-type but have no effect on Lewis-type acidic sites.

A similar situation in which two different oxides show acidic properties on combination was encountered by Moro-oka et al.[94][95] in their investigation of propylene oxidation. They observed an increase in the number of acidic sites when stannic oxide, believed to have only a few acidic sites, was combined with molybdenum trioxide. They also suggested that the acidic sites were hydroxyl groups.

The tin-antimony mixed oxides studied for this thesis were prepared in an analogous manner to the ones used by Godin et al.[23] They believed that the mixed oxides of composition >5 atom % Sb, consisted of two phases. One phase was believed to be a solid solution of antimony tetroxide in stannic oxide and the other was thought to be an antimony tetroxide phase. Maximum activity for 3,3-dimethylbut-1-ene isomerization was observed with the 49.5 atom % Sb and 26.8 atom % Sb mixed oxides of the L.T. and H.T. series, respectively. This suggests

that both phases are responsible for Brønsted-type acidity.

The greater activity of the mixed oxides presented in Table 8.4 compared with the corresponding ones in Table 8.3, indicates that Brønsted acidity increases when the outgassing temperature is raised from 293 K to 698 K. Flockhart et al.[59] studying cyclopropane isomerization over a zeolite catalyst, observed that Brønsted acidity increased with rise in temperature until an optimum temperature was reached. Above this temperature, Lewis acidity increased but Brønsted acidity decreased. A similar situation possibly exists for the tin-antimony mixed oxides. Other investigators[73] have reported that tin-antimony mixed oxides, calcined at 1173 K, showed Lewis acidity. The tin-antimony mixed oxides, outgassed at 698 K, may also have Lewis-type sites as well as a considerable number of Brønsted-type sites. Although all the tin-antimony mixed oxides of composition >6.2 atom % Sb showed an increase in activity when the outgassing temperature was raised to 698 K, two different activity patterns were observed for the two outgassing temperatures. This implies that the extent to which Brønsted acidity increases with rise in temperature, depends upon catalyst composition. Therefore, the temperature at which Lewis acidity starts to increase and Brønsted acidity to decrease will probably also depend on catalyst composition. A study of the infra-red spectra of adsorbed pyridine, similar to the one carried out by Ward[96], would have provided a method of estimating the concentration of either Brønsted-type, or Lewis-type acidic sites. Unfortunately, preliminary infra-red studies, mentioned in Section 8.15, revealed that this technique could not be applied to the tin-antimony mixed oxides, due to transmission difficulties. Thornton and Harrison[97] encountered similar difficulties in their infra-red investigation of stannic oxide.

They detected the presence of weakly bonded water on the surface of stannic oxide, after outgassing at 293 K. The water was believed to be held to the surface by several modes, one of which was hydrogen bonding to surface hydroxyl groups. A similar situation may also exist with the individual oxides and the 6.2 atom % Sb mixed oxide of the L.T. series, under the experimental conditions employed for the 3,3-dimethylbut-1-ene isomerization study. This would account for the inactivity of the three catalysts. However, the activity of the mixed oxides of composition >6.2 atom % Sb indicates the presence of Brønsted-type hydroxyls, after outgassing at 293 K.

Increasing the outgassing temperature to 698 K will result in the loss of the weakly bonded water from the surface, and will also result in dehydroxylation. The inactivity of the two individual oxides and the 6.2 atom % Sb mixed oxide, after outgassing at 698 K, implies that considerable dehydroxylation takes place, so that no suitable hydroxyl groups are available for 3,3-dimethylbut-1-ene isomerization. This is in keeping with the findings of Thornton and Harrison[97], who reported that stannic oxide showed considerable Lewis acidity at temperatures of ≥508 K.

A different situation exists for the tin-antimony mixed oxides, outgassed at 698 K. The observed increase in the activity of the H.T. series as compared with the L.T. series, Tables 8.3 and 8.4, indicates an increase in the number and/or the activity of the suitable hydroxyl groups. Loss of water from the surface will be a contributory factor. However, unlike the situation encountered with the individual oxides and the 6.2 atom % Sb mixed oxide, extensive dehydroxylation evidently does not occur if the atom % Sb is >6.2%.

In all cases, the isomerization of 3,3-dimethylbut-1-ene was

limited to the formation of 2,3-dimethylbut-1-ene and 2,3-dimethylbut-2-ene. This, according to Haag and Pines[29], indicates that the Brønsted-type acidic sites, present on the tin-antimony mixed oxides, are weak. Further rearrangement of 3,3-dimethylbut-1-ene only occurs on strongly acidic sites. Tables 8.1 and 8.2 of selectivities show that the product ratio (2,3-dimethylbut-2-ene/2,3-dimethylbut-1-ene) does not vary significantly with time, catalyst composition, or pretreatment. The average value of the product ratio ($\sim$5) is slightly higher than the one extrapolated from the data of Kilpatrick et al.[98] It would appear that the products are formed in approximately thermodynamic equilibrium proportions during the reaction. Similar observations concerning the product ratios were made by Kemball et al.[32] and Hoser and Krzyzanowski[99].

Decomposition of Isopropanol

In spite of the controversy concerning the mechanism of alcohol decomposition, discussed in Section 3.1, a number of investigators [100][101] have correlated the surface acidity of binary oxide catalysts with isopropanol dehydration. It was with this correlation in mind that a study of the decomposition of isopropanol was undertaken. As alcohol decomposition can take place by dehydrogenation and dehydration, it also provides a suitable model for studying the effect of catalyst composition and pretreatment on selectivity.

Tables 8.11 and 8.12 illustrate the striking change in selectivity which resulted when the outgassing temperature was raised from 293 K to 698 K. The tin-antimony mixed oxides, outgassed at 293 K, functioned essentially as dehydration catalysts but on changing the outgassing temperature to 698 K, selectivity towards dehydrogenation increased. This increase was particularly marked

in the tin-antimony mixed oxides of low antimony content.

Isopropanol dehydration, resulting in propylene formation, can take place on Brønsted-type acidic sites[45] or Lewis-type acidic sites[46]. Comparison of the activity patterns for 3,3-dimethylbut-1-ene isomerization, Figures 8.3 and 8.4, with those for propylene formation, Figures 8.9 and 8.10, gives an indication of the nature of the site responsible for isopropanol dehydration. The tin-antimony mixed oxides of composition greater than 6.2 atom % Sb, pretreated according to the L.T. and H.T. method, display similar activity patterns for 3,3-dimethylbut-1-ene isomerization and propylene formation. This suggests that both reactions take place on the same type of site. As discussed earlier, 3,3-dimethylbut-1-ene isomerization takes place with hydroxyl groups capable of displaying Brønsted-type acidity. Gentry and Rudham[45], studying the dehydration of isopropanol on X zeolites, observed propylene and di-isopropyl ether formation. Activity was attributed to hydroxyl groups, capable of displaying Brønsted acidity. Thus, the reaction schemes proposed by Gentry and Rudham[45] may also account for isopropanol dehydration over the mixed oxides of composition >6.2 atom % Sb and pretreated according to both methods.

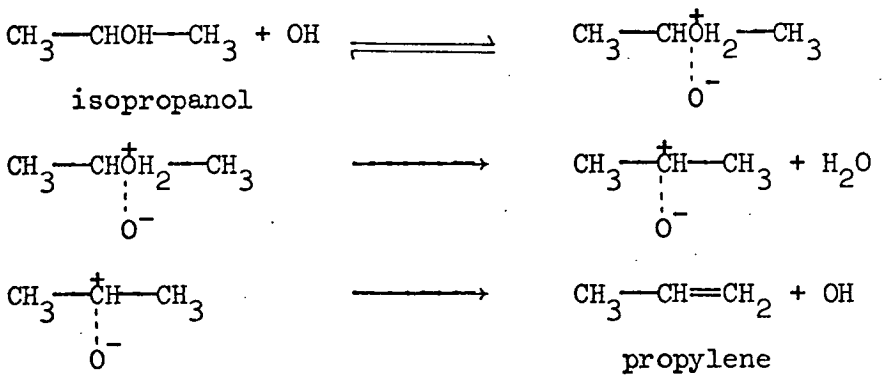

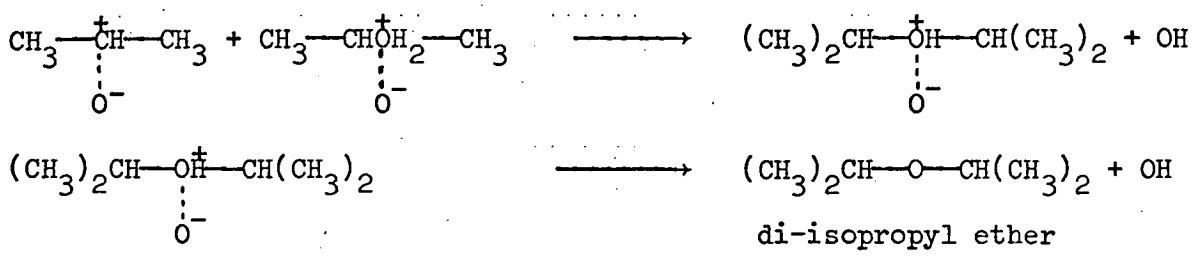

Previously mentioned was the fact that 3,3-dimethylbut-1-ene isomerization was found to take place more readily with the H.T. series, than with the L.T. series, indicating an increase in Brønsted acidity in the H.T. series. A similar situation might be expected with propylene formation from isopropanol. However, Section 8.9 reveals that this is not the case. Propylene formation was observed to occur more readily over the L.T. series. Hughes et al.[28] and Christie[92] noted that propylene readily poisoned the acidic sites of tin-antimony mixed oxides, outgassed at 723 K. Such a retarding effect will probably take place more readily with the H.T. series, (which display the greater Brønsted-type acidity) than with the L.T. series. Thus, the H.T. series will appear to be less active for propylene formation than the L.T. series. The fact that the mixed oxides of the H.T. series had the ability to dehydrogenate as well as dehydrate isopropanol alcohol will also be a factor contributing to the decrease in propylene formation.

Stannic oxide and catalyst samples of approximately 6 atom % Sb, pretreated according to the H.T. method, showed activity for propylene formation but not for 3,3-dimethylbut-1-ene isomerization. A mechanism involving Lewis-type sites, similar to the one proposed by Gentry et al.[46] would result in propylene formation and would not lead to 3,3-dimethylbut-1-ene isomerization. In keeping with this idea, Thornton and Harrison[97] reported that stannic oxide showed considerable

Lewis acidity at temperatures of ≥508 K. Table 8.14 shows that the activity of stannic oxide, for propylene formation, was greater than the activity of the 6.13 atom % Sb mixed oxide. These facts suggest that the tin ions may act as Lewis-type acidic sites. Thus, it may be possible to account for propylene formation over stannic oxide and the 6.13 atom % Sb mixed oxide, outgassed at 698 K, using a reaction scheme similar to the one proposed by Gentry et al.[46]

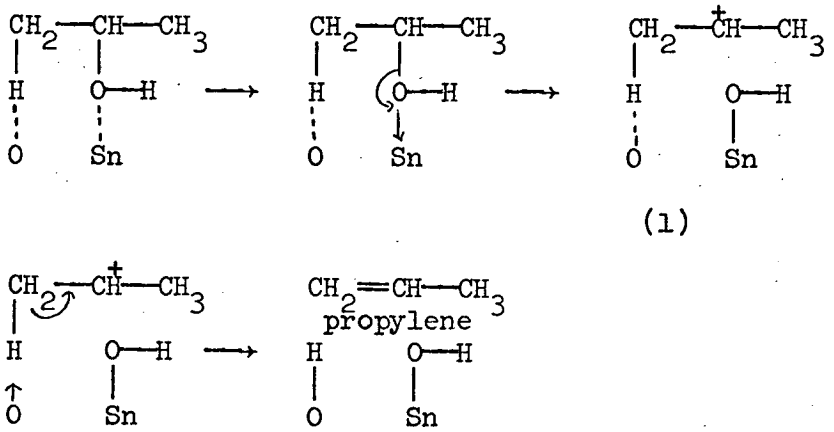

(1)

Interaction of the carbonium (1) with physically adsorbed isopropanol will give rise to an oxonium ion $((CH_3)_2HC)_2\overset{+}{O}H$. Abstraction of a proton by a basic oxide will result in di-isopropyl ether formation. Such a mechanism may account for the trace amount of di-isopropyl ether observed with the 6.13 atom % Sb mixed oxide of the H.T. series.

A striking feature is the fact that only the mixed oxides of the H.T. series displayed appreciable activity for isopropanol dehydrogenation. A number of investigators[46-48] believe that different sites are responsible for dehydration and dehydrogenation. Two observations suggest that a similar situation exists for the tin-antimony mixed oxides. One of these observations, illustrated in Tables 8.18 and 8.19, is the greater effect that pyridine treatment had on dehydration than on dehydrogenation. Pyridine[102] can adsorb

on both Brønsted-type and Lewis-type acidic sites. In keeping with this was the observation that pyridine treatment retarded the dehydration activity of the 6.13 atom % Sb and 26.8 atom % Sb mixed oxides. As discussed above, the most likely mechanisms for propylene formation with these tin-antimony mixed oxides involve Lewis-type and Brønsted-type acidic sites, respectively. The other observation, inferring separate sites, is the fact that different activity patterns were found for propylene formation and acetone formation, with the same range of tin-antimony mixed oxides. This is illustrated by Figure 8.10 and Table 8.15, respectively.

It is particularly interesting, that the catalytic action of stannic oxide, outgassed at 698 K, was directed almost exclusively to the dehydrogenation of isopropanol. Buiten[103], studying the decomposition of isopropanol over stannic oxide, molybdenum trioxide and a catalyst composed of both oxides, encountered a similar situation. Stannic oxide favoured the formation of acetone, but the combination of the two oxides resulted in a catalyst which preferentially formed propylene. In this case also, hydroxyl groups were believed to be involved in the mechanism for propylene formation. Thus, the tin oxide component of the tin-antimony mixed oxides, outgassed at 698 K, may possibly be responsible for the formation of acetone.

As already discussed in Section 3.1, Hauffe[16] and Wolkenstein[17] put forward contrasting theories to explain the role of the electronic factor in the decomposition of alcohols. Although Hauffe[16] and Wolkenstein[17] postulated theories to explain dehydration and dehydrogenation, their ideas concerning dehydrogenation only shall be considered. The foregoing discussion shows that isopropanol dehydration over the mixed oxides of $\geq$6.2 atom

% Sb, outgassed according to both methods, may be related to the acidic nature of the catalyst's surface.

Wolkenstein[17] considers the adsorption of alcohol as an acceptor process, whereas, Hauffe[16] regards it as a donor process. Although Wolkenstein and Hauffe regard the desorption of acetone as a donor process, only Hauffe believes it to be the rate-determining step. Thus, according to Hauffe's view, isopropanol dehydrogenation will be favoured by a p-type semiconductor. However, antimony tetroxide, a p-type semiconductor did not dehydrogenate isopropanol but stannic oxide, a n-type semiconductor, did. Such a result is consistent with Wolkenstein's view. According to Wolkenstein, the initial adsorption step is through the hydroxyl hydrogen. This can be regarded as an acceptor process and will be favoured by a n-type semiconductor. In accordance with such a view were the observations made by a group studying isopropanol decomposition over the n-type semiconductors manganese molybdate[47] and zinc oxide[104]. An increase in the Fermi levels of the two n-type semiconductors resulted in an increase in isopropanol dehydrogenation. However, they did not support Wolkenstein's view that the initial adsorption step of alcohol was rate-determining. Rajaram et al.,[47] observing that isopropanol dehydrogenation over manganese molybdate was inhibited by acetone, concluded that the desorption of acetone was the rate-determining step. They, unlike Wolkenstein and Hauffe, believed that the desorption of acetone had an acceptor character. In spite of the different views concerning the rate-determining step, a mechanism proposed by Viswanathan et al.[104] to explain isopropanol dehydrogenation over zinc oxide was, in general, in keeping with Wolkenstein's views. A similar mechanism may also account for isopropanol dehydrogenation over the H.T. series. The results

obtained with the H.T. series favour the view that stannic oxide, a n-type semiconductor, is responsible for isopropanol dehydrogenation.

1) Initial adsorption of the alcohol through the hydrogen of the hydroxyl group

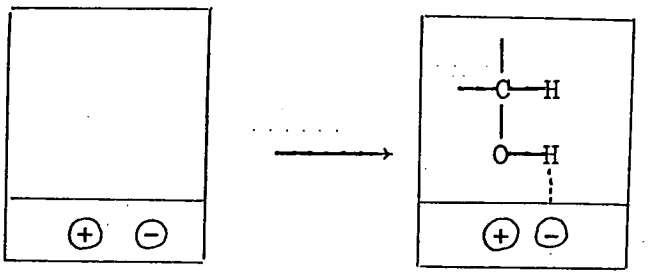

C_3H_7OH +

2) The primary adsorption state transforms into a two point adsorption involving both the hydrogen and oxygen of the hydroxyl group.

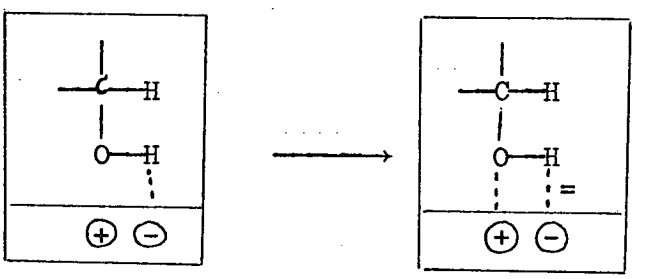

3) Acetone and hydrogen are desorbed leaving the surface in its original state.

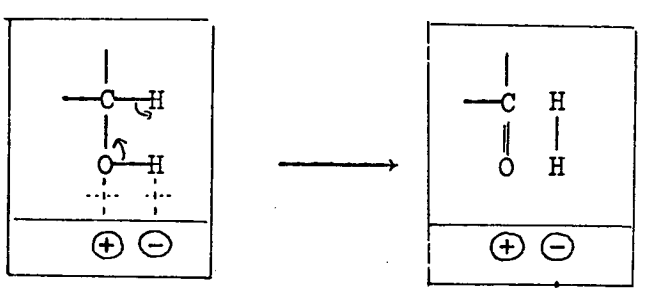

Thus, on stannic oxide, activity for dehydrogenation of isopropanol is associated with the donor levels and is rate-limited by an acceptor process. According to Wolkenstein, the rate-limiting step is the initial adsorption of the alcohol through the hydrogen of the hydroxyl group. On the other hand, Rajaram et al.,[47] from

their investigation with manganese molybdate, concluded that the desorption of acetone, an acceptor process, was the rate-determining step. However, there is insufficient evidence to infer which step is rate determining for isopropanol dehydrogenation over the H.T. series.

Cyclopropane Isomerization

Mentioned earlier in Section 4.4, was the fact that cyclopropane isomerization has been attributed to Brønsted-type[54] and Lewis-type acidic sites[56]. A comparison of the results obtained for cyclopropane isomerization, with the ones obtained for 3,3-dimethylbut-1-ene isomerization and isopropanol dehydration, provides further information about the acidic nature of the tin-antimony catalysts.

For the tin-antimony mixed oxides, pretreated according to the L.T. method, the activity pattern for cyclopropane isomerization is similar to the ones obtained for 3,3-dimethylbut-1-ene isomerization and isopropanol dehydration. This is illustrated by Figures 8.13, 8.3 and 8.9, respectively. Thus, taking into account the discussion concerning the most likely sites for 3,3-dimethylbut-1-ene isomerization and isopropanol dehydration over the mixed oxides of composition >6.2 atom % Sb, cyclopropane isomerization probably takes place via similar Brønsted-type acidic sites. Other investigators have also postulated a mechanism for cyclopropane isomerization which involved an initial step of proton addition. Roberts[54] postulated an n-propylcarbonium ion, whereas Baird and Aboderin[55] and Hightower and Hall[57] explained their observations by invoking a cyclo-propylcarbonium ion. The technique employed in the investigation of the tin-antimony mixed oxides does not allow a distinction to be made between the two forms.

The activity pattern for cyclopropane isomerization over the H.T. series mixed oxides, Figure 8.14, is unlike the ones obtained for 3,3-dimethylbut-1-ene isomerization and isopropanol dehydration, Figures 8.4 and 8.10, respectively. This suggests that different sites may be responsible for cyclopropane isomerization. Flockhart et al.,[59] studying a zeolite catalyst, concluded that an increase in the outgassing temperature resulted in the sites changing from Brønsted-type acidic sites to Lewis-type acidic sites. The possibility that cyclopropane isomerization takes place via two types of acidic sites may explain the different activity pattern. A similar explanation, to be discussed fully in a later section, is used to account for the but-1-ene isomerization activity pattern found with the mixed oxides of the H.T. series. This activity pattern, Figure 9.4, is similar to the cyclopropane isomerization one.

An interesting feature of the cyclopropane isomerization investigation is the fact that the mixed oxides of the H.T. series were found to be less active than the corresponding ones of the L.T. series. This is in accordance with the finding for isopropanol dehydration. The H.T. series mixed oxides displayed the lowest activity. The possibility that this decrease in activity is due to poisoning by propylene has already been discussed. A further indication of this poisoning effect is borne out by the difficulty, mentioned in Section 8.14, of obtaining Arrhenius data for the H.T. series. Other investigators[54][105] have also encountered irreversible adsorption of propylene in their cyclopropane isomerization studies.

Isomerization of n-Butenes

Fully discussed in chapter 5, is the manner in which n-butene isomerization can provide a useful general method of distinguishing between acid, base and metal catalysts. Mechanisms involving butenyl (allylic) carbonium ions[65] and secondary butyl carbonium ions[106] have been postulated to explain activity over Lewis-type and Brønsted-type acidic sites, respectively. Pines and Schaap[66] proposed an allylic carbanion to account for double-bond isomerization over base catalysts. Secondary butyl radicals[60] have been used to explain isomerization over metal catalysts. However, there are some cases where elucidation of the reaction mechanism has proved to be difficult. One such case is alumina. Hightower and Hall[64] concluded that the difficulty arose because various reactions, proceeding through different surface complexes, took place on different sites. Keeping in mind the fact that rationalization of the reaction mechanism may prove to be difficult, an investigation of n-butene isomerization over the tin-antimony catalysts was undertaken. It was hoped that the observations from such an investigation would correlate with the ones found for 3,3-dimethylbut-1-ene isomerization, cyclopropane isomerization and isopropanol dehydration.

In accordance with the general findings for the above three reactions, the individual oxides displayed no activity for n-butene isomerization. Activity was only detected for the tin-antimony mixed oxides. Itoh et al.[107], working with titanium dioxide and silicon dioxide, reported that a combination of the two oxides resulted in a catalyst showing high activity. The combination of the two oxides was thought to result in an increase

in the number of sites responsible for the formation of secondary butyl carbonium ions.

Contrary to the findings reported in this thesis, Kemball et al.[71] noted that stannic oxide showed considerable isomerization activity for but-1-ene and cis but-2-ene. In an earlier investigation, Takte and Rooney[70] postulated a mechanism involving 1-methyl-allyl radicals to account for but-1-ene isomerization. However, Kemball et al.[71] failed to establish such a correlation. An intramolecular mechanism involving a secondary carbonium ion was used to explain cis but-2-ene isomerization.

Although under oxidation conditions, it is interesting to note the observations of Trifirò et al.[69] and Sala and Trifirò[73], studying tin-antimony oxides. Trifirò et al.[69] reported that stannic oxide had very little isomerizing ability. The activity of antimony tetroxide was observed to be less than that of stannic oxide. In a later investigation, Sala and Trifirò[73] noted that antimony pentoxide showed activity for but-1-ene isomerization. Increasing the calcination temperature of the antimony pentoxide from 673 K to 1073 K resulted in complete loss of activity. However, the activity of the tin-antimony mixed oxides was not destroyed by a high calcination temperature. In view of their observations, it is perhaps not surprising that the tin-antimony mixed oxides were active and the individual oxides were inactive. A calcination temperature of 1123 K was used in the preparation of all the catalysts investigated for this thesis. In keeping with the view that high calcination temperatures possibly affect the isomerization activity of the individual oxides, are the experimental conditions which Kemball et al.[71] used. Stannic oxide, showing considerable isomerization activity, had been

pretreated at a low temperature of 473 K.

Attaching no significance to the slight variation of the initial product ratios observed for the tin-antimony mixed oxides of a particular series, the average initial cis but-2-ene/trans but-2-ene product ratios for the L.T. and H.T. series are 3.4 and 1.2, respectively. This is illustrated by Tables 9.1, 9.2 and 9.3. Tables 9.13, 9.14 and 9.15, show that the average initial trans but-2-ene/but-1-ene product ratios found for the L.T. and H.T. series are 3.6 and 3.5, respectively. Thus, it was only in the case of but-1-ene isomerization that different average initial product ratios were observed for the two methods of pretreatment.

Over the L.T. series, but-1-ene isomerization resulted in an average initial cis but-2-ene/trans but-2-ene product ratio of 3.4. This value suggests that a mechanism involving a secondary butyl radical is unlikely. Such a mechanism, discussed in Section 5.5, results in an initial trans but-2-ene/cis but-2-ene product ratio >1 at low temperatures. However, initial cis but-2-ene/trans but-2-ene product ratios >1 have been explained for but-1-ene isomerization over basic and acidic catalysts. Haag and Pines[67], studying catalysts such as sodium-on-alumina and lithium-on-alumina, believed that the double-bond shift occurred by a mechanism involving allylic carbanion intermediates. Such a mechanism was thought to account for a fast but-1-ene to cis but-2-ene interconversion, resulting in an initial cis but-2-ene/trans but-2-ene product ratio of 4. The high initial product ratio was thought to be due to the stability of the cis anion brought about by the formation of a cyclic intermediate. This intermediate is illustrated in Section 5.4.

Leftin and Hermana[65], studying but-1-ene isomerization over a silica-alumina catalyst, rationalized their observed initial product ratios in terms of a butenyl carbonium ion. Assuming a staggered conformation around C_3 in but-1-ene, trans and gauche conformations are possible. Lewis acid attack on the trans and gauche conformers, without rearrangement, will result in the formation of trans and cis but-2-ene, respectively. They argued that as two equivalent gauche structures for but-1-ene are possible, on statistical grounds, a maximum cis but-2-ene/trans but-2-ene ratio of 2 would be expected for catalysts possessing strong Lewis-type acidity. However, they did not preclude the possibility that higher cis but-2-ene/trans but-2-ene product ratios would be obtained if the adsorption-desorption rates for the gauche conformations were greater than those for the trans conformation.

Foster and Cvetanović[68], studying but-1-ene isomerization over a variety of acid catalysts, concluded that high initial cis but-2-ene/trans but-2-ene product ratios were consistent with a mechanism involving a carbonium ion. However, Haag and Pines[29], and Lucchesi et al.[108] believed that high initial product ratios, formed as a result of but-1-ene isomerization, could not be reconciled with conventional carbonium ion theory. Haag and Pines[29], studying alumina, observed initial cis but-2-ene/trans but-2-ene product ratios of 2-4. They also found similar rates for double-bond shift and cis but-2-ene to trans but-2-ene interconversion. This observation surprised them. Migration of the double-bond involves the breaking of a carbon-hydrogen bond and the formation of a new one, whereas cis but-2-ene to trans but-2-ene interconversion

requires untying of a π-bond. Thus, bond breaking was not occurring in the rate-determining step. The similarity in the rates of the two processes suggested that both occurred by the same mechanism. A secondary butyl carbonium ion was proposed as the common intermediate. The elimination of a proton from the secondary butyl carbonium ion proceeded through the rearrangement to a π-complex in a slow step, with a subsequent rapid loss of the proton. Such a mechanism was believed to account for the high initial product ratios. A diagram of the mechanism is given in Section 5.3.

The activity patterns for but-1-ene and cis but-2-ene isomerization over the L.T. series, Figures 9.3 and 9.11, are similar. This infers that double-bond shift and cis but-2-ene to trans but-2-ene isomerization take place on similar sites. An insight into the nature of these sites is gained from the fact that the but-1-ene and cis but-2-ene activity patterns are like the ones found for 3,3-dimethylbut-1-ene isomerization, cyclopropane isomerization and isopropanol dehydration, over the tin-antimony mixed oxides of the L.T. series. Thus, but-1-ene and cis but-2-ene isomerization, over the L.T. series, probably take place via Brønsted-type acidic sites. In keeping with a mechanism involving Brønsted-type acidic sites is the average initial trans but-2-ene/but-1-ene product ratio of 3.6. Mechanisms involving allylic carbanions[66], butenyl (allylic) carbonium[65] ions are expected to result in low initial trans but-2-ene/but-1-ene product ratios, due to the lack of rotation about the allylic intermediate. In keeping with this, Foster and Cvetanović[68] reported that but-2-ene isomerization over potassium hydroxide resulted in but-1-ene formation only.

In an early investigation Misono et al.,[109] studying

cis but-2-ene isomerization over a range of metal sulphates, were able to show that the initial product ratio depended upon the acid strength of the catalyst. The initial product ratio increased with increase in the acid strength of the catalyst. In a later study Misono and Yoneda[110], studying n-butene isomerization over aluminium sulphate as a typical strong acid catalyst and magnesium sulphate as a typical weak acid catalyst, attempted to clarify the correlation between selectivity and acid strength by the use of energy diagrams similar to the one used by Hightower and Hall[64]. The increase in the initial but-2-ene/but-1-ene product ratio, with increasing acid strength, was explained by a decrease in the height of the energy barrier to but-2-ene formation relative to but-1-ene formation.

The resemblance between the carbonium ion intermediate and the transition state was believed to increase as the stability of the carbonium ion decreased. A stable carbonium ion intermediate was said to be formed over the stronger acid catalyst aluminium sulphate. Thus, the energy barrier of but-2-ene formation was believed to be lower than that of but-1-ene formation due to the fact that the transition states reflected the energy differences of the n-butene isomers. Such an interpretation rationalized the high initial trans but-2-ene/but-1-ene product ratio (6.9) and the similarities in the reactivities of the n-butenes over aluminium sulphate. However, the energy differences between the transition states of the n-butene isomers for the weaker acid catalyst, magnesium sulphate, were believed to be small, due to the fact that a less stable carbonium ion intermediate was formed. This explained the low initial trans but-2-ene/but-1-ene product ratio (1.2) and the large differences between the reactivities of the n-butene isomers observed for magnesium sulphate.

Thus, according to the results of Misono and Yoneda[110], the average initial trans but-2-ene/but-1-ene product ratio of 3.6 and the lower reactivity for cis but-2-ene isomerization relative to but-1-ene isomerization suggests that the active sites of the L.T. series tin-antimony mixed oxides are moderately acidic. In accordance with this are the results for 3,3-dimethylbut-1-ene isomerization, which have been discussed earlier. The only products observed over the tin-antimony mixed oxides of the L.T. series, were 2,3-dimethylbut-1-ene and 2,3-dimethylbut-2-ene. This infers that strongly acidic sites[29] are not present.

Although the results for cis but-2-ene isomerization over the tin-antimony mixed oxides of the L.T. series can be correlated with the findings of Misono and Yoneda[110], the ones for but-1-ene isomerization do not. Misono and Yoneda[110], in accordance with the interpretations put forward by Hightower and Hall[64] for a common secondary butyl carbonium intermediate, found initial cis but-2-ene/trans but-2-ene product ratios of approximately 1 for both catalysts. However, the average initial cis but-2-ene/trans but-1-ene product ratio observed for the tin-antimony mixed oxides of the L.T. series was 3.4. Such a ratio is similar to the ones reported by Haag and Pines[29]. They postulated, discussed in Section 5.3, a mechanism involving π-complex formation to account for the high initial product ratios and the similarities in the rates for double-bond shift and cis but-2-ene to trans but-2-ene isomerization. However, the rates for the two types of isomerization over the tin-antimony mixed oxides of the L.T. series are different. This is illustrated by comparing the cis but-2-ene isomerization rates given in Table 9.13 with the corresponding ones

quoted in Table 9.1, for but-1-ene isomerization.

Mentioned earlier was the fact that the activity patterns for but-1-ene and cis but-2-ene isomerization were similar, suggesting that similar sites were involved. Separately, the results for but-1-ene and cis but-2-ene isomerization over the L.T. series mixed oxides are, in general, in accordance with the findings of Haag and Pines[29] and Misono and Yoneda[110], respectively. It is difficult to account completely for both reactions in terms of a single interpretation. However, all the evidence, for both reactions, favours a mechanism involving carbonium ions in which Brønsted-type acidic sites play a major role. This view is further supported by the effect that 2,6-dimethylpyridine pretreatment had on but-1-ene and cis but-2-ene isomerization.

Tables 9.7 and 9.18 show that pretreatment with 2,6-dimethylpyridine decreased the activity of the tin-antimony mixed oxides of the L.T. series for but-1-ene and cis but-2-ene isomerization, respectively, but had no significant effect upon the initial product ratios. This implies that double-bond shift and cis but-2-ene to trans but-2-ene interconversion are affected to the same extent. Jacobs and Heylen[111], studying 2,6-dimethylpyridine and pyridine adsorption on a series of zeolites by means of infra-red spectroscopy, obtained evidence to support the idea that 2,6-dimethylpyridine shows a high selectivity towards Brønsted-type acidic sites in the presence of Lewis-type acidic sites. Weaker bonds were believed to be formed with Lewis-type acidic sites due to the steric effects of the methyl groups in positions 2 and 6. In a later investigation, Jacobs et al.[106] used the same technique to show that hydroxyl groups were responsible for n-butene isomerization over a series of zeolites. Thus, the poisoning effect of pretreatment with 2,6-dimethylpyridine on the

activity for but-1-ene and cis but-2-ene isomerization is consistent with a mechanism involving Brønsted-type acidic sites.

A comparison between the n-butene isomerization results of the mixed oxides of the L.T. series with those of the H.T. series reveals a number of interesting facts. A similar average initial trans but-2-ene/but-1-ene product ratio was observed for both series. However, but-1-ene isomerization over the mixed oxides of the L.T. and H.T. series gave rise to average initial cis but-2-ene/trans but-2-ene product ratios of 3.4 and 1.2, respectively. Unlike the situation encountered with the mixed oxides of the L.T. series, two different activity patterns were observed for but-1-ene and cis but-2-ene isomerization with the mixed oxides of the H.T. series.

Initial cis but-2-ene/trans but-2-ene product ratios close to 1 are considered by a number of investigators[64][68][110] to be in accordance with a mechanism involving a carbonium ion. The way in which Hightower and Hall[64] accounted for such a value, has already been described in Section 5.3. Thus, a possible mechanism for but-1-ene isomerization, over the mixed oxides of the H.T. series, may be one involving a secondary butyl carbonium ion. However, Figures 9.4 and 8.4 show that the activity pattern found for but-1-ene isomerization is unlike the one obtained for 3,3-dimethylbut-1-ene isomerization. As 3,3-dimethylbut-1-ene isomerization is believed to involve carbonium ion formation[29], it is surprising to find that their activity patterns differ. The isomerization of but-1-ene resulted in an activity pattern similar to the one observed for cyclopropane isomerization over the H.T. series mixed oxides, Figure 8.14.

Mentioned earlier, was the possibility that cyclopropane isomerization, over the mixed oxides of the H.T. series, takes place

via Brønsted-type and Lewis-type acidic sites, simultaneously. A similar situation may exist for but-1-ene isomerization. Thus, over the mixed oxides of the H.T. series, 3,3-dimethylbut-1-ene isomerization takes place via Brønsted-type acidic sites only, but cyclopropane and but-1-ene isomerization may take place via Brønsted-type and Lewis-type acidic sites. Such a situation would account for the fact that the activity patterns for cyclopropane and but-1-ene isomerization are unlike the one observed for 3,3-dimethylbut-1-ene isomerization. A situation in which cis but-2-ene isomerization occurred over the two types of acidic sites was reported by Ballivet et al.[112][113]. Ballivet et al.[112][113], studying cis but-2-ene isomerization over four silica-aluminas, attributed their activity to both types of acidic sites. Activity was found to decrease according to two experimental laws, one of which was correlated qualitatively with Lewis-type acidic sites and the other with Brønsted-type acidic sites.

It is possible, to some extent, to account for an initial cis but-2-ene/trans but-2-ene product ratio of 1.2 by a mechanism involving a butenyl carbonium ion as well as by one involving a secondary butyl carbonium ion. Leftin and Hermana[65], studying but-1-ene isomerization over silica-alumina, observed initial cis but-2-ene/trans but-2-ene product ratios of 1.2-1.7. Lewis-type acidic sites resulting in butenyl carbonium ions, were thought to be responsible for but-1-ene isomerization.

Several other factors support the possibility that but-1-ene isomerization, over the mixed oxides of the H.T. series, takes place via Brønsted-type and Lewis-type acidic sites. Consistent with a mechanism involving Brønsted-type acidic sites[111] is the decrease in but-1-ene isomerization activity observed for a mixed oxide of

the H.T. series, which had been pretreated with 2,6-dimethylpyridine. This is illustrated by Table 9.8. Several investigators made observations believed to be consistent with but-1-ene isomerization via Lewis-type acidic sites. Sala and Trifirò[73] found that the ability of a tin-antimony mixed oxide to isomerize but-1-ene increased with rise in calcination temperature. This observation and the inhibiting effect of water were thought to support a mechanism involving Lewis-type acidic sites. Alieva et al.[72], studying but-1-ene isomerization over a tin-antimony mixed oxide (atomic ratio Sn:Sb = 4:1) reported that the addition of alkali metals resulted in a decrease in activity. This was believed to be due to the neutralization of Lewis-type acidic sites. Thus, there is evidence to support the idea that but-1-ene and cyclopropane isomerization, over the mixed oxides of the H.T. series, may take place via Brønsted-type and Lewis-type acidic sites. However, the results obtained for cis but-2-ene isomerization seem to favour carbonium ion formation via Brønsted-type acidic sites only.

There are two factors which support the view that cis but-2-ene isomerization, over the mixed oxides of the H.T. series, takes place via Brønsted-type acidic sites. One of these is the fact that similar average initial trans but-2-ene/but-1-ene product ratios are observed for the L.T. and H.T. series. These values are 3.6 and 3.5 for the L.T. and H.T. series, respectively. (The fact that an initial trans but-2-ene/but-1-ene product ratio of 3.6 is consistent with a carbonium ion mechanism has already been discussed for the L.T. series mixed oxides). The second factor is the decrease in activity of a H.T. series mixed oxide, Table 9.19, after pretreatment with 2,6-dimethylpyridine. However, the fact that maximum activity for cis but-2-ene isomerization takes place

with the 7.4 atom % Sb and 8.7 atom % Sb mixed oxides, Figure 9.12, is not consistent with a mechanism involving Brønsted-type acidic sites. Maximum activity for 3,3-dimethylbut-1-ene isomerization is observed with the 26.8 atom % Sb mixed oxide, Figure 8.4.

A number of investigators have observed deactivation taking place during n-butene isomerization. Baird and Lunsford[114], studying but-1-ene isomerization over magnesium oxide, concluded that preferential adsorption of cis but-2-ene resulted in deactivation of the sites responsible for the carbanion mechanism. A similar conclusion was made by Peri[115] who believed that Lewis-type acidic sites were responsible for but-1-ene isomerization and the strong adsorption of cis but-2-ene on γ-alumina. Jacobs et al.[106], investigating n-butene isomerization over a series of zeolites, observed that there was a rapid conversion of but-1-ene to but-2-ene prior to deactivation. Infrared spectroscopy revealed the presence of hydrogen deficient polymeric species on the surface and also showed that hydroxyl groups were irreversibly involved.

The number of Brønsted-type and Lewis-type acidic sites, present on the mixed oxides of the H.T. series, will depend on the composition of the catalyst. Selective sites, Brønsted-type or Lewis-type, may adsorb cis but-2-ene strongly and give rise to deactivation. Thus, the extent of deactivation by cis but-2-ene will be a function of the catalyst composition. This may account for the fact that cis but-2-ene isomerization, over the mixed oxides of the H.T. series, gave rise to an activity pattern unlike the one obtained for 3,3-dimethylbut-1-ene isomerization. The average initial trans but-2-ene/but-1-ene product ratio of 3.5 and the retarding effect of pretreatment with 2,6-dimethylpyridine suggests, like 3,3-dimethylbut-1-ene isomerization, that Brønsted-type acidic sites may be

responsible for cis but-2-ene isomerization over the mixed oxides of the H.T. series. If deactivation by strongly adsorbed cis but-2-ene accounts for the fact that maximum activity was observed with the 7.4 atom % Sb and 8.7 atom % Sb mixed oxides, instead of the 26.8 atom % Sb mixed oxide, then the 19.6 atom % Sb and 26.8 atom % Sb mixed oxides must be particularly susceptible to poisoning by cis but-2-ene. On the other hand, the mixed oxides of the L.T. series display similar activity patterns for 3,3-dimethylbut-1-ene and cis but-2-ene isomerization suggesting that deactivation by cis but-2-ene does not occur to any significant extent.

In keeping with the view that deactivation by cis but-2-ene occurs more readily with the mixed oxides of the H.T. series than with those of the L.T. series is the fact that a low average initial cis but-2-ene/trans but-2-ene product ratio is observed for the H.T. series. However, the activity patterns for but-1-ene and cis but-2-ene isomerization are different. This suggests that unlike the situation encountered for cis but-2-ene isomerization, deactivation by cis but-2-ene is not the major factor which determines the but-1-ene isomerization activity pattern for the H.T. series. Thus, the possibility that the activity pattern for but-1-ene isomerization over the H.T. series mixed oxides is a function of both types of acidic sites is not ruled out. On the other hand, most of the evidence infers that cis but-2-ene isomerization takes place via Brønsted-type acidic sites and the factor influencing the shape of the activity pattern may be the extent to which cis but-2-ene is irreversibly adsorbed by a particular mixed oxide.

An interesting observation was the fact that increasing the pressure of the reactant but-1-ene resulted in a decrease in the activity of a H.T. series mixed oxide, Table 9.9. Such an

observation is in keeping with the view that the mixed oxides of the H.T. series are susceptible to deactivation by cis but-2-ene. Increasing the pressure of but-1-ene, leading to an initial increase in double-bond shift, will result in an increase in cis but-2-ene formation.

Conclusion

Combining stannic oxide and antimony tetroxide results in an acidic catalyst. The number and nature of the acidic sites are determined by the percentage composition of the catalyst and their pretreatment.

Isopropanol dehydration, 3,3-dimethylbut-1-ene, cyclopropane and n-butene isomerization over the tin-antimony mixed oxides, outgassed at 293 K for 5 hr , are believed to take place on Brønsted-type acidic sites.

For the tin-antimony mixed oxides of composition >6.2 atom % Sb, outgassed at 698 K for 16 hr , Brønsted-type acidic sites are thought to be responsible for isopropanol dehydration, 3,3-dimethyl-but-1-ene and cis but-2-ene isomerization. However, Brønsted and Lewis-type acidic sites may account for cyclopropane and but-1-ene isomerization.

Evidence suggests that the ability of the H.T. series catalysts to dehydrogenate isopropanol is associated with stannic oxide, an n-type semiconductor.

CHAPTER 11

Oxidative Dehydrogenation of n-Butenes

11.1 Chromatographic Column

The column and operating conditions were identical to those used for the n-butene isomerization studies described in Section 9.1. The retention times, measured according to Section 7.7 were:-

but-1-ene = 1.0 min

trans but-2-ene = 3.5 min

cis but-2-ene = 5.0 min

butadiene = 7.6 min

11.2 Relative Sensitivity Factors

Measured according to Section 7.8:-

but-1-ene = 1

trans but-2-ene = 1.3

cis but-2-ene = 1.3

butadiene = 1.2

11.3 Experimental Procedure

The samples were pretreated according to the two methods described in Section 7.11. The reaction mixture was made up in bulb G, Figure 7.1, 60 min. before the start of the reaction. This allowed time for a completely homogeneous mixture to be obtained. It contained air to n-butene in the ratio of 6:1.

At the end of the outgassing period, the sample was isolated from the pumping system at a pressure of 133 $\mu N\ m^{-2}$ (10^{-6} Torr). The

OXIDATIVE DEHYDROGENATION OF BUT-1-ENE

474 K

49.5 ATOM % Sb H.T. Series

FIGURE 11.1

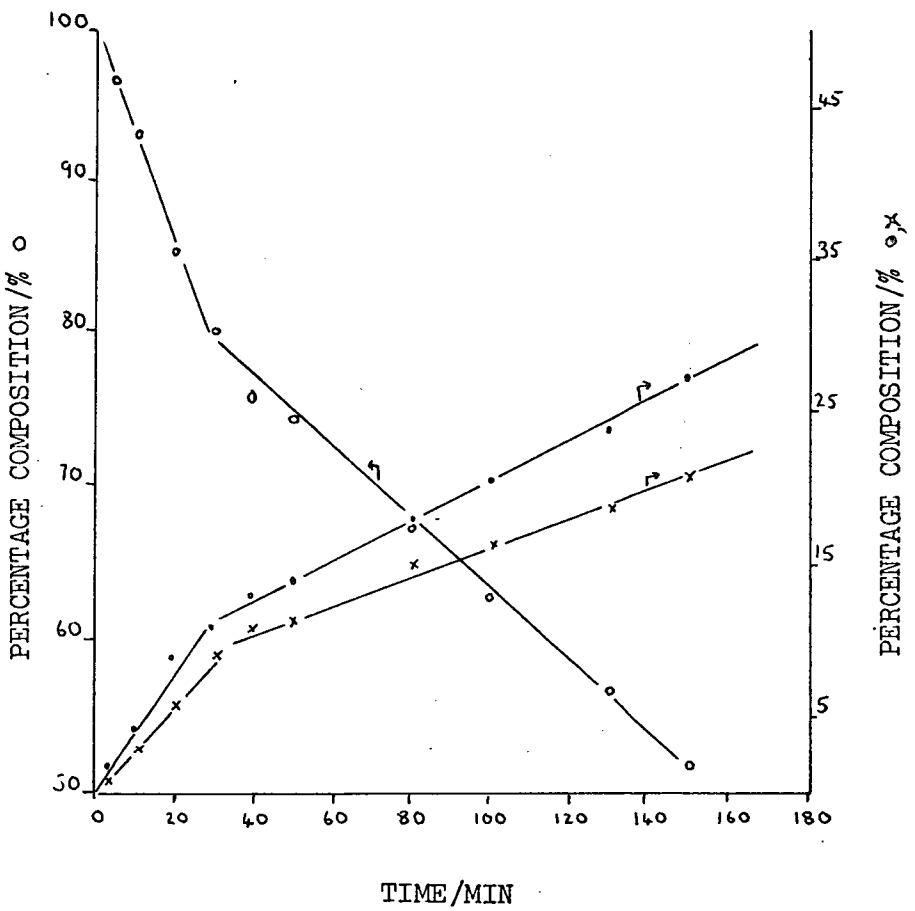

reaction vessel at a temperature of 474 K, the reaction mixture was admitted by expansion to give a total pressure of 5.99 kN m^{-2} (45 Torr). The partial pressure of n-butene was 0.86 kN m^{-2} (6.4 Torr), which was equivalent to 3.63×10^{19} molecules. The standard experimental procedure was then carried out.

11.4 Treatment of Results

For both series, the oxidative dehydrogenation of but-1-ene, cis but-2-ene and trans but-2-ene was accompanied by considerable isomerization. A reaction temperature of 474 K was found to be the most suitable one for all three reactants. The isomerization rates were obtained from plots of the sum of the percentage compositions of the isomerization products against time. Percentage composition versus time plots were also used to measure the rates of butadiene appearance. Initial product ratios were obtained during stage S_1.

11.5 Oxidative Dehydrogenation of But-1-ene with the H.T. Series

The products formed were cis but-2-ene, trans but-2-ene and butadiene. A typical percentage composition versus time plot is illustrated by Figure 11.1. Selectivity towards isomerization and butadiene formation was found to vary with the catalyst composition. The selectivities are presented in Table 11.1.

TABLE 11.1

H.T. Series Outgassed at 698 K for 16 hr

Reaction Temperature 474 K

Cat.Comp./ Atom % Sb	Se_1/% at 10 min		Se_2/% at 80 min	
	Ct	bd	Ct	bd
6.2		100		100
8.7	13.8	86.2	16.0	84.0
19.6	42.9	57.1	38.4	61.6
26.8	60.5	39.5	59.2	40.8
49.5	55.5	44.5	54.4	45.6
75.0	90.0	10.0	91.1	8.9

ct = cis but-2-ene + trans but-2-ene

bd = butadiene

The 6.2 atom % Sb and 8.7 atom % Sb mixed oxides showed the greatest selectivity for butadiene formation. The 75.0 atom % Sb mixed oxide was the least selective catalyst for butadiene formation. There was no significant change in selectivity with time.

The sum of the rates of appearance of cis but-2-ene and trans but-2-ene R_{1ct}, R_{2ct} and the rates of appearance of butadiene R_{1bd}, R_{2bd}, are presented in Tables 11.2 and 11.3 respectively.

H.T. Series Outgassed at 698 K for 16 hr

Reaction Temperature 474 K

TABLE 11.2

Cat.Comp./ Atom % Sb	$R_{1ct}/10^{-3}$ % min^{-1} m^{-2}	$R_{2ct}/10^{-3}$ % min^{-1} m^{-2}	initial cis/trans
0	0	0	-
6.2	0	0	-
8.7	21	5.0	1.4
19.6	77	19	1.8
26.8	420	108	1.4
49.5	196	49	1.9
75.0	440	140	1.5
100	0	0	-

TABLE 11.3

Cat.Comp./ Atom % Sb	$R_{1bd}/10^{-3}$ % min^{-1} m^{-2}	$R_{2bd}/10^{-3}$ % min^{-1} m^{-2}
0	0	0
6.2	26	19
8.7	460	95
19.6	190	46
26.8	81	27
49.5	145	39
75.0	30	11
100	0	0

ACTIVITY PATTERNS FOR THE OXIDATIVE DEHYDROGENATION OF BUT-1-ENE WITH THE H.T. SERIES

474 K

ISOMERIZATION PRODUCTS FORMATION

FIGURE 11.2

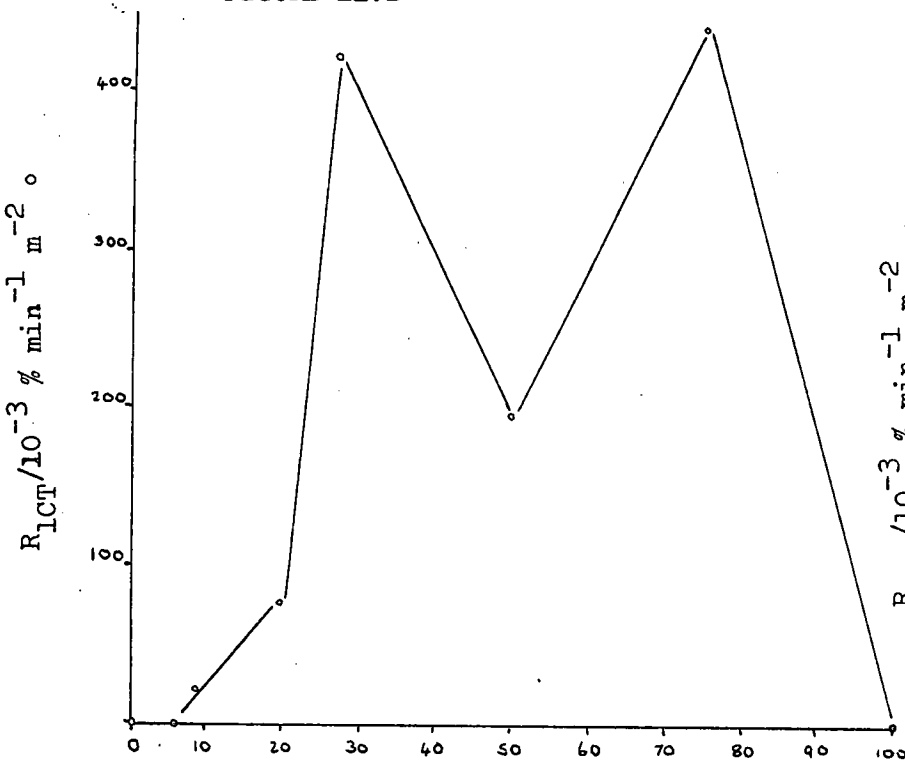

BUTADIENE FORMATION

FIGURE 11.3

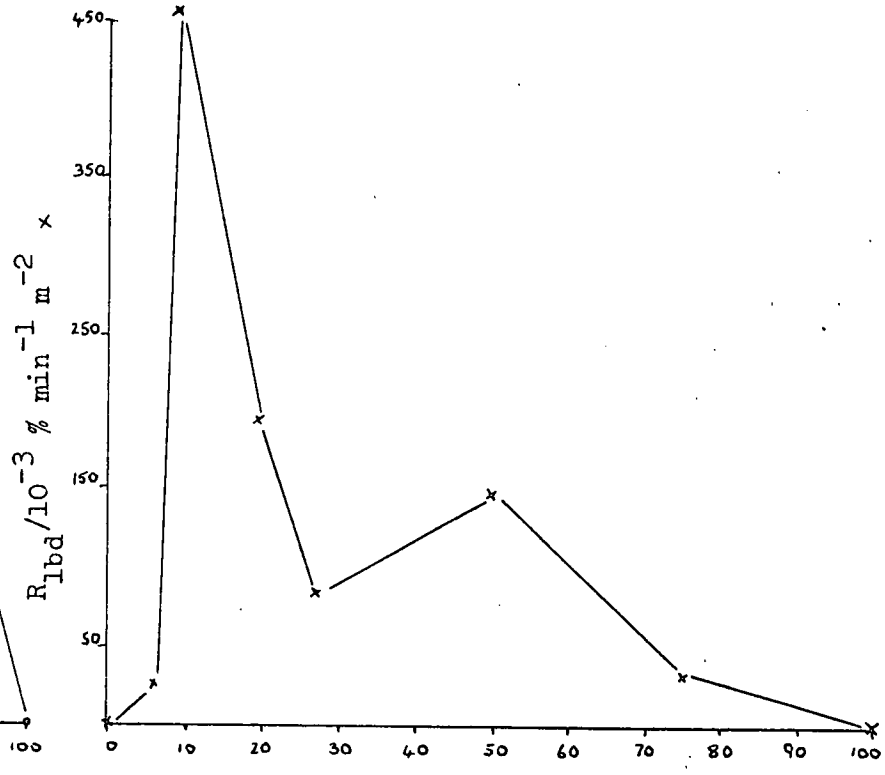

CAT.COMP./ATOM % Sb

The initial cis but-2-ene/trans but-2-ene product ratios indicated that the formation of cis but-2-ene was favoured. Stannic oxide and antimony tetroxide showed no activity for butadiene formation or but-1-ene isomerization. The 6.2 atom % Sb mixed oxide was only active for butadiene formation. The 8.7 atom % Sb and 19.6 atom % Sb mixed oxides showed more activity for butadiene formation than for but-1-ene isomerization. The remaining mixed oxides in the series, were found to be more active for but-1-ene isomerization.

The opposite trends observed in the two activity patterns for the tin-antimony mixed oxides are illustrated by Figures 11.2 and 11.3. Maximum activity for but-1-ene isomerization and butadiene formation was seen with the 75.0 atom % Sb and 8.7 atom % Sb mixed oxides, respectively. For the catalyst composition region of 8.7 atom % Sb to 26.8 atom % Sb, an increase in the antimony content resulted in a decrease in butadiene formation and an increase in but-1-ene isomerization. Increasing the antimony content to give a catalyst composition of 49.5 atom % Sb led to an increase in butadiene formation and a decrease in but-1-ene isomerization. A further increase in the antimony content to give a catalyst composition of 75.0 atom % Sb resulted in a decrease in butadiene formation and an increase in but-1-ene isomerization.

Rate values for repeat experiments are given in Tables 11.4 and 11.5.

H.T. Series Outgassed at 698 K for 16 hr

Reaction Temperature 474 K

TABLE 11.4

Cat.Comp./ Atom % Sb	$R_{1ct}/10^{-3}$ % min^{-1} m^{-2}	$R_{2ct}/10^{-3}$ % min^{-1} m^{-2}	initial cis/trans
6.2*	0	0	-
6.2	0	0	-
26.8*	420	108	1.4
26.8	403	102	1.9

TABLE 11.5

Cat.Comp./ Atom % Sb	$R_{1bd}/10^{-3}$ % min^{-1} m^{-2}	$R_{2bd}/10^{-3}$% min^{-1} m^{-2}
6.2*	26	19
6.2	24	18
26.8*	81	27
26.8	75	29

*values quoted in Tables 11.2 and 11.3

The average difference in the rate values was 5%. Changes of greater than $\pm$5% in the activity patterns were taken to be significant.

11.6 Reaction of But-1-ene at 474 K in the Absence of Air

An experiment was carried out to find the extent of butadiene formation in the absence of air, at 474 K. The 8.7 atom % Sb mixed oxide, pretreated according to the H.T. method, was used. The but-1-ene pressure was the same as the partial pressure of but-1-ene used in the reaction mixture given in Section 11.3. The rates of but-1-ene isomerization and butadiene formation are presented in Tables 11.6 and 11.7.

Reaction of But-1-ene at 474 K

H.T. Series Outgassed at 698 K for 16 hr

Reaction Temperature 474 K

TABLE 11.6

Cat.Comp./ Atom % Sb	$R_{1ct}/10^{-3}$ % min^{-1} m^{-2}	$R_{2ct}/10^{-3}$ % min^{-1} m^{-2}	initial cis/trans
8.7*	21	5.0	1.4
8.7	32	9.4	1.3

TABLE 11.7

Cat.Comp./ Atom % Sb	$R_{1bd}/10^{-3}$ % min^{-1} m^{-2}	$R_{2bd}/10^{-3}$ % min^{-1} m^{-2}
8.7*	460	95
8.7	40	5

*values for air+but-1-ene mixture quoted in Tables 11.2 and 11.3

OXIDATIVE DEHYDROGENATION OF CIS BUT-2-ENE
474 K

26.8 Atom % Sb H.T. Series

FIGURE 11.4

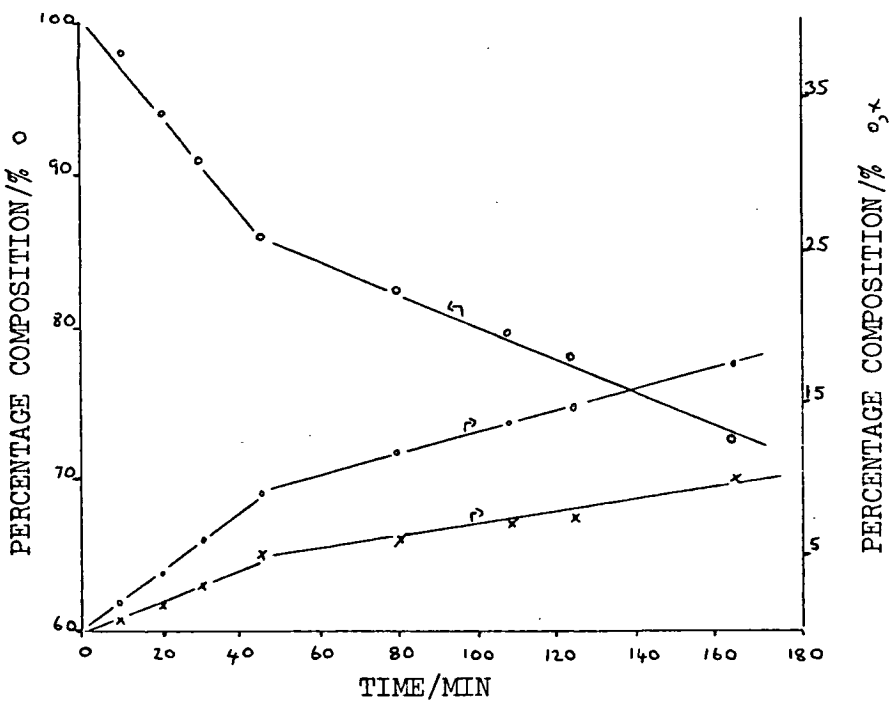

o CIS BUT-2-ENE

o TRANS BUT-2-ENE + BUT-1-ENE
x BUTADIENE

The absence of air resulted in an increase in but-1-ene isomerization and a reduction in butadiene formation.

11.7 Oxidative Dehydrogenation of Cis But-2-ene with the H.T. Series

Figure 11.4 illustrates a typical percentage composition versus time plot. The products formed were trans but-2-ene, but-1-ene and butadiene. Selectivity for cis but-2-ene isomerization and butadiene formation was found to depend on the catalyst composition. The selectivities are presented in Table 11.8.

TABLE 11.8

H.T. Series Outgassed at 698 K for 16 hr

Reaction Temperature 474 K

Cat.Comp./ Atom % Sb	Se_1/% at 20 min		Se_2/% at 80 min	
	tb	bd	tb	bd
6.2*	47.1	52.9	40.7	59.3
8.7	55.3	44.7	52.2	47.8
19.6	36.6	63.4	36.0	64.0
26.8	66.7	33.3	63.2	36.8
49.5	88.5	11.5	81.8	18.2
75.0	81.2	18.8	80.3	19.7

trace* amount only of but-1-ene

tb = trans but-2-ene + but-1-ene

bd = butadiene

Selectivity did not change significantly with time. The majority of the mixed oxides showed a greater selectivity for cis but-2-ene isomerization than for butadiene formation. The greatest selectivity for butadiene formation was found with the 19.6 atom % Sb mixed oxide. The sum of the rates of appearance of trans but-2-ene and but-1-ene R_{1tb}, R_{2tb} and the rates of appearance of butadiene R_{1bd}, R_{2bd} are given in Tables 11.9 and 11.10, respectively.

H.T. Series Outgassed at 698 K for 16 hr

Reaction Temperature 474 K

TABLE 11.9

Cat.Comp./ Atom % Sb	$R_{1tb}/10^{-3}$ % min^{-1} m^{-2}	$R_{2tb}/10^{-3}$ % min^{-1} m^{-2}	initial trans/but-1-ene
0	0	0	-
6.2*	6.8	4.1	~100% trans
8.7	20	9.0	3.1
19.6	49	25	3.5
26.8	45	21	3.0
49.5	36	20	2.6
75.0	47	24	2.6
100	0	0	-

ACTIVITY PATTERNS FOR THE OXIDATIVE DEHYDROGENATION OF CIS BUT-2-ENE WITH THE H.T. SERIES 474 K

Isomerization Products Formation
FIGURE 11.5

BUTADIENE FORMATION

Figure 11.6

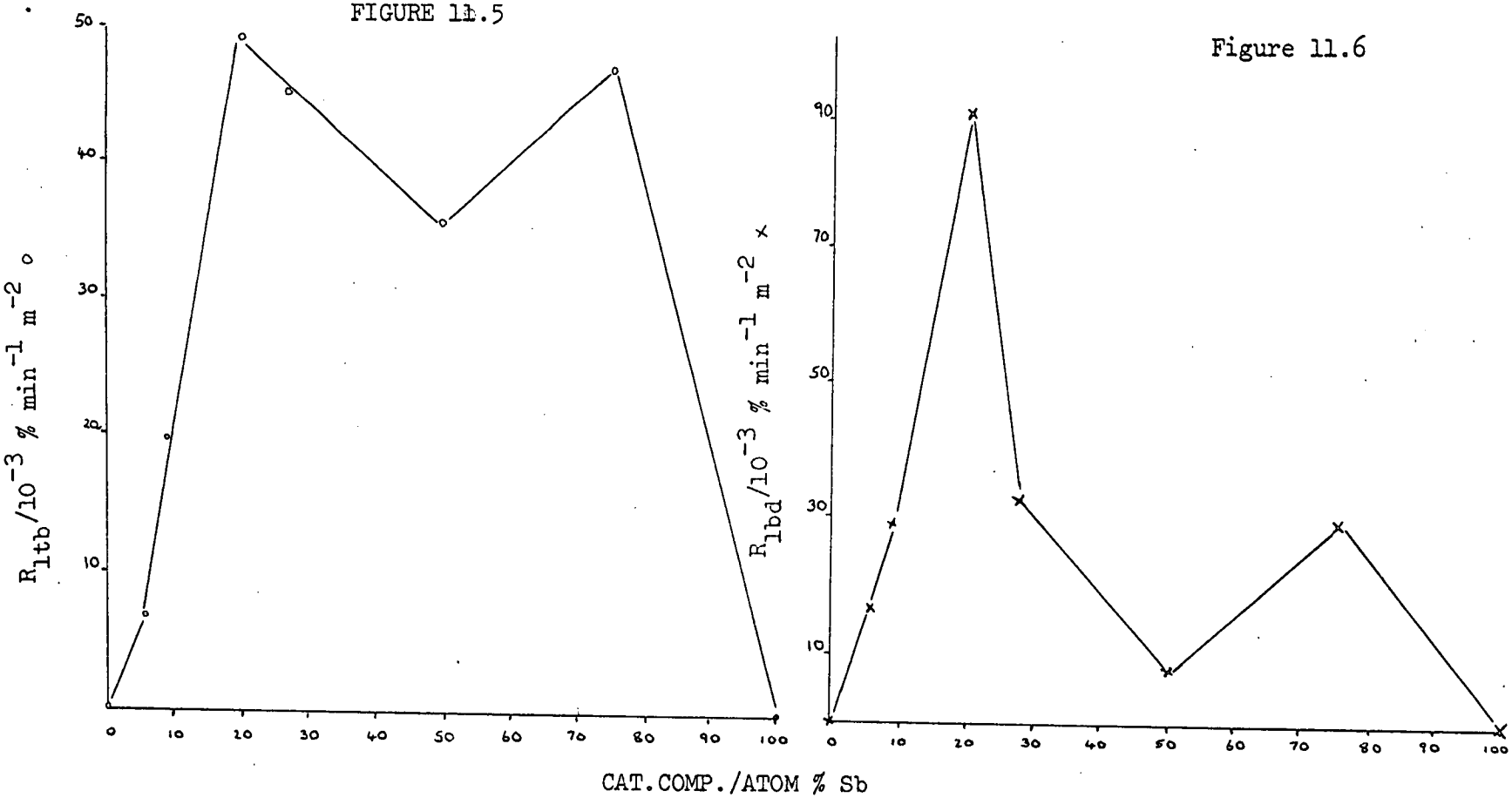

TABLE 11.10

Cat.Comp./ Atom % Sb	$R_{1bd}/10^{-3}$ % min^{-1} m^{-2}	$R_{2bd}/10^{-3}$ % min^{-1} m^{-2}
0	0	0
6.2	17	4.8
8.7	29	11
19.6	89	30
26.8	33	9.8
49.5	8.1	6.6
75.0	30	9.0
100	0	0

*traces only of but-1-ene

Stannic oxide and antimony tetroxide were found to be inactive. The percentage of but-1-ene formed with the 6.2 atom % Sb mixed oxide never exceeded 0.5%. The initial trans but-2-ene/but-1-ene product ratios indicated that trans but-2-ene formation was favoured. Similar activity patterns, with maximum activity with the 19.6 atom % Sb mixed oxide, were found for cis but-2-ene isomerization and butadiene formation. The activity patterns are presented in Figures 11.5 and 11.6. In the catalyst composition region of 6.2 atom % Sb to 19.6 atom % Sb, an increase in the antimony content resulted in an increase in activity. Activity was reduced with increasing antimony content in the catalyst composition region of 19.6 atom % Sb to 49.5 atom % Sb. A further increase in activity was observed when the antimony content was increased to 75.0 atom % Sb.

Repeat experiments gave an indication of the reproducibility in the rate values. The rate values are presented in Tables 11.11 and 11.12.

H.T. Series Outgassed at 698 K for 16 hr

Reaction Temperature 474 K

TABLE 11.11

Cat.Comp./ Atom % Sb	$R_{1tb}/10^{-3}$ % min^{-1} m^{-2}	$R_{2tb}/10^{-3}$ % min^{-1} m^{-2}	initial trans/but-1-ene
8.7*	20	9.0	3.1
8.7	19	8.7	3.2
75.0*	47	24	2.6
75.0	45	22	2.4

TABLE 11.12

Cat.Comp./ Atom % Sb	$R_{1bd}/10^{-3}$ % min^{-1} m^{-2}	$R_{2bd}/10^{-3}$ % min^{-1} m^{-2}
8.7*	29	11
8.7	27	11
75.0*	30	9.0
75.0	28	8.7

Values* quoted in Tables 11.9 and 11.10.

The average difference in the rate values was 5%. Consequently, changes of greater than $\pm 5\%$ were regarded as significant.

OXIDATIVE DEHYDROGENATION OF TRANS BUT-2-ENE

474 K

26.8 Atom % Sb H.T. Series

FIGURE 11.7

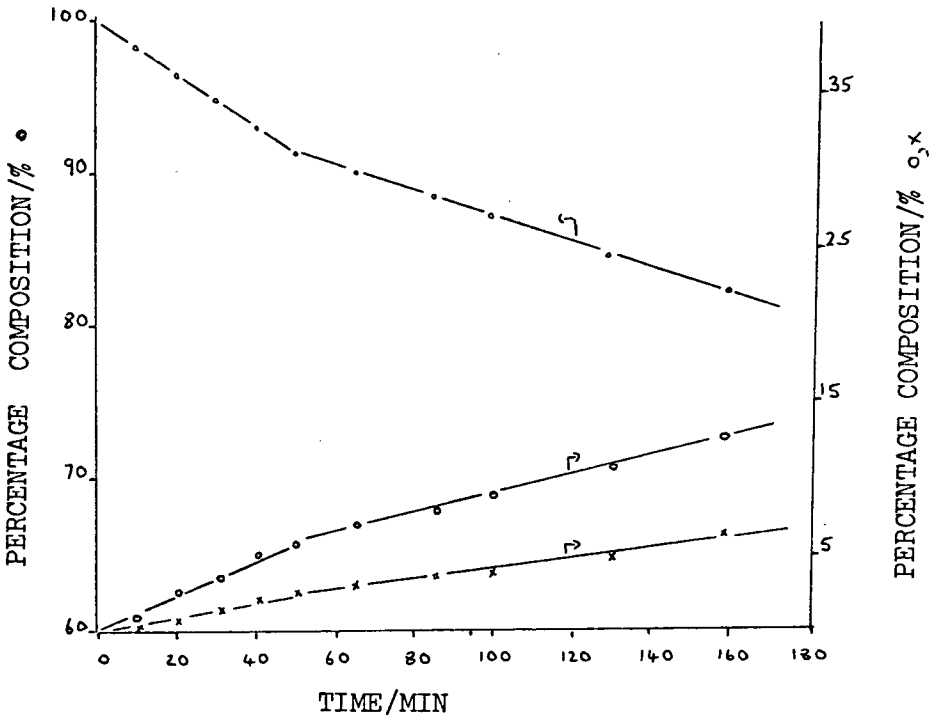

• TRANS BUT-2-ENE

o CIS BUT-2-ENE + BUT-1-ENE

x BUTADIENE

11.8 Oxidative Dehydrogenation of Trans But-2-ene with the H.T. Series

A typical percentage composition versus time plot is presented in Figure 11.7. The products formed were cis but-2-ene, but-1-ene and butadiene. Selectivity towards isomerization or butadiene formation was found to depend on the catalyst composition. The selectivities are presented in Table 11.13.

TABLE 11.13

H.T. Series Outgassed at 698 K for 16 hr

Reaction Temperature 474 K

Cat.Comp./ Atom % Sb	Se_1/% at 20 min		Se_2/% at 80 min	
	cb	bd	cb	bd
6.2*	60.0	40.0	59.1	40.9
8.7	47.3	52.7	50.0	50.0
19.6	46.6	53.4	46.7	53.3
26.8	78.4	21.6	70.1	29.9
49.5	68.5	31.5	66.7	33.3
75.0	80.5	19.5	75.9	24.1

trace* amounts only of but-1-ene

cb = cis but-2-ene + but-1-ene

bd = butadiene

Selectivity did not alter significantly with time. The majority of mixed oxides showed a greater selectivity for trans but-2-ene isomerization than for butadiene formation. Maximum selectivity for butadiene formation was observed with the 19.6 atom

% Sb mixed oxide. The sum of the rates of appearance of cis but-2-ene and but-1-ene R_{1cb}, R_{2cb} and the rates of appearance of butadiene R_{1bd}, R_{2bd}, are presented in Tables 11.14 and 11.15.

H.T. Series Outgassed at 698 K for 16 hr

Reaction Temperature 474 K

TABLE 11.14

Cat.Comp./ Atom % Sb	$R_{1cb}/10^{-3}$ % min^{-1} m^{-2}	$R_{2cb}/10^{-3}$ % min^{-1} m^{-2}	initial cis/but-1-ene
0	0	0	-
6.2*	2.3	1.3	~100% cis
8.7	8.1	2.6	3.3
19.6	47	19	4.5
26.8	34	14	3.0
49.5	18	5.7	4.3
75.0	25	8.8	4.5
100	0	0	-

ACTIVITY PATTERNS FOR THE OXIDATIVE DEHYDROGENATION OF TRANS BUT-2-ENE WITH H.T. SERIES

474 K

ISOMERIZATION PRODUCTS FORMATION
FIGURE 11.8

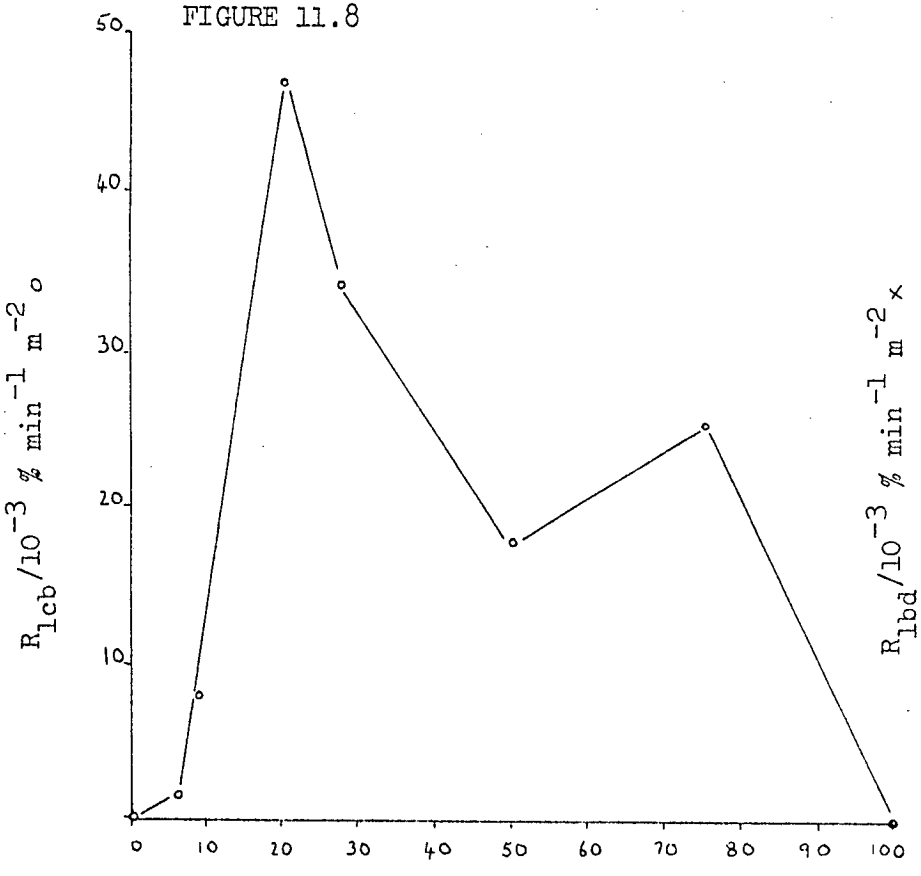

BUTADIENE FORMATION
FIGURE 11.9

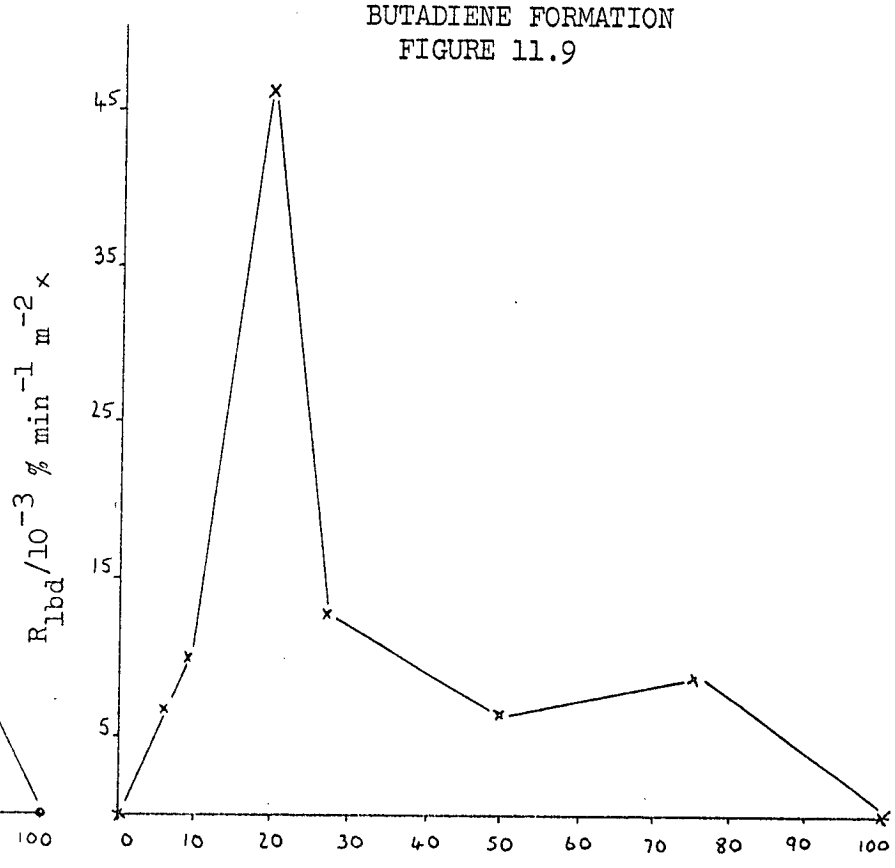

CAT.COMP./ATOM % Sb

TABLE 11.15

Cat.Comp./ Atom % Sb	$R_{1bd}/10^{-3}$ % min^{-1} m^{-2}	$R_{2bd}/10^{-3}$ % min^{-1} m^{-2}
0	0	0
6.2	6.7	2.3
8.7	10	9.0
19.6	46	15
26.8	13	10
49.5	6.8	2.4
75.0	9.1	3.4
100	0	0

*traces only of but-1-ene

No activity was observed for stannic oxide and antimony tetroxide. The percentage of but-1-ene formed with the 6.2 atom % Sb mixed oxide never exceeded 0.5%. The initial cis but-2-ene/but-1-ene product ratios indicated that the formation of cis but-2-ene was favoured. Similar activity patterns, Figures 11.8 and 11.9, were obtained for trans but-2-ene isomerization and butadiene formation. Maximum activity was observed with the 19.6 atom % Sb mixed oxide. An increase in the antimony content in the catalyst composition region of 6.2 atom % Sb to 19.6 atom % Sb resulted in an increase in activity. Activity was reduced with increasing antimony content in the catalyst composition region of 19.6 atom % Sb to 49.5 atom % Sb. A further increase in activity was observed at the catalyst composition of 75.0 atom % Sb.

OXIDATIVE DEHYDROGENATION OF BUT-1-ENE

474 K

26.8 Atom % Sb L.H. Series

FIGURE 11.10

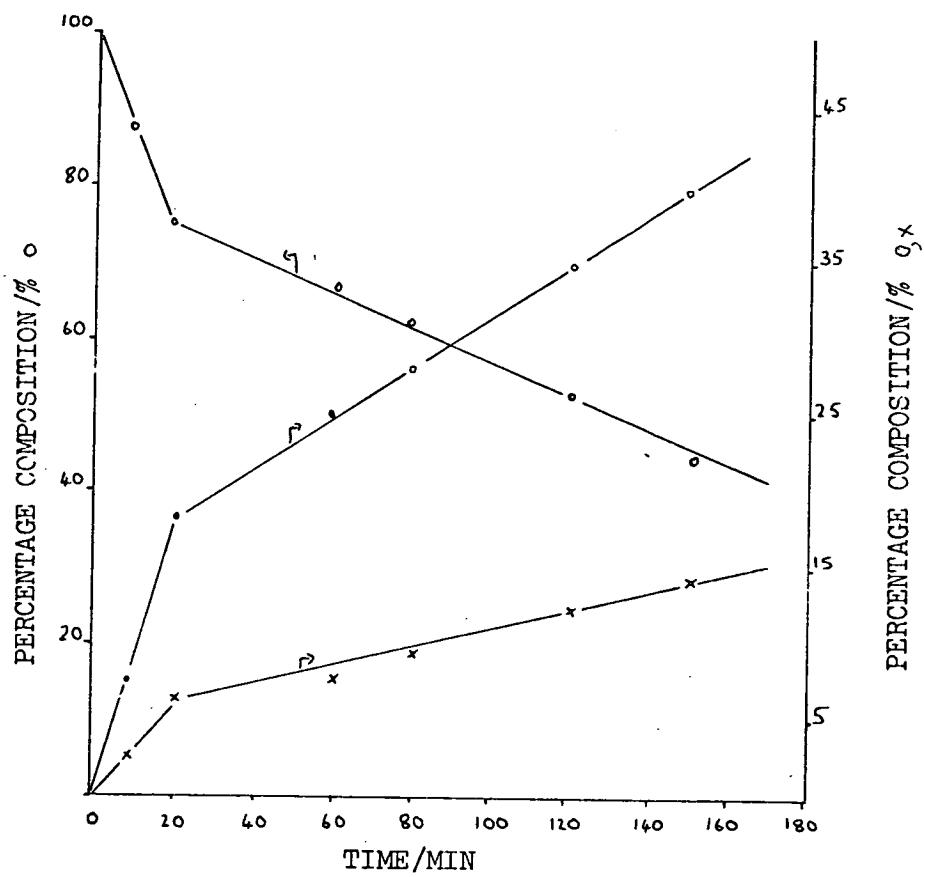

o BUT-1-ENE

o CIS BUT-2-ENE + TRANS BUT-2-ENE

x BUTADIENE

An indication of the reproducibility in the rate values is given in Tables 11.16 and 11.17.

H.T. Series Outgassed at 698 K for 16 hr

Reaction Temperature 474 K

TABLE 11.16

Cat.Comp./ Atom % Sb	$R_{1cb}/10^{-3}$ % min^{-1} m^{-2}	$R_{2cb}/10^{-3}$ % min^{-1} m^{-2}	initial cis/but-1-ene
6.2*	2.3	1.3	∿100% cis
6.2	2.2	1.2	∿100% cis

TABLE 11.17

Cat.Comp./ Atom % Sb	$R_{1bd}/10^{-3}$ % min^{-1} m^{-2}	$R_{2bd}/10^{-3}$ % min^{-1} m^{-2}
6.2*	6.7	2.3
6.2	7.0	2.2

Values* quoted in Tables 11.14 and 11.15.

The average difference in the rates was 5%. Changes of greater than ±5% in the activity patterns were considered to be significant.

11.9 Oxidative Dehydrogenation of But-1-ene with the L.T. Series Mixed Oxides

Figure 11.10 illustrates a typical percentage composition versus time plot. The products formed were cis but-2-ene, trans but-2-ene and

butadiene. Selectivity changed with catalyst composition, but did not alter significantly with time. The selectivities for but-1-ene isomerization and butadiene formation are presented in Table 11.18.

TABLE 11.18

L.T. Series Mixed Oxides Outgassed at 293 K for 5 hr

Reaction Temperature 474 K

Cat.Comp./ Atom % Sb	Se_1/% at 10 min		Se_2/% at 50 min	
	ct	bd	ct	bd
8.7	44.7	55.3	43.7	56.3
19.6	30.0	70.0	25.8	74.2
26.8	62.2	37.8	61.4	38.6
49.5	50.9	49.1	52.6	47.4
75.0	31.2	68.8	35.5	64.5

ct = cis but-2-ene + trans but-2-ene

bd = butadiene

The 19.6 atom % Sb mixed oxide showed the greatest selectivity for butadiene formation. The rates of but-1-ene isomerization R_{1ct}, R_{2ct} and butadiene appearance R_{1bd}, R_{2bd}, for a few selected mixed oxides, are presented in Tables 11.19 and 11.20.

ACTIVITY PATTERNS FOR THE OXIDATIVE DEHYDROGENATION OF BUT-1-ENE WITH THE L.T. SERIES MIXED OXIDES

474 K

ISOMERIZATION PRODUCTS FORMATION

FIGURE 11.11

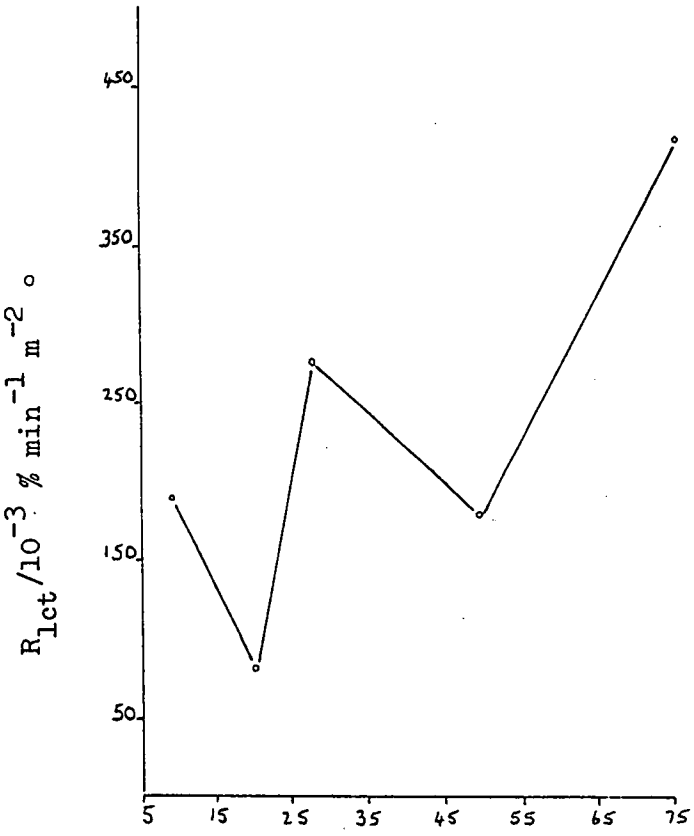

BUTADIENE FORMATION

FIGURE 11.12

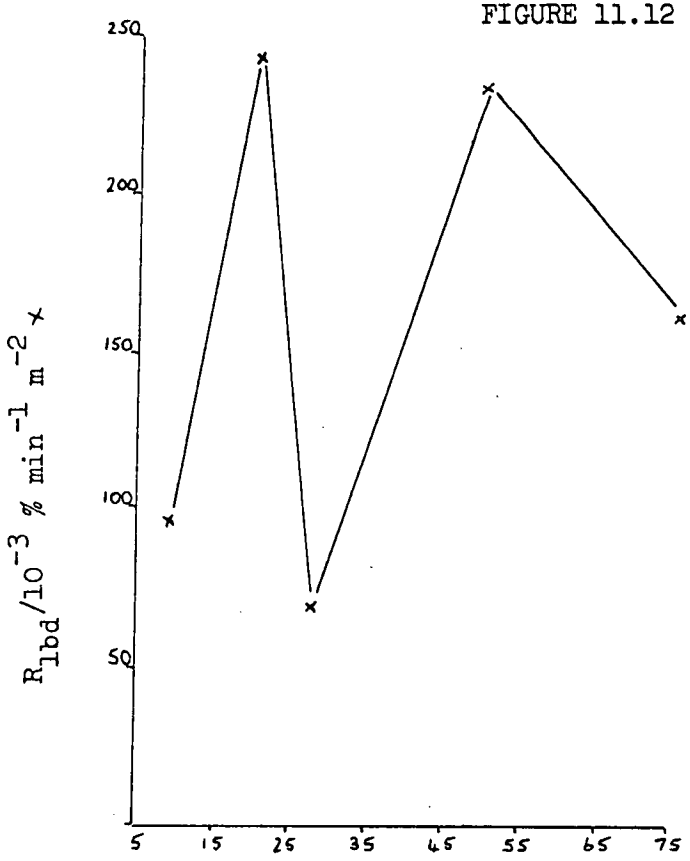

CAT.COMP./ATOM % Sb

L.T. Series Mixed Oxides Outgassed at 293 K for 5 hr

Reaction Temperature 474 K

TABLE 11.19

Cat.Comp./ Atom % Sb	$R_{1ct}/10^{-3}$ % min^{-1} m^{-2}	$R_{2ct}/10^{-3}$ % min^{-1} m^{-2}	initial cis/trans
8.7	192	44	1.4
19.6	81	21	1.9
26.8	279	46	2.0
49.5	182	41	2.1
75.0	418	61	2.0

TABLE 11.20

Cat.Comp./ Atom % Sb	$R_{1bd}/10^{-3}$ % min^{-1} m^{-2}	$R_{2bd}/10^{-3}$ % min^{-1} m^{-2}
8.7	96	42
19.6	243	55
26.8	70	33
49.5	235	44
75.0	162	37

The initial cis but-2-ene/trans but-2-ene product ratios indicated that cis but-2-ene was preferentially formed.

The two different activity patterns are illustrated by Figures 11.11 and 11.12. An increase in but-1-ene isomerization was accompanied by a decrease in butadiene formation and vice versa.

Tables 11.21 and 11.22 give an indication of the reproducibility in the rate values.

L.T. Series Mixed Oxide Outgassed at 293 K for 5 hr

Reaction Temperature 474 K

TABLE 11.21

Cat.Comp./ Atom % Sb	$R_{1ct}/10^{-3}$ % min^{-1} m^{-2}	$R_{2ct}/10^{-3}$ % min^{-1} m^{-2}	initial cis/trans
19.6*	81	21	1.9
19.6	75	20	1.8

TABLE 11.22

Cat.Comp./ Atom % Sb	$R_{1bd}/10^{-3}$ % min^{-1} m^{-2}	$R_{2bd}/10^{-3}$ % min^{-1} m^{-2}
19.6*	243	55
19.6	230	51

*Values quoted in Tables 11.19 and 11.20.

The average difference in the rate values was 6%. Differences of greater than ±6% in the rate values were considered to be significant.

11.10 Oxidative Dehydrogenation of Cis But-2-ene with the L.T. Series Mixed Oxides

The products formed were trans but-2-ene, but-1-ene and butadiene.

OXIDATIVE DEHYDROGENATION OF CIS BUT-2-ENE

474 K

49.5 Atom % Sb L.T. Series

FIGURE 11.13

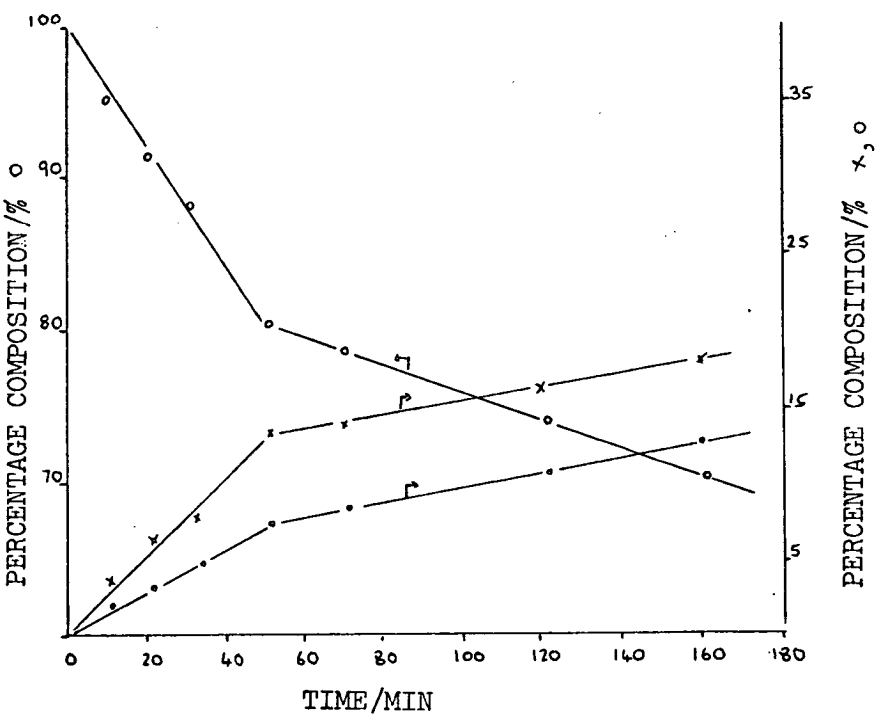

o CIS BUT-2-ENE

× BUTADIENE

o TRANS BUT-2-ENE + BUT-1-ENE

Figure 11.13 illustrates a typical percentage composition versus time plot. Selectivities for cis but-2-ene isomerization and butadiene formation are given in Table 11.23.

L.T. Series Mixed Oxides Outgassed at 293 K for 5 hr

Reaction Temperature 474 K

TABLE 11.23

Cat.Comp./ Atom % Sb	Se_1/% at 10 min		Se_2/% at 50 min	
	tb	bd	tb	bd
8.7*	23.1	76.9	28.2	71.8
19.6	43.3	56.7	42.9	57.1
26.8	42.7	57.3	40.0	60.0
49.5	36.4	63.6	35.0	65.0
75.0	51.3	48.7	51.6	48.4

traces* only of but-1-ene

tb = trans but-2-ene + but-1-ene

bd = butadiene

Selectivity altered with catalyst composition but not with time. The 8.7 atom % Sb mixed oxide showed the greatest selectivity for butadiene formation. The rates of cis but-2-ene isomerization R_{1tb}, R_{2tb} and butadiene appearance R_{1bd}, R_{2bd} are presented in Tables 11.24 and 11.25.

L.T. Series Mixed Oxides Outgassed at 293 K for 5 hr

Reaction Temperature 474 K

TABLE 11.24

Cat.Comp./ Atom % Sb	$R_{1tb}/10^{-3}$ % min^{-1} m^{-2}	$R_{2tb}/10^{-3}$ % min^{-1} m^{-2}	initial trans/but-1-ene
8.7*	16	4.4	~100% trans
19.6	27	13	1.9
26.8	37	18	1.1
49.5	60	21	2.2
75.0	173	52	2.0

TABLE 11.25

Cat.Comp./ Atom % Sb	$R_{1bd}/10^{-3}$ % min^{-1} m^{-2}	$R_{2bd}/10^{-3}$ % min^{-1} m^{-2}
8.7*	22	8.1
19.6	41	16
26.8	58	18
49.5	101	20
75.0	169	45

traces* only of but-1-ene

The initial trans but-2-ene/but-1-ene product ratios indicated that the formation of trans but-2-ene was favoured. The percentage of

ACTIVITY PATTERNS FOR THE OXIDATIVE DEHYDROGENATION OF CIS BUT-2-ENE WITH THE L.T. SERIES MIXED OXIDES

474 K

ISOMERIZATION PRODUCTS FORMATION

FIGURE 11.14

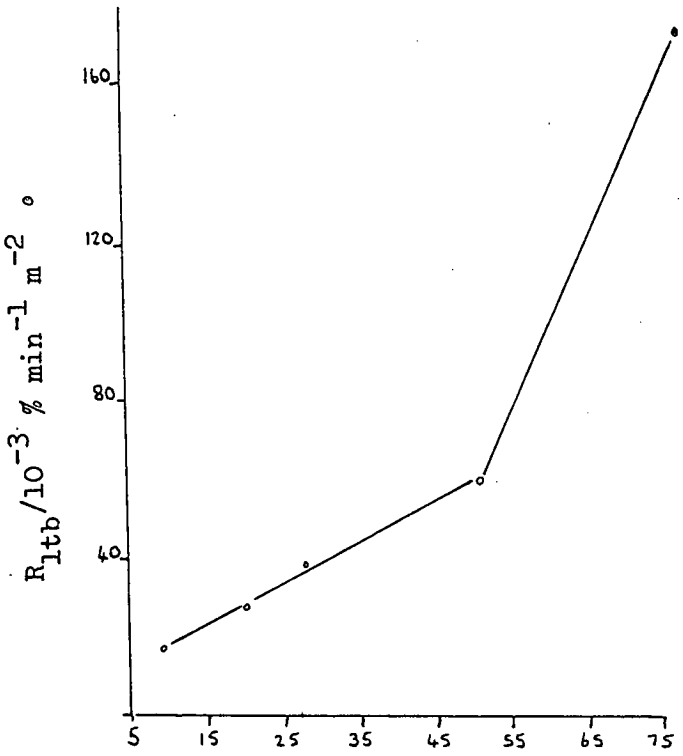

BUTADIENE FORMATION

FIGURE 11.15

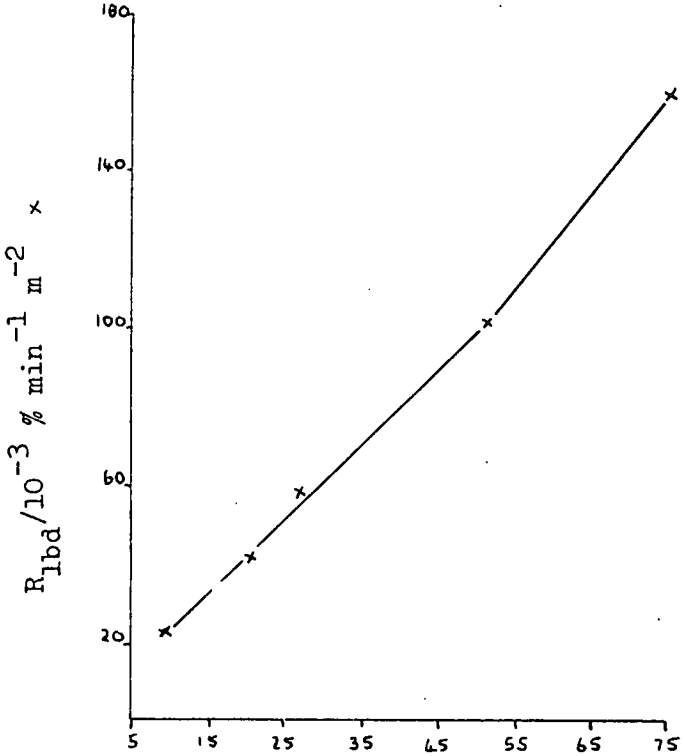

CAT.COMP./ATOM % Sb

but-1-ene formed with the 8.7 atom % Sb mixed oxide never exceeded 0.5%. Similar activity patterns, with maximum activity at the 75.0 atom % Sb mixed oxide, were obtained for cis but-2-ene isomerization and butadiene formation. Increasing the antimony content resulted in an increase in activity. These activity patterns are illustrated by Figures 11.14 and 11.15.

Rate values for repeat experiments are given in Tables 11.26 and 11.27.

L.T. Series Mixed Oxides Outgassed at 293 K for 5 hr

Reaction Temperature 474 K

TABLE 11.26

Cat.Comp./ Atom % Sb	$R_{1tb}/10^{-3}$ % min^{-1} m^{-2}	$R_{2tb}/10^{-3}$ % min^{-1} m^{-2}	initial trans/but-1-ene
19.6*	27	13	1.9
19.6	26	12	1.9

TABLE 11.27

Cat.Comp./ Atom % Sb	$R_{1bd}/10^{-3}$ % min^{-1} m^{-2}	$R_{2bd}/10^{-3}$ % min^{-1} m^{-2}
19.6*	41	16
19.6	39	15

Values* quoted in Tables 11.24 and 11.25.

The average difference in the rate values was 6%. Differences of greater than $\pm$6% in the two activity patterns were considered to be significant.

11.11 Area Occupied by the Solid Solution

Using the method put forward by Lazukin et al.,[24] an estimation of the fractional surface area of the solid solution in the two-phase tin-antimony mixed oxides was obtained from the following formula:-

$$\left[{}^{s}\text{ solid solution} \right] = \frac{{}^{s}\text{ solid solution} \times {}^{p}\text{ solid solution}}{{}^{s}\text{ mixed oxide}}$$

^{p} solid solution and ^{s} solid solution are, respectively, weight percentage and specific surface area of the solid solution, ^{s} mixed oxide is the specific surface area of the mixed oxide.

Godin et al.,[23] using tin-antimony catalysts prepared in a similar manner to the ones studied for this thesis, concluded that the solubility limit of antimony in stannic oxide was approximately 5 atom % Sb. In order to obtain an indication of the fraction of the mixed oxide area occupied by the solid solution, the solubility limit was set at 6.2 atom % Sb. This has a surface area of 16.4 m^2 and was the value used for ^{s} solid solution in the above formula. The composition of the two phases of a range of tin-antimony mixed oxides is shown in Table 11.28

TABLE 11.28

Phase Composition of Mixed Oxides

Cat.Comp./ Atom % Sb	Amounts of Sn and Sb, in solid solution/%		Amounts of Sb remaining as Sb_2O_4/%	Percentage of phases in mixed oxides weight/%		Computed surface fraction of mixed oxides, in their constituent phases/%		Specific surface area of mixed oxides/$m^2\ g^{-1}$
	Sn	Sb		solid solution	Sb_2O_4	solid solution	Sb_2O_4	
6.2	93.8	6.2	0	100	0	100	0	16.4
8.7	91.3	6.0	2.7	97.3	2.7	89.2	10.8	17.9
19.6	80.4	5.3	14.3	85.8	14.2	67.7	32.3	20.8
26.8	73.2	4.8	22.0	78.2	21.8	69.7	30.3	18.4
49.5	50.5	3.3	46.2	54.0	46.0	70.9	29.1	12.5
75.0	25	1.7	73.3	26.8	73.2	62.8	37.2	7.0

The rates of appearance of butadiene for but-1-ene dehydrogenation over the H.T. and L.T. series, with respect to the specific surface area of the solid solution only, are presented in Tables 11.29 and 11.30, respectively.

Table 11.29

H.T. Series Outgassed at 698 K for 16 hr

Reaction Temperature 474 K

Cat.Comp./ Atom % Sb	$R_{1bd}/10^{-3}$ % min^{-1} m^{-2}	$R_{2bd}/10^{-3}$ % min^{-1} m^{-2}
6.2	26	19
8.7	515	106
19.6	280	68
26.8	116	39
49.5	204	55
75.0	48	17

Table 11.30

L.T. Series Outgassed at 293 K for 5 hr

Reaction Temperature 474 K

Cat.Comp./ Atom % Sb	$R_{1bd}/10^{-3}$ % min^{-1} m^{-2}	$R_{2bd}/10^{-3}$ % min^{-1} m^{-2}
8.7	107	47
19.6	358	81
26.8	101	47
49.5	330	62
75.0	258	59

Calculating butadiene formation with respect to the specific surface area of the solid solution instead of the total specific surface area of the mixed oxide had no appreciable effect on the shape of the

activity patterns for but-1-ene dehydrogenation. This is illustrated by comparing Tables 11.29 and 11.30 with Tables 11.3 and 11.20, respectively.

A similar observation can be made for butadiene formation from cis but-2-ene and trans but-2-ene.

11.12 Summary

The individual oxides, pretreated according to the H.T. method, were inactive for the three n-butenes.

The activity patterns of the tin-antimony mixed oxides for the but-2-enes, both series, were unlike the corresponding ones for but-1-ene. However, the following trends are common to both series of mixed oxides.

i) An increase in but-1-ene isomerization was accompanied by a decrease in butadiene formation and vice versa. This is shown by Figures 11.2, 11.3 and 11.11, 11.12.

ii) An increase or decrease in cis but-2-ene or trans but-2-ene isomerization was accompanied by a similar change in butadiene formation. This is shown by Figures 11.5, 11.6, 11.8, 11.9 and 11.14, 11.15.

n-Butene isomerization observed in the presence and absence of air, at reaction temperatures of 474 K and 293 K, respectively, have different activity patterns.

Maximum activity for but-1-ene and cis but-2-ene isomerization with the H.T. series; in the presence of air, was found with the 75.0 atom % Sb and 19.6 atom % Sb mixed oxides, respectively. In the absence of air, the 19.6 atom % Sb and 7.4, 8.7 atom % Sb mixed oxides showed the greatest activity for but-1-ene and cis but-2-ene isomerization,

respectively. This is illustrated by comparing Figures 11.2 and 11.5 with the corresponding Figures 9.4 and 9.12.

For the L.T. series, maximum activity for but-1-ene and cis but-2-ene isomerization, in the presence of air, was found with the 75.0 atom % Sb mixed oxide. In the absence of air, the 49.5 atom % Sb mixed oxide was observed to be the most active catalyst for but-1-ene and cis but-2-ene isomerization. These observations are illustrated by comparing Figures 11.11 and 11.14 with the corresponding Figures 9.3 and 9.11.

CHAPTER 12

Discussion

Under the reaction conditions employed, activity was observed with the tin-antimony mixed oxides but not with the individual oxides. However, a number of investigators have shown that stannic oxide and the oxides of antimony are able to oxidize propylene to acrolein[24][79][80] and n-butenes to butadiene[69][71][73]. Generally, the oxides of antimony have been found to be less active, but more selective than stannic oxide. Few ideas have been put forward to explain the reaction mechanism for oxidation with the individual oxides. The majority of investigations have been concerned with the mixed oxides. In the references given above, only Sala and Trifiró[73] attempted to explain the oxidizing properties of the individual oxides. The oxidizing sites of antimony pentoxide were attributed to the presence of antimony-oxygen double bonds and/or surface defects. The presence of free electrons in the non-stoichiometric stannic oxide were believed to be responsible for the formation of butadiene.

The role of the allylic intermediate, in connection with propylene and n-butene oxidation, is well established. In keeping with this are the results obtained by Godin et al.[23] and Christie[92], studying propylene oxidation over tin-antimony mixed oxides which had been prepared in a manner similar to the ones investigated for this thesis. Godin et al.[23] used C^{13}-labelled propylene to confirm an allylic intermediate. Christie[92], studying propylene/D_2O exchange, concluded that the exchange mechanism involved the loss of an allylic hydrogen atom to form a symmetrical allylic intermediate. Such a mechanism could be used to account for the fact that only 5 of the

6 hydrogen atoms were exchangeable. Thus, taking into account the findings of Godin et al.[23] and Christie[92], it is reasonable to assume that allylic intermediates are also responsible for butadiene formation with the tin-antimony mixed oxides.

There are a number of different opinions concerning the nature of the chemical species responsible for the oxidizing properties of the tin-antimony mixed oxides. According to Godin et al.[23] the active sites were octahedrally co-ordinated Sb^{5+} ions. Wakabayashi et al.[25] believed that the sites responsible for oxidation were Sn^{4+} ions and that antimony labilized the tin-oxygen bonds. Trimm and Gabbay[87] also suggested that the active sites were Sn^{4+} ions, but they believed that the antimony oxides may have been involved in the allylic abstraction of the hydrogen from the olefins. Despite these discrepancies, a large proportion of the information found in the literature suggests that the solid solution of antimony oxide in stannic oxide may be responsible for its oxidizing properties.

The views held by Crozat and Germain[80] are particularly interesting. The mechanism responsible for propylene oxidation was believed to be similar to the one obtained for a bismuth-molybdate system. Thus, according to Crozat and Germain[80], the roles of the ions Sb^{5+} and Sn^{4+} were thought to be similar to those of Mo^{6+} and Bi^{3+}, respectively. The mechanism proposed by Crozat and Germain[80], Section 6.3, involved the formation of π-allyl-complexes with Sb^{5+} ions, resulting in the reduction of Sn^{4+} ions to Sn^{3+} ions. A redox mechanism also involving both cations was put forward by Peacock et al.[85] to explain propylene oxidation over bismuth molybdate catalysts. Additional support for the possible role played by Sn^{4+} ions, in the redox mechanism, comes from the investigation carried out by Margolis[116], studying

propylene oxidation over a tin-molybdenum mixed oxide. The mechanism proposed by Margolis[116] involved the formation of π-allyl-complexes with Mo^{6+} ions and the reduction of Sn^{4+} ions.

Thus, if the redox mechanisms for propylene oxidation over tin-antimony mixed oxides and bismuth-molybdate are similar, the mechanism for oxidative dehydrogenation of n-butenes, for both systems, may also contain similarities. A large amount of information concerning the oxidative dehydrogenation properties of bismuth-molybdates is available in the literature. The work carried out by Matsuura and Schuit[117][118], concerning the adsorption and reaction of adsorbed species on bismuth-molybdates, has led to a significant increase in the understanding of the mechanism for the oxidative dehydrogenation of n-butenes. The mechanism proposed by Matsuura and Schuit[117][118] involved participation by Mo^{6+} and Bi^{3+} ions. In view of the possibility that the roles of Mo^{6+} and Bi^{3+} ions may be analogous to Sb^{5+} and Sn^{4+} ions, some of the ideas developed by Matsuura and Schuit[117][118], for bismuth-molybdates, may also apply to the tin-antimony mixed oxides.

According to the earlier work of Matsuura and Schuit[117], the formation of butadiene from n-butene is a bifunctional process which involves the simultaneous cooperation of two centres called A and B. Evidence obtained from the adsorption studies indicated that the identities and roles of these centres were as follows:-

i) A-centre is an O_A^{2-} ion associated with a Bi^{3+} ion. It is the site at which reoxidization of the catalyst takes place and it is also the site from which a water molecule, arising from butadiene formation, leaves.

ii) B-centre consists of two O_B^{2-} ions and an anion vacancy. It is associated with the Mo^{6+} ion and is the site responsible for the adsorption of n-butenes.

Correlating the A and B centres with Sn^{4+} and Sb^{5+} ions, respectively, a possible mechanism for oxidative dehydrogenation of n-butenes over tin-antimony mixed oxides is as follows:-

$$C_4H_8 + Sb^{5+} + O_{B_1}^{2-} + A.V. \rightarrow [C_4H_7....Sb]^{5+} + O_{B_1}^{-}H + e \quad (1)$$

$$[C_4H_7....Sb]^{5+} + O_{B_2}^{2-} \rightarrow C_4H_6 + O_{B_2}^{-}H + e + Sb^{5+} + A.V. \quad (2)$$

$$Sn^{4+} + 2e \rightarrow Sn^{2+} \quad (3)$$

$$O_{B_1}^{-}H + O_{B_2}^{-}H + O_A^{2-} \rightarrow O_{B_1}^{2-} + O_{B_2}^{2-} + H_2O + A.V. \quad (4)$$

$$Sn^{2+} + \tfrac{1}{2}O_2 + A.V. \rightarrow Sn^{4+} + O_A^{2-} \quad (5)$$

$[C_4H_7....Sb]^{5+}$ represents an allyl anion π-bonded to Sb^{5+}. Support for such an intermediate comes from the work of Godin et al.[23] and Christie[92], studying propylene oxidation over tin-antimony mixed oxides. However, the participation of σ-bonded allylic intermediates cannot be ruled out. A.V. is an anion vacancy.

In accordance with the views held by Crozat and Germain[80] and Peacock et al.,[85] for the tin-antimony mixed oxides and bismuth-molybdates respectively, the electrons generated as a result of steps (1) and (2) lead to the reduction of the cation, which is not involved with the allylic-complex, Sn^{4+} step (3).

The two hydrogen atoms, attached to $O_{B_1}^{2-}$ and $O_{B_2}^{2-}$, migrate to O_A^{2-} and are desorbed as water. This results in an anion vacancy (step 4) and is in accordance with the views of Matsuura and Schuit[118]. The role played by Sn^{2+}, in the reoxidization step (5), is similar to one given by Crozat and Germain[80].

For the L.T. and H.T. series mixed oxides, the rates of

butadiene formation from the three n-butenes, decrease in the order but-1-ene>cis but-2-ene>trans but-2-ene. Such a sequence is in keeping with the findings of Adams et al.[119]. The order for the rate of abstraction of allylic hydrogens is tertiary>secondary> primary. The allylic hydrogens abstracted in step (1) for but-1-ene and but-2-ene are secondary and primary ones, respectively. Thus, the rate of formation of butadiene from the n-butenes is in keeping with the view held by Trimm and Gabbay[87] that the rate-determining step is the abstraction of the allylic hydrogen.

The activity patterns presented for butadiene formation and n-butene isomerization provide further support for the view that butadiene formation is more favourable from but-1-ene than from the two but-2-enes. When but-1-ene is the reactant, isomerization results in a decrease in the amount of but-1-ene available for oxidative dehydrogenation. In general, a catalyst which has a high activity for but-1-ene isomerization has a low activity for butadiene formation and vice versa. Isomerization of cis but-2-ene or trans but-2-ene, with the exception of the 6.2 atom % Sb mixed oxide, resulted in the formation of but-1-ene. Thus, a catalyst having a high activity for cis or trans but-2-ene isomerization also possess a high activity for butadiene formation and vice versa.

The mechanism proposed to explain butadiene formation requires the cooperation of the Sb^{5+} and Sn^{4+} ions, which are present in the solid solution of antimony oxide in stannic oxide and is in keeping with views, held by Godin et al.[23] and Lazukin et al.[24] that the solid solution is responsible for activity. However, unlike their observations, a change in the

composition of the catalyst generally resulted in a change in activity and/or selectivity. This was noted with the L.T. and H.T. series mixed oxides for all the n-butenes studied. Calculating butadiene formation with respect to the specific surface area of the solid solution or the total specific surface area of the mixed oxide gave rise to two similar activity patterns. An illustration of this effect is given in Section 11.11. The work carried out by Godin et al.[23] and Lazukin et al.[24] concerned propylene oxidation, but the investigation for this thesis involved the oxidative dehydrogenation of n-butenes. In accordance with the observations made by a number of other investigators[69][73][86] isomerization as well as oxidative dehydrogenation occurred. The way in which isomerization influences butadiene formation has already been discussed. Unlike the situation encountered for propylene oxidation, the oxidative dehydrogenation of n-butene will depend on two factors. One factor, common to both oxidation reactions, is the role played by the solid solution of antimony oxide in stannic oxide. The second factor, encountered with the n-butenes only, is the process of isomerization. Isomerization, in the absence of air, was found to vary with catalyst composition. A similar observation was made when oxidation conditions were used. Thus, any change in n-butene isomerization will give rise to a change in butadiene formation. This may account for the variation in butadiene formation observed in the catalyst composition region of 6.2 atom % Sb to 75.0 atom % Sb, both series, in spite of the belief that the solid solution of antimony oxide in stannic oxide is responsible for its formation.

Such an argument assumes that the sites responsible for n-butene isomerization and butadiene formation are different. If

the sites were the same, activity for n-butene isomerization would not be expected to vary significantly over the catalyst composition 6.2 atom % to 75.0 atom % Sb. Butadiene formation would also remain effectively constant.

Shown in Table 11.2, is the fact that the 6.2 atom % Sb mixed oxide was inactive for but-1-ene isomerization but active for butadiene formation. Simons et al.[120], studying oxidative dehydrogenation of n-butenes over uranium-antimony mixed oxides also observed butadiene formation only. This emphasises the fact that the formation of allylic intermediates does not always lead to isomerization. Other evidence available in the literature[69][73] also supports the view that the two processes, with the tin-antimony mixed oxides, take place on different sites. However, Matsuura and Schuit[118] concluded that similar sites were responsible for butadiene formation and n-butene isomerization over bismuth-molybdates.

The summary given in Section 11.12 illustrates the fact that the activity patterns for n-butene isomerization, in the absence of air, were unlike the corresponding ones obtained in the presence of air. However, this observation does not entirely rule out the possibility that n-butene isomerization, in the presence and absence of air, takes place on similar sites. Section 9.7, shows that pretreatment with butadiene was found to poison but-1-ene isomerization, taking place in the absence of air. Thus, the ability of the tin-antimony mixed oxides to isomerize n-butenes, under oxidation conditions, is likely to be influenced by the amount of butadiene formed. If the poisoning effect of butadiene is a function of catalyst composition the activity patterns for n-butene isomerization, taking place in the presence of butadiene

formation, would not be expected to be the same as the corresponding ones obtained in the absence of butadiene formation. Thus, it may be possible to apply arguments similar to the ones given in Chapter 10, to explain n-butene isomerization taking place under oxidation conditions.

Section 11.6 illustrates the fact that butadiene formation can take place in the absence of air. This observation shows that the lattice oxygens are capable of abstracting allylic hydrogens. However, butadiene formation was reduced indicating that gaseous oxygen plays a role in the reoxidization of the catalyst. Also noted was the fact that but-1-ene isomerization increased. This provides further support for the retarding influence of butadiene on but-1-ene isomerization.

Step (5) shows reoxidation of the tin-antimony mixed oxides taking place at the reduced centre A, with gas phase oxygen. However, Matsuura and Schuit[117] also suggested that reoxidation of bismuth-molybdate could take place by diffusion of lattice oxygen from the bulk of the catalyst. Christie[92], studying propylene oxidation in the presence of $^{18}O_2$, was able to show that the diffusion of oxygen through the catalyst played a major role in the reoxidation of the tin-antimony mixed oxides, studied for this thesis. Thus, reoxidation of the reduced catalyst may take place by lattice oxygen transfer and/or by the adsorption of gas phase oxygen at the reduced sites.

Conclusion

A redox mechanism, involving the cations Sb^{5+} and Sn^{4+} found in the saturated solid solution of antimony tetroxide in stannic oxide, is thought to be responsible for butadiene formation. Evidence suggests

that the accompanying n-butene isomerization does not take place through the allylic intermediates which are responsible for butadiene formation. There exists the possibility that n-butene isomerization, under oxidation conditions, may take place on the same type of sites responsible for n-butene isomerization, occurring at low temperatures in the absence of air.

REFERENCES

1. Van Marum, J., J. der Phys., 3, 359 (1796).
2. Kirchhoff, G.R., Schweigger's Journal, 4, 108 (1812).
3. Davy, H., Phil. Trans., 7, 77 (1817).
4. Dobereiner, J., Schweigger's Journal, 34, 91 (1822).
5. Berzelius, J., Jahresber. Chem., 15, 237 (1836).
6. Ostwald, W., Phyzik Z., 3, 313 (1902).
7. Faraday, M., Phil. Trans., 114, 55 (1834).
8. Sabatier, P., La Catalyse en Chemie Organique (Paris and Liege, 1913).
9. Langmuir, I., Phys. Rev., 6, 79 (1915).
10. Hinshelwood, C.N., "The Kinetics of Chemical Change" (Clarendon Press, Oxford, 1940).
11. Laidler, K.J., "Catalysis", ed. Emmett, P.H., (Reinhold, New York, 1954).
12. Rideal, E.K., Sabatier Lecture: J. Soc. Chem. Ind., 62, 335 (1943).
13. Eley, D.D., Quart. Rev., 3, 209 (1949).
14. Roberts, J.K., Proc. Roy. Soc. A., 152, 445 (1935).
15. Weisz, P.B., J. Chem. Phys., 20, 1483 (1952).
16. Hauffe, K., Adv. Catalysis, 7, 213 (1955).
17. Wolkenstein, Th., Adv. Catalysis, 12, 189 (1960).
18. Stone, F.S., Adv. Catalysis, 13, 1 (1962).
19. Winter, E.R.S., Disc. Faraday Soc., 28, 183 (1959).
20. Belański, A., Deren, J., Haber, J., Sloczyński, J., Trans. Faraday Soc. 58, 166 (1962).
21. Dowden, D.A., Wells, D., 2nd Actes Intern. Congr. Catalyse, Paris, 1960 2, 1499 (Techip, Paris, 1961).

22. Balandin, A.A., Adv. Catalysis, 19, 1 (1969).

23. Godin, G.W., McCain, C.C., Porter, E.A., Proc. 4th Intern. Congr. on Catalysis, Moscow, 1968, 1, 271 (Akademiai Kiado, Budapest, 1971).

24. Lazukin, V.I., Rubanik, M. Ya., Zhugailo, Ya. V., Kurganov, A.A., Katalis i Katalizatory, 3, 54 (1967).

25. Wakabayashi, K., Kamiya, Y., Ohta, N., Bull. Chem. Soc. Japan, 41, 2776 (1968).

26. Roginskaya, Yu. E., Dulin, D.A., Stroeva, S.S., Kul'kova, N.V., Gel'bshtein, A.I., Kinet. Katal. 9, 943 (1968).

27. Simon, A., Theler, E., Z. Anorgan. und Allgem. Chem., 161, 113 (1927); 162, 253 (1927).

28. Hughes, B., Kemball, C., Tyler, K.J., J. Chem. Soc. Faraday I, 71, 1285 (1975).

29. Pines, H., Haag, W.O., J. Amer. Chem. Soc., 82, 2471 (1960).

30. Haag, W.O., Pines, H., J. Amer. Chem. Soc., 82, 2488 (1960).

31. Kemball, C., Leach, H.F., Skundric, B., Taylor, K.C., J. Catalysis, 27, 416 (1972).

32. Kemball, C., Leach, H.F., Moller, B.W., J. Chem. Soc. Faraday I, 69, 624 (1973).

33. Bunnett, J.F., Angew. Chem. Intern., 1, 225 (1962).

34. Gould, E.S., "Mechanism and Structure in Organic Chemistry", 472 (Holt Intern. Norwich 1969).

35. Pines, H., Manassen, J., Adv. Catalysis, 16, 49 (1966).

36. Knözinger, H., Angew. Chem. Intern., 7, 791 (1968).

37. Brey jr. W.S., Krieger, K.A., J. Amer. Chem. Soc., 71, 3637 (1949).

38. Topchieva, K.V., Yun-Pin, K., Smirnova, I.V., Adv. Catalysis, 9, 799 (1957).

39. Hensel, J., Pines, H., J. Catalysis, 24, 197 (1972).

40. Pines, H., Hensel, J., Šimonik, J., J. Catalysis, 24, 206 (1972).

41. Šimonik, J., Pines, H., J. Catalysis, 24, 211 (1972).

42. Pines, H., Šimonik, J., J. Catalysis, 24, 220 (1972).

43. Licht, E., Schächter, Y., Pines, H., J. Catalysis, 31, 110 (1973).

44. Licht, E., Schächter, Y., Pines, H., J. Catalysis, 34, 338 (1974).

45. Gentry, S.J., Rudham, R., J. Chem. Soc. Faraday I, 70, 1685 (1974).

46. Gentry, S.J., Rudham, R., Wagstaff, K.P., J. Chem. Soc. Faraday I, 71, 657 (1975).

47. Rajaram, P., Sastri, M.V.C., Viswanathan, B., Srinivasan, V., Z. Physik. Chem. Neue Folge, 89, 154 (1974).

48. Kibby, C.L., Hall, W.K., J. Catalysis, 29, 144 (1973).

49. Schwab, G.H., Schwab-Agallidis, E., J. Amer. Chem. Soc., 71, 1806 (1949).

50. Balta, I., Borcsök, S., Solymosi, F., Szabó, Z.G., Proc. 3rd Intern. Congr. on Catalysis, Amsterdam, 1964, 2, 1340 (North-Holland, Amsterdam, 1965).

51. McCaffrey, E.F., Klissurski, D.G., Ross, R.A., Proc. 5th Intern. Congr. on Catalysis, Miami Beach, 1972, 1, 151 (North-Holland, Amsterdam, 1973).

52. Coutts, N.M., Ph.D. Thesis University of Edinburgh, (1973).

53. Newham, J., Chem. Revs., 63, 123 (1963).

54. Roberts, R.M., J. Phys. Chem., 63, 1400 (1959).

55. Baird, R.L., Aboderin, A.A., J. Amer. Chem. Soc., 86, 252 (1964).

56. Larson, J.G., Gerberich, H.R., Hall, W.K., J. Amer. Chem. Soc., 87, 1880 (1965).

57. Hightower, J.W., Hall, W.K., J. Amer. Chem. Soc., 90, 851 (1968).

58. Bartley, B.H., Habgood, H.W., George, Z.M., J. Phys. Chem., 72, 1689 (1968).

59. Flockhart, B.D., McLoughlin, L., Pink, R.C., Chem. Comm., 818 (1970).

60. Bond, G.C., Wells, P.B., Adv. Catalysis, 15, 91 (1964).

61. Ipatieff, V.N., Corson, B.B., Ind. Eng. Chem., 27, 1069 (1935).

62. Farkas, A., Farkas, L., Ind. Eng. Chem., 34, 716 (1942).

63. Turkevich, J., Smith, R.K., J. Chem. Phys., 16, 466 (1948).

64. Hightower, J.W., Hall, W.K., J. Phys. Chem., 71, 1014 (1967).

65. Leftin, H.P., Hermana, E., Proc. 3rd Intern. Congr. on Catalysis, Amsterdam, 1964, 2, 1064 (North-Holland, Amsterdam, 1965).

66. Pines, H., Schaap, L.A., Adv. Catalysis, 12, 117 (1960).

67. Haag, W.O., Pines, H., J. Amer. Chem. Soc., 82, 387 (1960).

68. Foster, N.F., Cvetanović, R.J., J. Amer. Chem. Soc., 82, 4274 (1960).

69. Trifirò, F., Villa, P.L., Pasquon, I., La Chimica e L'Industria, 52, 857 (1970).

70. Takte, D.G., Rooney, J.J., Chem. Comm., 612 (1969).

71. Kemball, C., Leach, H.F., Shannon, I.R., J. Catalysis, 29, 99 (1973).

72. Alieva, M.M., Adzhamov, K. Yu., Shikhalizade, G.M., Vartanov, A.A., Chem. Abstr., 77, 156825y (1972).

73. Sala, F., Trifirò, F., J. Catalysis, 34, 68 (1974).

74. Voge, H.H., "Oxidation of Organic Compounds", Amer. Chem. Soc., 76, 242 (Washington, 1968).

75. Hucknall, D.J., "Selective Oxidation of Hydrocarbons" (Academic Press Inc., London, 1974).

76. Mars, P., Van Krevelen, D.W., Chem. Engng. Sci. Suppl., 3, 41 (1964).

77. Adams, C.R., Proc. 3rd Intern. Congr. on Catalysis, Amsterdam, 1964, 1, 240 (North-Holland, Amsterdam, 1965).

78. Sachtler, W.M.H., De Boer, N.H., Proc. 3rd Intern. Congr. on Catalysis, Amsterdam, 1964, 1, 252 (North-Holland, Amsterdam, 1965).

79. Belousov, V.H., Gershingorina, A.V., Kinet. Katal., 12, 541 (1971).

80. Crozat, M., Germain, J.E., Bull. Soc. Chim. France, 3, 1125 (1973).

81. Wakabayashi, K., Kamiya, Y., Ohta, N., Bull. Chem. Soc. Japan, 40, 2172 (1967).

82. Seiyama, T., Yamazoe, N., Egashira, M., Proc. 5th Intern. Congr. on Catalysis, Miami Beach, 1972, 2, 997 (North-Holland, Amsterdam, 1973).

83. Fattore, V., Fuhrman, Z.A., Manara, G., Notari, B., J. Catalysis, 37, 215 (1975).

84. Batist, Ph.A., Kapteijns, C.J., Lippens, B.C., Schuit, G.C.A., J. Catalysis, 7, 33 (1967).

85. Peacock, J.M., Sharp, M.J., Parker, A.J., Ashmore, P.G., Hockey, J.A., J. Catalysis, 15, 379 (1969).

86. Sekushova, Kh.Z., Vartanov, A.A., Alkhazov, T.G., Belen'kii, M.S., Chem. Abstr., 73, 3283n (1970).

87. Trimm, D.L., Gabbay, D.S., Trans. Faraday Soc., 67, 2782 (1971).

88. Leck, J.H., "Pressure Measurement in Vacuum Systems" (Chapman and Hall, London 1964).

89. "Handbook of Chemistry and Physics" 53 (The Chemical Rubber Co. Ohio 1972-1973).

90. Brunauer, S., Emmett, P.H., Teller, E., J. Amer. Chem., Soc., 60, 309 (1938).

91. Howe, R.F., Davidson, D.E., Whan, D.A., J. Chem. Soc. Faraday I, 68, 2266 (1972).

92. Christie, J.R., Ph.D. Thesis University of Edinburgh; J. Chem. Soc. Faraday I, 72, 334 (1976).

93. Roca, F.F., De Mourgues, L., Trambouze, Y., J. Catalysis, 14, 107 (1969).

94. Moro-oka, Y., Takita, Y., Ozaki, A., J. Catalysis, 27, 177 (1972)

95. Takita, Y., Ozaki, A., Moro-oka, Y., J. Catalysis, 27, 185 (1972)

96. Ward, J.W., J. Catalysis, 9, 225 (1967).

97. Thornton, E.W., Harrison, P.G., J. Chem. Soc. Faraday I, 71, 461 (1975).

98. Kilpatrick, J.E., Prosen, E.J., Pitzer, K.S., Rossini, J.D., J. Res. Nat. Bur. Stand., 36, 559 (1946).

99. Hoser, H., Krzyzanowski, S., J. Catalysis, 38, 366 (1975).

100. Dzisko, V.A., Proc. 3rd Intern. Congr. on Catalysis, Amsterdam, 1964 1, 422 (North-Holland, Amsterdam, 1965).

101. Ai, M., Suzuki, S., J. Catalysis, 30, 362 (1973).

102. Parry, E.P., J. Catalysis, 2, 371 (1963).

103. Buiten, J., J. Catalysis, 13, 373 (1969).

104. Viswanathan, B., Sastri, M.V.C., Srinivasan, V., Z. Physik. Chem. Neue Folge, 79, 216 (1972).

105. Hall, W.K., Larson, J.G., Gerberich, H.R., J. Amer. Chem. Soc., 85, 3711 (1963).

106. Jacobs, P.A., Declerck, L.J., Vandamme, L.J., Uytterhoeven, J.B., J. Chem. Soc. Faraday I, 71, 1545 (1975).

107. Itoh, M., Hattori, H., Tanabe, K., J. Catalysis, 35, 225 (1974).

108. Lucchesi, P.J., Baeder, D.L., Longwell, J.P., J. Amer. Chem. Soc., 81, 3235 (1959).

109. Misono, M., Saito, Y., Yoneda, Y., J. Catalysis, 9, 135 (1967).

110. Misono, M., Yoneda, Y., J. Phys. Chem., 76, 44 (1972).

111. Jacobs, P.A., Heylen, C.F., J. Catalysis, 34, 267 (1974).

112. Ballivet, D., Barthomeuf, D., Trambouze, Y., J. Catalysis, 26, 34 (1972).

113. Ballivet, D., Barthomeuf, D., Trambouze, Y., J. Catalysis, 34, 423 (1974).

114. Baird, M.J., Lunsford, J.H., J. Catalysis, 26, 440 (1972).

115. Peri, J.B., Actes Du Deuxieme Congres. International De Catalyse Paris, Paris, 1960, 1, 1333 (Technip, Paris, 1961).

116. Margolis, L.Ya., J. Catalysis, 21, 93 (1971).

117. Matsuura, I., Schuit, G.C.A., J. Catalysis, 20, 19 (1971).

118. Matsuura, I., Schuit, G.C.A., J. Catalysis, 25, 314 (1972).

119. Adams, C.R., Voge, H.H., Morgan, C.Z., Armstrong, W.E., J. Catalysis, 3, 379 (1964).

120. Simons, Th.G.J., Houtman, P.N., Schuit, G.C.A., J. Catalysis, 23, 1 (1971).